FLAMMABILITY CHARACTERISTICS OF HYDROGEN AND ITS MIXTURES WITH LIGHT HYDROCARBONS AT ATMOSPHERIC AND SUB-ATMOSPHERIC PRESSURES

A Dissertation

by

THUY MINH HAI LE

Submitted to the Office of Graduate Studies of
Texas A&M University
in partial fulfillment of the requirements for the degree of

DOCTOR OF PHILOSOPHY

Chair of Committee, M. Sam Mannan
Committee Members, James Holste
Charles Glover
Eric Petersen
Head of Department, M. Nazmul Karim

August 2013

Major Subject: Chemical Engineering

Copyright 2015 Thuy Minh Hai Le

ABSTRACT

Knowledge of flammability limits is essential in the prevention of fire and explosion. There are two limits of flammability, upper flammability limit (UFL) and lower flammability limit (LFL), which define the flammable region of a combustible gas/vapor. This research focuses on the flammability limits of hydrogen and its binary mixtures with light hydrocarbons (methane, ethane, *n*-butane, and ethylene) at sub-atmospheric pressures.

The flammability limits of hydrogen, light hydrocarbons, and binary mixtures of hydrogen and each hydrocarbon were determined experimentally at room temperature (20ºC) and initial pressures ranging from 1.0 atm to 0.1 atm. The experiments were conducted in a closed cylindrical stainless steel vessel with upward flame propagation. It was found that the flammable region of hydrogen initially widens when the pressure decreases from 1.0 atm to 0.3 atm, then narrows with the further decrease of pressure. In contrast, the flammable regions of the hydrocarbons narrow when the pressure decreases. For hydrogen and the hydrocarbons, pressure has a much greater impact on the UFLs than on the LFLs.

For binary mixtures of hydrogen and the hydrocarbons, the flammable regions of all mixtures widen when the fraction of hydrogen in the mixture increases. When the pressure decreases, the flammable regions of all mixtures narrow. The applications of Le Chatelier's rule and the Calculated Adiabatic Flame Temperature (CAFT) model to the

flammability limits of the mixtures were verified. It was found that Le Chatelier's rule could predict the flammability limits much better than the CAFT model.

The adiabatic flame temperatures (AFTs), an important parameter in the risk assessment of fire and explosion, of hydrogen and the hydrocarbons were also calculated. The influence of sub-atmospheric pressures on the AFTs was investigated. A linear relationship between the AFT and the corresponding flammability limit is derived. Furthermore, the consequence of fire relating to hydrogen and the hydrocarbons is discussed based on the AFTs of the chemicals.

DEDICATION

To my mother, Huong Thi Nguyen, and father, Tri Si Le, who always believe in me and have supported me tirelessly from day one.

To my husband, Ha Hai Nguyen, who inspires me to go above and beyond.

This is a tribute to the three of you.

ACKNOWLEDGEMENTS

I would like to express my deepest gratitude to Dr. M. Sam Mannan, my advisor, who has been a great source of guidance, support, encouragement, and inspiration throughout my years of studying and working on my research. Whenever I am confused and lost, his calmness and encouragement motivate me to keep reading and working until I could find my direction. He has also provided me countless opportunities to work with many experts and scholars who have helped me not only in my research but also in other aspects of process safety engineering which are essential for my future career. I am proud to be his student and a member of the Mary Kay O'Connor Process Safety Center.

I would like to thank my committee members, Dr. James Holste, Dr. Charles Glover, and Dr. Eric Petersen, for their advice, thought-provoking suggestions, availabilities and commitments.

Many thanks to Dr. Chad Victor Mashuga, whose help in the initial stage of my research was crucial. Dr. Mashuga has spent days in my lab teaching me and working with me on my apparatus and the setup of the Lab-View program. Many of my research ideas came from Dr. Mashuga's work. More importantly, Dr. Mashuga has inspired me to reach out and help fellow students as much as I can.

I would like to acknowledge Randy Marek for his invaluable help on the construction and repair of my experimental apparatus. Without Randy's support, many of my experiments could not have been possible.

I am grateful to Dr. Hans Pasman for his advice and insightful ideas relating to my research project. Dr. Pasman has helped me answer many questions which enable me to understand fundamental concepts of combustion much better.

I would also like to thank all the students and staff members of the Mary Kay O'Connor Process Safety Center for making my years of study much easier, funnier and memorable.

I could not thank enough my family for always standing by me, enduring my moments of anxiety and stress, celebrating my achievements, and loving me unconditionally. Thank you, mother, for your many sacrifices without which my education would not have been possible. Thank you, father, for your words of encouragement and comforting. Finally, thank you, my dear husband, for always being there, in sadness and happiness. Words cannot express how much I love you all.

TABLE OF CONTENTS

Page

Page

LIST OF FIGURES

Page

Page

Page

Page

Page

Page

LIST OF TABLES

Page

Page

1. INTRODUCTION[*]

1.1. Flammability limits

A flammable gas or vapor burns in air over a limited range of compositions bounded by two limits of flammability: upper flammability limit (UFL), and lower flammability limit (LFL). UFL is the maximum concentration of gas in air and LFL is the minimum concentration of gas in air capable of propagating flame upon ignition as defined by the ASTM[1] and the U.S. Bureau of Mines.[2-3] In European standards such as EN 1839 and EN 1127-1,[4] UFL and LFL are referred to as upper explosion limit (UEL) and lower explosion limit (LEL), respectively. It is worth noting that according to the European definition, explosion limits are not part of the explosion/flammable range; for example, LEL is the highest concentration of gas which just fails to propagate flame upon ignition.[4]

[*] Part of this section is reprinted with permission from "Upper Flammability Limits of Hydrogen and Light Hydrocarbons in Air at Subatmospheric Pressures" by H. Le, S. Nayak, M. S. Mannan, 2012. *Industrial & Engineering Chemistry Research*, 51(27), 9396-9402. DOI: 10.1021/ie300268x. Copyright 2012 American Chemical Society

[*] Part of this section is reprinted with permission from "Lower Flammability Limits of Hydrogen and Light Hydrocarbons in Air at Subatmospheric Pressures" by H. Le, Y.Liu, M. S. Mannan, 2013. *Industrial & Engineering Chemistry Research*, 52(3), 1372-1378. DOI: 10.1021/ie302504h. Copyright 2013 American Chemical Society

Controlling the concentrations of gases and vapors outside their flammability ranges is a major consideration in occupational safety and health. Flammable gases are stored safely by keeping the gas concentrations above their UFLs. A number of methods are also employed to prevent the existence of a flammable gas-air mixture including the use of inert substances such as nitrogen or carbon dioxide to dilute the gas before it comes in contact with air.[5] For example, nitrogen is commonly used in the procedure to take a vessel containing a flammable gas out of service without creating a flammable environment. The calculation of the amount of nitrogen needed requires the knowledge of the LFL of the gas as illustrated in the following equation:[5]

$$\text{OSFC}=\frac{\text{LFL}}{1\text{-z}\left(\frac{\text{LFL}}{21}\right)} \qquad [1.1]$$

where OSFC is the out of service fuel concentration, and z is the stoichiometric oxygen coefficient from the combustion reaction between the flammable gas and oxygen. The knowledge of LFL is also important in the design of ventilation systems to control flammable gas releases. One of the design criteria for ventilation systems provided by the National Fire Protection Association NFPA 30[6] states the ventilation for inside process areas must be sufficient to keep concentrations of gases at a 5-foot radius from all sources below 25% of the gas LFL. UFLs and LFLs are regularly used in fire consequence modeling and fire risk assessment.[7] All above examples show that knowledge of flammability limits is essential in the prevention of fire and explosion when handling flammable gases or vapors.

Flammability limits are affected by a number of factors which can be grouped into three categories:[2-3, 8-9] apparatus parameters (e.g., size, location of igniter or direction of flame propagation, ignition energy), operator (e.g., flammability limit criterion), and the physical condition of the gas mixture (e.g., turbulence, temperature, pressure). For this reason, it is important that the report of any flammability limit must include the specifications of the experimental apparatus, the criterion of flammability, and the experimental conditions. It is equally important that the right flammability limits are selected and used according to the operation conditions, most notably temperature and pressure. An overview of the influence of each category on flammability limits is provided below.

As one of the apparatus parameters, the size of the combustion vessel is an important factor affecting flammability limits. The propagation of flame requires sufficient energy to be transferred from the burned gas to the adjacent unburned gas. Therefore, anything which reduces this available energy will affect the flammability limits. In general, the flammable region widens when the vessel's diameter increases; however, when the diameter increases over 5 cm, the flammable region rarely shows more than a few tenths of a percent increase.[2] There is a minimum diameter below which too much heat will be lost through the wall and the flame propagation will not be initiated; this diameter is called quenching diameter. All vessels designed to measure flammability limits must have diameters larger than quenching diameters so the quenching effect is eliminated.[10]

The location of the igniter or the direction of flame propagation is another important apparatus parameter influencing flammability limits. There are three common directions of flame propagation: upward propagation, horizontal propagation, and downward propagation. When a flammable mixture is ignited, a flame is formed and travels away from the ignition source in all direction. The hot expanded combustion products tend to rise and introduce upward convective currents; therefore, flames propagate more readily upward than downward. If the upward movement of the burned gases is faster than the flame speed, which is usually small at flammability limit concentrations, the flame cannot travel downward. Therefore, a flammability range determined with upward flame propagation tends to be larger than that determined with downward flame propagation. In fact, experiments were carried out with three propagation directions in the same cylindrical vessel for methane-air and ammonia-air mixtures; it was found that the flammable range is the largest (smaller LFL and bigger UFL) with upward propagation followed by horizontal propagation and downward propagation.[2] Therefore, from a safety point of view, it is recommended to determine flammability limits with upward flame propagation (bottom ignition source) so that the most conservative results are obtained.

Ignition source is another factor affecting the determination of flammability limits. If a weak source of ignition is used, some flammable mixtures, particularly those near flammability limits, will not propagate flame. The ignition source should be strong enough to provide sufficient energy to induce flame propagation consistently, but it should not be so strong that spurious indications of propagation are observed.[10] It is

recommended that the amount of energy is in the range of 10 J to 20 J[11-12] so that the most conservative flammability limits are obtained and the reproducibility of experiments is maintained.[13]

The choice of criterion for flammability is an important consideration in the determination of flammability limits. In general, there are two common criteria: i) flame propagation (or flame detachment) by visual observation (or thermal detection), and ii) pressure rise after ignition by pressure measurement. Examples of the use of flame propagation criterion can be found in the U.S. Bureau of Mines method,[2] ASTM E-681 method,[1] the German standard DIN 51649-1,[14] and the European standard EN 1839(T).[11] The choice of the pressure rise criterion is more ambiguous in which there are two pressure rise thresholds. American standards such as ASTM E 918[15] and ASTM E 2079[16] recommend 7% pressure increase, whereas European standards such as EN 1839 (B)[11] require a pressure rise of 5%. The pressure rise criterion may not be applicable to gases with small pressure increases after ignition; for example, some refrigerants have a pressure rise of only 2% even when a flammable mixture is ignited.[17] Studies have been carried out to compare flammability limits determined by the two criteria, flame propagation and pressure rise.[4, 10] For example, Schröder and Molnarne[4] found that LFLs measured by the pressure rise method are generally higher than those measured by the flame propagation criterion; they attributed this to the lesser sensitivity of the pressure threshold criterion versus the flame propagation criterion. For gases which are difficult to ignite, flammability limits obtained by the two criteria tend to differ more.[4] It is necessary that users of flammability limits understand the applicability of each

criterion to their practical conditions. In the prevention of fire and explosion, flammability limits determined by either criterion are useful. However, in the situation where the prevention of flame spreading in a flowing flammable gas mixture is concerned, the flame propagation criterion is the correct choice. Thus, for flammable materials classification purpose as described in the international standard ISO 10156 No. 4.2,[18] it is recommended to apply the flame propagation criterion.

A number of methods have been developed and used to determine flammability limits of gases and vapors. These methods usually employ different apparatus designs and flammability criteria. There is no universal standard method for flammability limit measurement. In fact, the attempt to standardize flammability limit determination method has achieved little success. It is critical that the researcher and user of flammability limits understand the parameters affecting the limits and the user's particular application to design and chose the right method and flammability data. In light of the above discussion on the influence of apparatus parameters and flammability criteria on flammability limit, it is recommended that:

- The size of the test vessel should be large enough to simulate free flame propagation conditions and to minimize the combustion heat loss through the vessel wall. The diameter of the vessel must be larger than quenching diameters.
- If a cylindrical test vessel is used, the igniter should be installed at the bottom of the vessel so the most conservative flammability limits are obtained.

- The amount of ignition energy should be in the range of 10 J to 20 J to obtain conservative flammability limits and maintain the reproducibility of experiments.
- The flame propagation criterion should be used if the prevention of flame spreading in a flowing flammable gas mixture is concerned. For flammable materials classification purpose, it is also recommended to apply the flame propagation criterion.

Our experimental method to determine flammability limits satisfies all the above recommendations and will be described in detail in Section 3.

The influence of the physical condition of the gas mixture, especially the initial temperature and pressure, has received a great interest in the literature because it directly relates to the actual application of flammability limits. Flammable gases and vapors are handled in various operation conditions including atmospheric condition (e.g., storage tanks), or non-atmospheric temperature and pressure conditions (e.g., a reactor). It is critical that the right flammability limits are used for the actual application to achieve the best prevention of fire and explosion. The following discussion as well as the majority of this dissertation will focus on the effect of the physical condition, particularly the initial pressure, on flammability limits.

The effect of temperature on flammability limits has been studied extensively in the literature.[2-3] In general, the flammability region widens (UFL increases and LFL decreases) when the initial temperature of the gas mixture increases. This is understandable since the enthalpy of the initial mixture increases if the initial

temperature increases. To propagate flame, heat from the burned mixture is transferred to the adjacent unburned mixture so that its temperature is raised to the point where combustion reaction happens. If the initial temperature of the unburned mixture increases, less heat is required to raise its temperature; thus it will burn more readily resulting in a wider flammability region. The opposite happens when the initial temperature of gas mixture decreases. Many studies have been carried out with different gases and vapors at initial temperatures ranging from very low (less than zero degree Celsius) to very high (hundreds of degree Celsius). It was found that the LFLs and UFLs of most gases vary linearly with changes in the initial temperature.[2-3, 19-22] For example, the LFLs and UFLs of the alkanes (paraffin hydrocarbons) depend linearly on the initial temperature as described very well by the modified Burgess-Wheeler Law below[3]:

$$LFL_t = LFL_{25} - \frac{0.75}{\Delta H_c}(t - 25) \qquad [1.2]$$

$$UFL_t = UFL_{25} + \frac{0.75}{\Delta H_c}(t - 25) \qquad [1.3]$$

where LFL_t and UFL_t are the LFL and UFL at the initial temperature t (degree Celsius), LFL_{25} and UFL_{25} are the LFL and UFL at 25ºC, and ΔH_c is the heat of combustion (kcal/mol). For unsaturated hydrocarbons (e.g., ethylene, acetylene), and other gases, the flammability limits also vary linearly with the temperature, but the modified Burgress-Wheeler Law shows less accuracy in the prediction of the dependence of their flammability limits on temperature.[2-3, 19-22]

The influence of pressure on flammability limits is neither simple nor uniform but is specific for each gas. Unlike temperature, an increase in the initial pressure does not always widen the flammability range. For some gases, a mixture which is flammable at atmospheric pressure may not be able to propagate flame at a higher pressure. In these cases, the flammability range narrows with an initial increase of pressure to a point where it is the narrowest, then the flammability range widens again with further increases in pressure.[2-3] Such behavior is observed for several gases such as hydrogen or carbon monoxide.[2] In addition, flammability limits do not always vary linearly with pressure as observed with temperature.[19, 21-23] It has been found that combustion reaction mechanism plays an important role in the influence of pressure on flammability limits,[24-26] which explains the specific effect of pressure for each gas. While the influence of elevated pressure (higher than 1.0 atm) on flammability limits has been studied extensively in the literature,[2-3, 19, 21-23] the effect of low pressures (less than 1 atm) is much less investigated. Therefore, to enhance our understanding about the influence of pressure on flammability limits, and to better prevent fire and explosion at low pressure conditions (e.g., vacuum distillation, vacuum furnace), it is necessary to study the effect of low pressures on flammability limits, which is the focus of this study.

To end the discussion on flammability limits, it is worth noting the difference between "normal flame" which associates with flammability limits and "cool flame" which is attributed to the gas phase oxidation at low temperature where the peroxy oxidation chemistry occurs in a fuel rich region above the UFL.[27] Cool flame has a typical blue-green color, a smaller cross section and propagates a shorter distance than a

normal flame as observed by various researchers.[27-29] If a series of sparks[28] (or hot-wire [29]) was used as the ignition source, the gas mixture was heated locally (near the igniter) before it ignited. This would lead to the low temperature oxidation mechanism where peroxy oxidation chemistry occurs, and result in the cool flame formation and propagation. In this study, an exploding fuse wire ignition source similar to that outlined in ASTM E 918 – 83 was used to obtain flammability limits associated with the "normal flame" and avoid the "cool flame" formation.

1.2. Hydrogen flammability

Hydrogen is produced and used in various industrial processes ranging from the oil and gas industry to food manufacturing.[30] Hydrogen is also increasingly explored as a promising alternative to traditional fossil fuels primarily due to its environmental benefits. Except for some levels of NO_x, the combustion of hydrogen emits no toxic substances and pollutants such as CO, CO_2, SO_x or soot.[31-32] In addition, hydrogen energy is regarded as renewable and abundant since hydrogen can be produced from water. The amount of hydrogen generated worldwide is estimated in the magnitude of million tons a year and worth billions of U.S. dollars annually.[30] Table 1 provides an example of the commodity production and shipment of hydrogen in the U.S. in 2003 and 2004. The data was collected and compiled by the U.S. Department of Commerce for major industrial gases including hydrogen.[33] It can be seen from Table 1 that the production of hydrogen increases significantly in both quantity (23%) and value of shipments (21%) from 2003 to 2004. Currently the largest amount of hydrogen is used in the syntheses of methanol and ammonia, and in the refining industry for: i) the treatment

of heavy crude oil, ii) the production of reformulated gasoline, and iii) the de-sulfurization of middle distillate diesel fuel.

Table 1: Total primary production of hydrogen in the U.S. in 2003 and 2004[33]
[Quantity in million cubic feet, Value in thousands of dollars]

2003			2004		
Quantity Produced	Quantity shipped	Value of shipments	Quantity Produced	Quantity shipped	Value of shipments
507,624	355,112	695,796	624,548	479,982	844,455

The high volume of hydrogen produced and the increasing presence of hydrogen in the industry require that hazards and risk associated with hydrogen to be carefully assessed and prevented. It is recommended that great precautions should be taken when handling hydrogen whether in its pure state or in mixtures with other chemicals since hydrogen poses a unique risk of fire and explosion. Table 2 lists the physical properties of hydrogen at atmospheric condition (1 atm, 298 K).

Table 2: Physical properties of hydrogen at 1 atm, 298K

Property	Value	Unit
Physical state	Gas	-
Flammability limits[2]	4% – 75%	Volume % fuel in air
Diffusion coefficient in air[34]	0.61	cm^2/s
Auto-ignition temperature[35]	572	^oC
Minimum ignition energy[35]	0.018	mJ
Heat of combustion[36]	285.8	kJ/mol
Maximum burning velocity in air[3]	3.25	m/s
Maximum pressure during combustion[37]	7.8	bara
Deflagration index K_G[37]	550	bar m/s

It can be seen from Table 2 that hydrogen has a wide range of flammability compared to common hydrocarbon fuels such as methane (5 – 15 vol %)[3], propane (2.1 – 9.5 vol %)[3] and gasoline (1.3 – 7.1 vol % for vapor phase).[38] In addition, the minimum ignition energy required to ignite a flammable hydrogen mixture is very small at 0.018 mJ, which is 15 times smaller than that for methane (0.28 mJ).[35] The wide flammability range and the low ignition energy suggest that the probability of fire or explosion is very high for hydrogen; thus, it is a very hazardous flammable substance. Hydrogen also poses an increased consequence due to its very large deflagration index K_G, which is an indicator of the robustness of explosion: the higher the K_G the more severe the explosion consequence. The K_G of hydrogen is about 10 times the value of methane and 5 times

that of gasoline at atmospheric condition.[34, 39] And since hydrogen has a very large burning velocity, roughly 7 times larger than that of methane or gasoline,[40] a hydrogen flame will be more likely to accelerate and transition to a detonation whose consequence is extremely severe with the over pressure up to 40 times the initial pressure.[3] Hydrogen also has a higher tendency to leak compared to other chemicals due to its small molecular size, low viscosity and low molecular weight. A hydrogen flame may be dangerous since it is nearly invisible and emits little infrared heat which makes it difficult to be detected and people may make inadvertent contact with the flame and be injured. In summary, based on its physical properties, hydrogen poses a great hazard and risk of fire and explosion.

Indeed, research into the accidents involving hydrogen shows that 84% of the accidents included fire and/or explosion.[34] The consequences of the accidents were serious with 12% resulting in deaths, 13% leading to serious injuries and 33% resulting in other injuries (out of a base size of 215 accidents).[34] It is worth to note that most of the accidents happened in the chemical sector (39% of accidents) and refining/petrochemical industry (22% of accidents) where hydrogen is largely used or produced.[34] Examples of major hydrogen accidents are the Hindenburg Disaster in 1937[41] which killed 36 people,[41] the Norway ammonia plant hydrogen fire/explosion in 1985 which claimed the lives of 2 people and completely destroyed the facility,[42] and the Fukushima Daiichi Plant hydrogen explosions which decimated the nuclear plant and exacerbated the nuclear disaster after the earthquake/tsunami in Japan in 2011.[43-44]

It is highly recommended that great attention and protection are provided when handling hydrogen. In order to do so, it is essential that the flammability limits of hydrogen and its mixtures are careful studied and understood. Reference to the literature shows that there is limited data on hydrogen flammability limits, whether in its pure state or in mixtures with hydrocarbons, at non-atmospheric conditions. Particularly, when the influence of pressure was studied, there was an apparent tendency to examine the flammability limit at high pressures while sub-atmospheric pressure condition was almost uninvestigated. For example, data reported by Coward and Jones [2] shows that the flammability limits of hydrogen first narrowed when the initial pressure increased to 20 atm, then steadily widened at higher pressures. However, it is unclear how the flammability limits behave at sub-atmospheric pressures. The increasing presence of hydrogen in various laboratory and industrial processes operating at different conditions, including sub-atmospheric pressure condition such as vacuum furnaces, vacuum drying, and vacuum distillation strongly justifies the need to study the flammability limits of hydrogen at reduced pressures.[45] This study, therefore, focuses on measuring and understanding the flammability limits of hydrogen at sub-atmospheric pressures. In addition, the flammability limits of hydrocarbons commonly found in mixtures with hydrogen such as methane, ethane, *n*-butane and ethylene,[46] will also be determined at both atmospheric and sub-atmospheric pressures to facilitate the understanding and prediction of flammability limits of mixtures of hydrogen and hydrocarbons.

1.3. Flame temperature

Besides flammability limits, flame temperature is an important parameter in the study of combustion as well as the risk assessment of fire and explosion. In the study of combustion, the knowledge of flame temperature has been applied extensively in the modeling and calculation of various combustion parameters including burning velocity, flammability limits, and flame characteristics (e.g., geometry, soot formation). For example, the burning velocity has been found to vary proportionally to flame temperature[47-50] since the higher flame temperature promotes dissociation reactions which introduce more free radicals into the flame; thus enhancing the overall combustion reaction rate and increasing the burning velocity, and vice versa.[51-52] Flame temperature is also widely used to predict flammability limits of gas mixtures based on a theoretical threshold flame temperature below which a flame cannot propagate or sustain itself. It has been shown that this method is an effective tool to estimate the flammability region of various fuel mixtures at different operating conditions such as elevated temperature and pressures.[3, 53-55] In the risk assessment of fire and explosion, knowledge of flame temperature is applied to estimate the consequence of various fire scenarios such as flash fire, jet fire, pool fire.[7] The following equation is an example of the calculation of the radiation heat flux from flame temperature:[56]

$$E = \varepsilon\sigma T^4 \qquad [1.4]$$

where E is radiation heat flux (W/cm^2), T is the absolute temperature of the flame (K), ε is the emissivity of the flame, and σ is the Stefan–Boltzmann constant. The radiation heat flux is then used to estimate the thermal impact on humans and structures from a

fire.[56] Flame temperature is also a critical parameter in the design and performance of combustion devices.[57]

Adiabatic flame temperature (AFT) is the flame temperature without heat loss to the surrounding; thus, it is considered the maximum flame temperature.[57] For this reason, AFT is widely used to predict various fire/explosion safety parameters such as flammability of fuel mixtures,[54, 58] limiting oxygen concentration,[55] and potential impacts of fire/explosion for consequence analysis. AFT is also applied in the estimation of the burning velocity in various studies.[47-50] AFT could be calculated based on the law of thermodynamics and chemical equilibrium. There is a number of methods developed to calculate AFT ranging from simple empirical equations/graphs[59-60] to more complex computer codes.[44, 54, 61-62]

In this work, the adiabatic flame temperatures of hydrogen and the hydrocarbons flammability limits of the chemicals were calculated at room temperature and initial pressures ranging from 1.0 atm to 0.1 atm using the CHEMKIN package[62] with thermochemical and transport properties from the database compiled by Kee et al.[63-64] and the reaction mechanism from GRI Mech 3.0[65] and the Combustion Chemistry Center.[66] This computer package has been validated extensively with experimental data[65-66] and used by a great number of researchers to accurately estimate flame temperature and other properties of combustion process.[48-49, 67-68] The calculated flame temperatures of hydrogen and hydrocarbons at the obtained flammability limits will also be used to predict the flammability of mixtures of hydrogen and hydrocarbons at both atmospheric and sub-atmospheric pressures.

1.4. Thesis outline

Following the discussion of the basic concepts of this research – flammability limits, hydrogen properties and flammability, flame temperature – as well as the motivation for the research, section 2 provides the research objectives. Section 3 describes the experimental setup and procedure including the details of the apparatus and the determination of flammability limits used in this research. Section 4 presents the obtained flammability limits of pure hydrogen and hydrocarbons at atmospheric and sub-atmospheric pressures. An analysis of the influence of pressure on the flammability limits of hydrogen and hydrocarbons, and an assessment of the hazards and risks of fire and explosion for these gases under the effect of pressure are also provided in Section 4. Section 5 provides the calculated adiabatic flame temperatures of hydrogen and hydrocarbons at sub-atmospheric pressures. Methods to calculate the temperatures are discussed and compared. The effect of pressure on flame temperature is investigated; the relationship between the flammability limits and adiabatic flame temperatures is analyzed; and finally, based on the adiabatic flame temperatures, the hazards/risks of fire pertaining to hydrogen and the hydrocarbons are discussed. Section 6 presents the experimental results of the flammability limits of binary mixtures of hydrogen and hydrocarbons at sub-atmospheric pressures. The influence of pressure on the flammability limits of the mixtures is analyzed. The effect of hydrogen in the mixtures on the flammability limits is investigated. The applications of Le Chatelier's rule and the CAFT model to predict flammability limits of mixtures of hydrogen with hydrocarbons

at atmospheric and low pressures are verified and compared. Finally, Section 7 concludes the research and provides recommendations for future endeavors in the field.

2. RESEARCH OBJECTIVES

This research has four objectives:

- The first objective is to design and conduct experiments to determine the flammability limits of pure hydrogen and of binary mixtures of hydrogen and light hydrocarbons (methane, ethane, *n*-butane, and ethylene) at room temperature and sub-atmospheric pressures ranging from 1.0 atm to 0.1 atm. This experimental study provides: i) an essential data set on the flammability limits of hydrogen and its mixtures with hydrocarbons at low pressure conditions, and ii) a basis for theoretical analyses.
- The second objective is to investigate the influence of low pressures (equal and smaller than 1.0 atm) on the flammability limits of pure hydrogen and of hydrogen mixtures with hydrocarbons. This, together with the impact of elevated pressures (greater than 1.0 atm) extensively studied in the literature, provides a complete understanding of the complex influence of pressure on the flammability limits of hydrogen and its mixtures with hydrocarbons. For comparison with hydrogen, the impact of sub-atmospheric pressures on the flammability limits of the hydrocarbons (methane, ethane, *n*-butane, and ethylene) is analyzed. For the mixtures, the role of hydrogen in the blended fuel with regard to the flammability limits is studied. Finally, the fire risk/hazard relating to hydrogen at low pressure conditions is evaluated.

- The third objective is to assess the influence of low pressure on the adiabatic flame temperatures at the flammability limits of hydrogen and the hydrocarbons. Different methods to calculate adiabatic flame temperatures are carried out and compared. The relationship between the adiabatic flame temperatures and the flammability limits and are derived. And the consequence of fire relating to hydrogen and the hydrocarbons is discussed based on the adiabatic flame temperatures of the chemicals.
- The fourth objective is to verify the application of Le Chatelier's rule to predict the flammability limits of mixtures of hydrogen and light hydrocarbons at atmospheric and sub-atmospheric pressures. The application of the Calculated Adiabatic Flame Temperature model to the flammability limits of the mixtures is also performed and compared with Le Chatelier's rule.

3. EXPERIMENT SETUP AND PROCEDURE[*]

3.1. Experiment apparatus

The apparatus used in this research for the determination of flammability limits was designed and constructed by Wong[8] according to the recommendations discussed in Section 1.1. Overall, the design of the apparatus is similar to that used by U.S. Bureau of Mines[2] and the European standard EN 1839 (T).[4, 69] Figure 1 illustrates the configuration of the apparatus whose main design features include: the fuel and air loading system, the mixing vessel, the reaction vessel, the sensors, and the ignition source. The following subsections provide details about each of the features.

[*] Part of this section is reprinted with permission from "Upper Flammability Limits of Hydrogen and Light Hydrocarbons in Air at Subatmospheric Pressures" by H. Le, S. Nayak, M. S. Mannan, 2012. *Industrial & Engineering Chemistry Research*, 51(27), 9396-9402. DOI: 10.1021/ie300268x. Copyright 2012 American Chemical Society

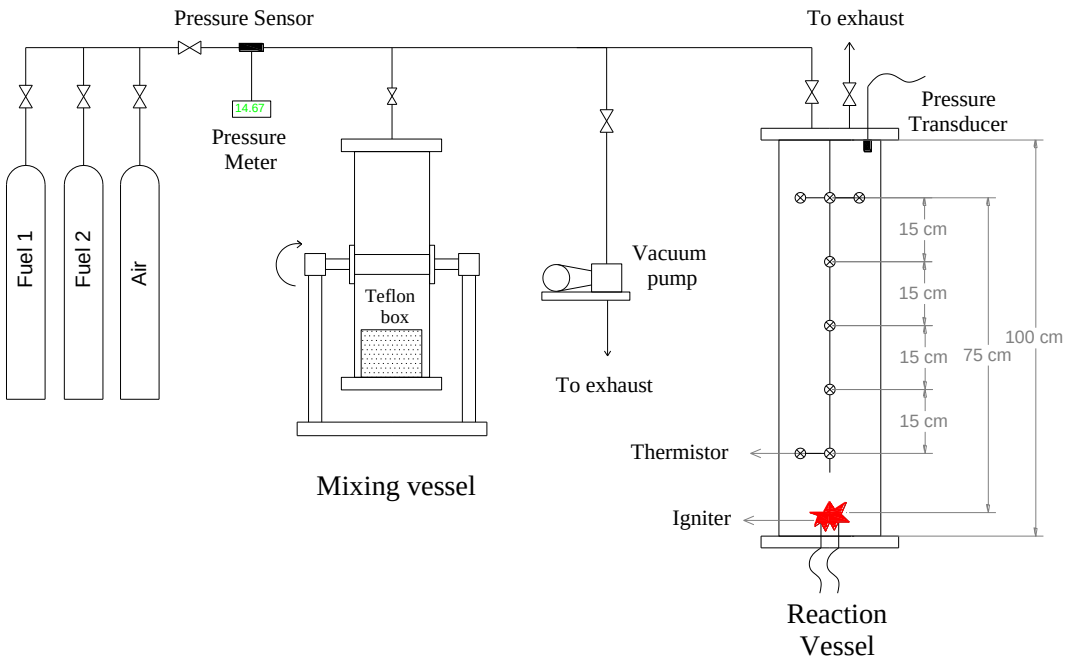

Figure 1: Apparatus configuration

3.1.1. The fuel and air loading system

Ultra high purity fuels (hydrogen, hydrocarbons) and air were used in this research so that highly accurate flammability limits can be obtained. The specifications of the fuels and air are provided in Table 3.

Table 3: Specifications of chemicals used in the experiments*

	H_2	CH_4	C_2H_6	C_4H_{10}	C_2H_4	Air
Purity	99.999%	99.99%	99.995%	99.98%	99.995% (H_2O < 1ppm)	Ultra zero certified

*Supplier: Matheson Tri Gas

The gases (fuel and air) were stored separately in pressurized cylinders located outside of the laboratory for safety purpose. The loading of the gases for experiments was carried out through a gas loading manifold which is illustrated in Figure 2. The gas quantities used in the experiments were determined based on partial pressure basis measured by a pressure transducer (Omega PX603, 0.4% accuracy, 0.04%/F thermal zero and span effect) also installed in the manifold. The loading of each gas was isolated from each other and from other sections of the apparatus by plug valves (Swagelok®). The manifold is connected to a vacuum pump so that it could be evacuated completely between each gas loading step to avoid contamination. The manifold also has connecting lines to the reaction vessel and the mixing vessel. All gas lines are 1/4 in. tubing, 0.028 in. thick and made of stainless steel (Type 316) with Swagelok® compression fittings.

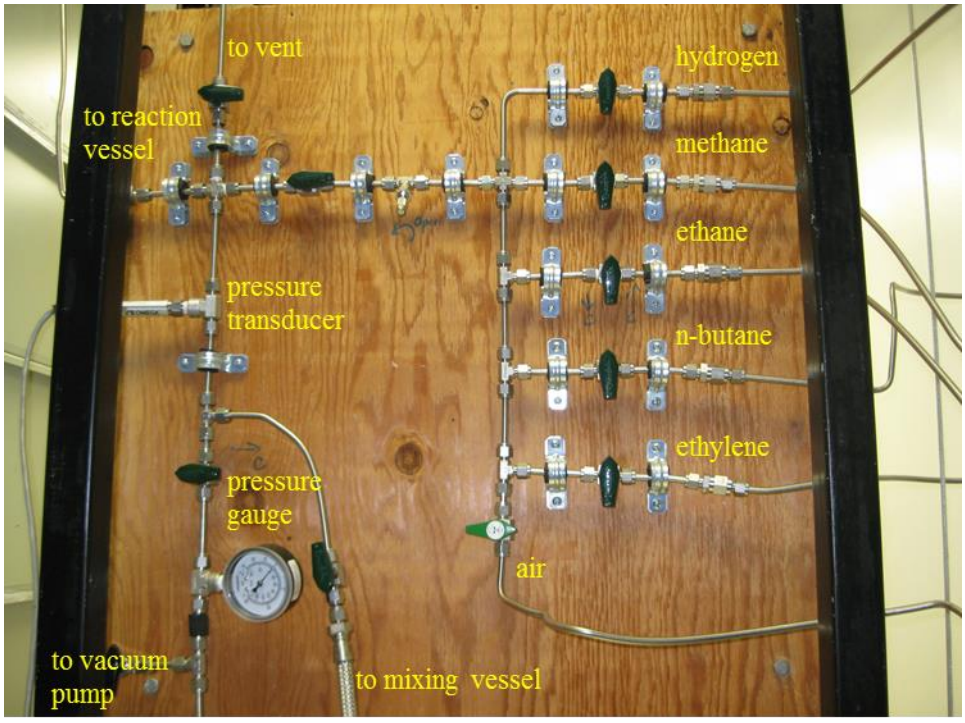

Figure 2: Gas loading manifold

3.1.2. The mixing vessel

The mixing vessel is a stainless steel pipe 29.75 inches long which a 3.88-inch inner diameter with flanges (7/8 inch thick, 8 bolts and Buna-n gaskets) at both ends. The volume of the vessel is 4.9 L. The vessel is connected to the gas loading manifold with a quick connect fitting and a flexible stainless steel hose. The quick connect fitting allows the vessel to be disconnected from the gas loading manifold when it rotates to mix the gases inside. The rotation of the vessel is powered by a DC motor mounted next to the vessel on top of the mixing stand made of 1.25 inch square steel tubing welded together. Figure 3 presents a picture of the mixing vessel and the arrangement of the motor. To facilitate the mixing, a Teflon® cylindrical block with a diameter slightly

smaller than the vessel's inner diameter was placed inside the vessel. When the vessel rotates lengthwise, the Teflon® block glides along the vessel's length creating highly turbulent zones in the front of and behind the moving block, thus allowing fast and complete mixing of the gas components. The design of the mixing vessel and Teflon® block is shown in Figure 4. For each test mixture, the mixing vessel rotated for 5 minutes, approximately 300 inversions. This mixing method was proved by Wong[8] to be able to achieve complete mixing of gases.

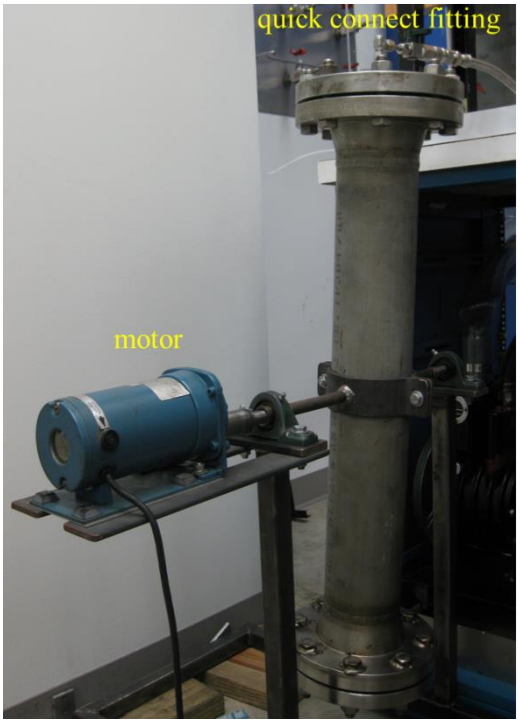

Figure 3: Mixing vessel assembly

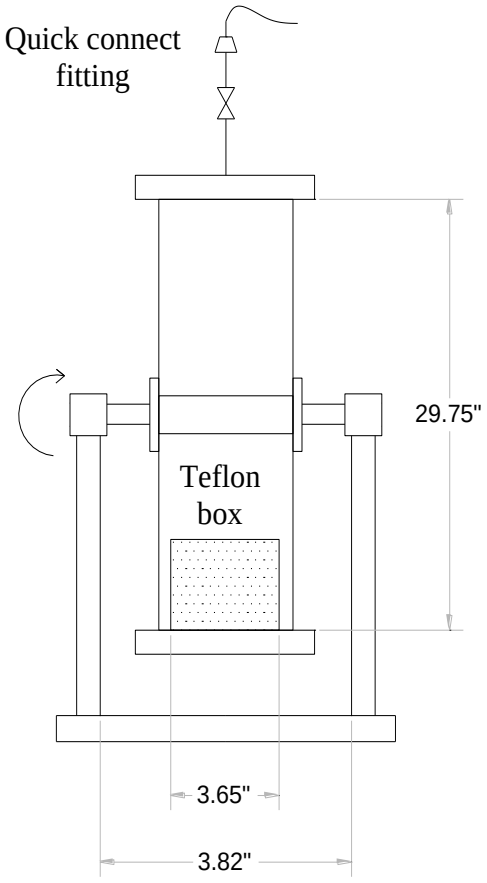

Figure 4: Mixing vessel configuration

3.1.3. The reaction vessel

The design of the reaction vessel is similar to those of the U.S Bureau of Mines[2] and the European standard EN 1839 (T).[11] The reaction vessel is where the combustion reaction takes place, so it must be strong enough to withstand heat and over pressure. A stainless steel pipe schedule 40, 4 inch nominal (11.43 cm outer diameter, 10.22 cm inner diameter) was chosen to be the body of the vessel. The body is 100 cm long and enclosed at both ends by welded flanges with a 7.78-cm outer diameter, 1.778 cm thick,

and 12 threaded bolt holes. The vessel was tested hydrostatically to 82.74 bar (1200 psi) which is much higher than possible overpressures from combustion reactions happening at atmospheric or sub-atmospheric pressures. The total volume of the vessel is 8.2 L. Thus the vessel is large enough to simulate free flame propagation and minimize combustion heat loss through the wall so that quenching effect will not take place, but not too large for the ease of operation and cleaning. Installed on top of the vessel is a dynamic pressure transducer (Omega DPX 101) to measure the pressure inside the vessel, and a pressure relief valve (Swagelok®, R4 Proportional Relief Valve) set at 500 psig for further protection from overpressure. Inside the vessel contains 8 thermistors (thermal sensors) located at the center used for flame propagation detection. Details about the sensors are presented later in section 3.1.4. At the center bottom of the vessel is a port for the insertion of an igniter whose details are discussed in section 3.1.5. Figure 5 illustrates the overall configuration of the reaction vessel including the relative locations of the pressure transducer, the thermistors, and the igniter; and Figure 6 shows a picture of the outside of the vessel.

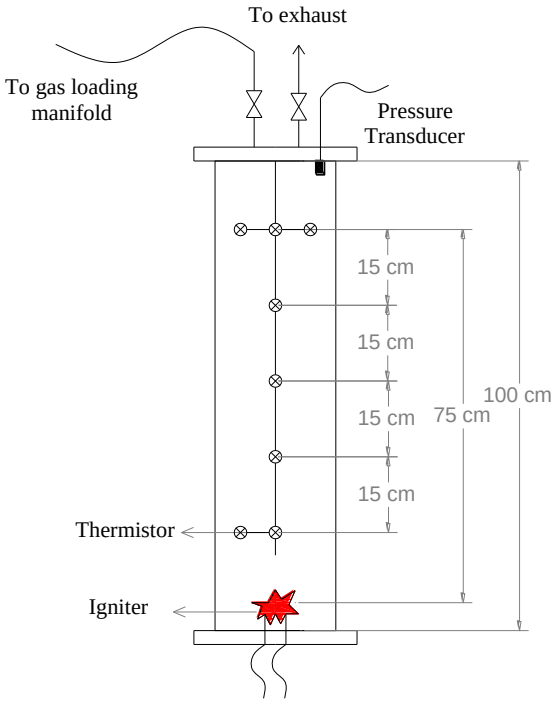

Figure 5: Reaction vessel configuration

Figure 6: Reaction vessel (outside)

3.1.4. The sensors

As recommended in Section 1.1, flame propagation was chosen as the flammability criterion in this research, and thermal sensors were used to detect the flame detachment inside the reaction vessel. There are a total of 8 thermistors used in the experimental apparatus; all of them were installed in the reaction vessel. The arrangement of the thermistors is illustrated in Figure 5. The type of thermal sensor used was a thermistor, which is an electronic component that exhibits a change in resistance with a change in its body temperature. Specifically, the sensor used is a negative temperature coefficient (NTC) thermistor, which has an inverse proportion between resistance and temperature. In this research, the NTC bead-type thermistor (Fastip Thermoprobe® thermistor) was selected among other thermistors since it offers high reliability and high stability, fast response times, and operation at high temperature (higher than 150ºC). A bead type thermistor consists of a small diameter glass coated thermistor bead hermitically sealed at the tip of a shock resistant glass rod; see Figure 7 for a detailed illustration and dimension. The hermetic seal provides roughly ten-fold increase in the stability of the thermistor. The bead is exposed as much as possible at the tip of the glass rod to provide the fastest response times. The units are rugged and unaffected by severe environmental exposure including high temperature combustion. For more specifications and future reference, NTC thermistor code FP07DB104N supplied by GE Thermometrics Inc. having 0.10 second response time in still air, 100 kΩ with 25% variance, laboratory tested to be 107 kΩ was used. A picture of a NTC

bead-type thermistor code FP07DB104N is shown in Figure 8. A signal from each thermistor was received and measured by a Wheatstone bridge circuit,[70] illustrated in Figure 9, used to measure an unknown electrical resistance (of the thermistor) by balancing two legs of a bridge circuit, one leg of which includes the unknown component.

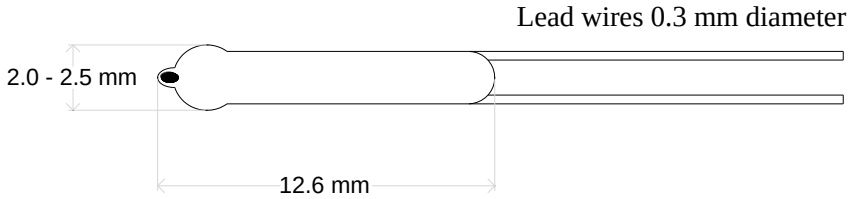

Figure 7: Thermistor configuration and dimension

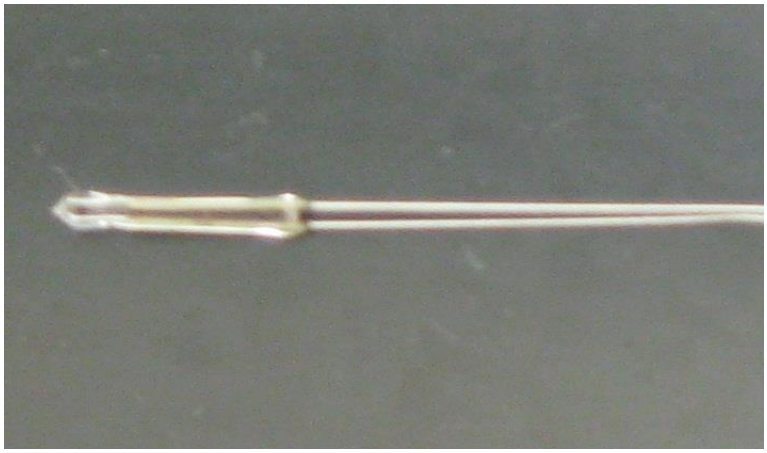

Figure 8: NTC thermistor code FP07DB104N supplied by GE Thermometrics Inc.

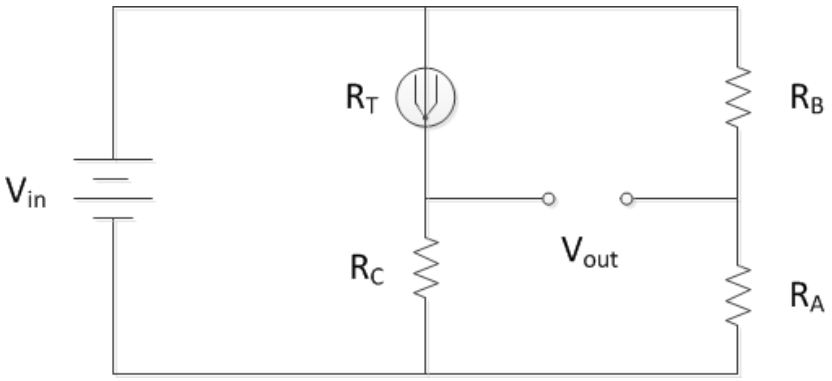

Figure 9: Wheatstone bridge circuit

To measure the pressure inside the reaction vessel, a pressure transducer was installed on the top plate of the vessel. The pressure transducer was an Omega DPX 101 piezoelectric quartz transducer which has a range of 0 to 250 psi pressure rise, with 0 to 5 V nominal output signal, 1μs rise time, 1% amplitude linearity, and a temperature effect of 0.03%/ ºF.

Signals from the pressure transducer and eight thermistors were obtained by a Keithley data acquisition card (Keithley® KPCI-3102, 225 signals per second at 0.05% accuracy) installed in a desktop computer, and the experimental process was controlled by a LabView® (National Instruments, version 7.1) program.

3.1.5. The ignition source

There are two most commonly used ignition sources in the literature: exploding fuse wire and high voltage sparks (electric arcs).[2, 4] As mentioned in Section 1.1, an ignition source must provide sufficient energy to induce flame propagation consistently. Between the exploding fuse wire and high voltage sparks, exploding fuse wire has

greater power density, thus can provide more useful energy to ignite a gas mixture.[10] Exploding fuse wire ignition source was also proven to have a consistent pattern of power and energy input; therefore it is more reliable in maintaining the repeatability of experiments.[71] This research used exploding fuse wire ignition source capable of providing 10 J of energy consistently for each experiment. The amount of 10 J is recommended so that the most conservative flammability limits can be obtained, as discussed in Section 1.1.[11-12] The ignition source consists of: i/ a 10 mm piece of AWG 40 tinned copper wire, ii/ a 500 VA isolation transformer (Hammond 171 E) at 115 V, iii/ a zero-crossing solid state relay (Omega, model # SSRL240DC100). An illustration of the ignition source system circuitry is shown in Figure 10.

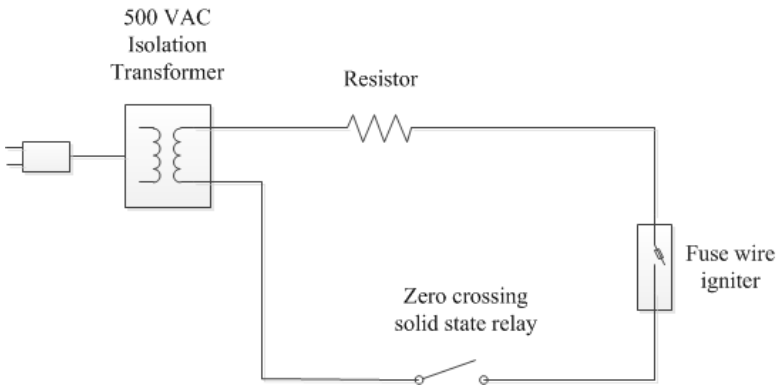

Figure 10: Ignition source system circuitry

The igniter consists of: i) a wire holder section which is a pair of copper rods with a spring loaded wire grip section mounted on a cylindrical platform made of non-conducting polymer, and ii) a vessel seal section which is a Cajon® VCO O-ring face seal connector gland and screw cap; the center of the gland is fitted with a stainless steel

plug where the circuitry wiring is routed through and the plug is filled with epoxy to provide a hermitic seal. The wire holder section was connected to the vessel seal section with a short ¼ in stainless steel tube which also contains the circuit wiring. The igniter was inserted to the reaction vessel for each experiment through a port consisting of a tapped 1 in NPT hole with the VCO face seal male connector (with Viton® O-ring) at the bottom center of the vessel. Figure 11 provides a picture of the igniter assembly.

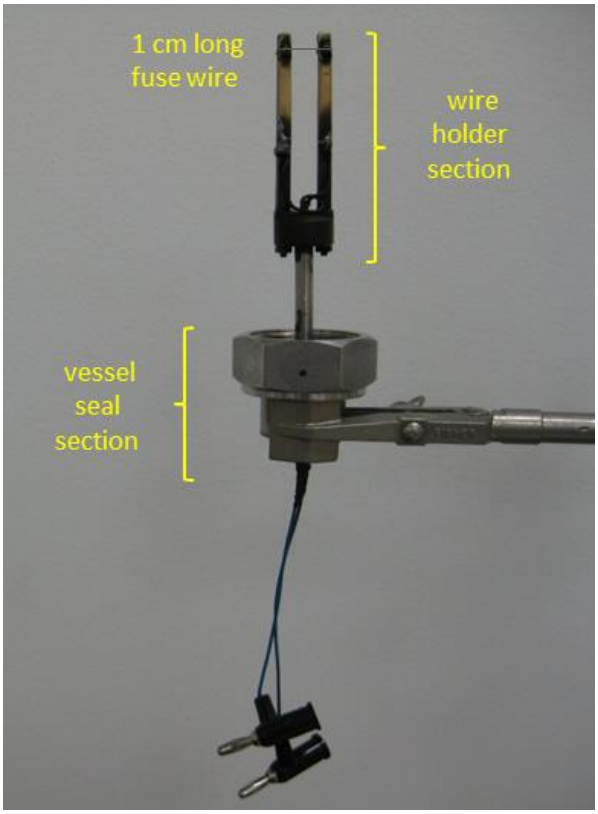

Figure 11: Igniter assembly

3.2. Experiment procedure

Before each experiment, the whole system (gas loading manifold, mixing vessel and reaction vessel) was vacuumed to remove remaining gases. Figure 12 shows the configuration (open/closed) of each valve on the gas loading manifold for this step. Fuel(s) and air were loaded into the mixing vessel one by one through the gas loading manifold. Note that fuel(s) should be introduced first into the mixing vessel. Figure 13 illustrates an example of the configuration of the valves on the manifold for the loading of hydrogen. Similar configurations were set for the loading of other fuels or air except the valve at the gas feed line was opened depending on which gas was to be added into the mixing vessel. Between each loading, the loading manifold must be evacuated to avoid contamination. Figure 14 shows the configuration of the valves for this manifold vacuuming step. The quantities of the fuel(s) and air were determined based on their partial pressures displayed by the pressure meter. The loading of fuels and gas was operated manually; and great care was taken to make sure that the desired fuel concentration was achieved.

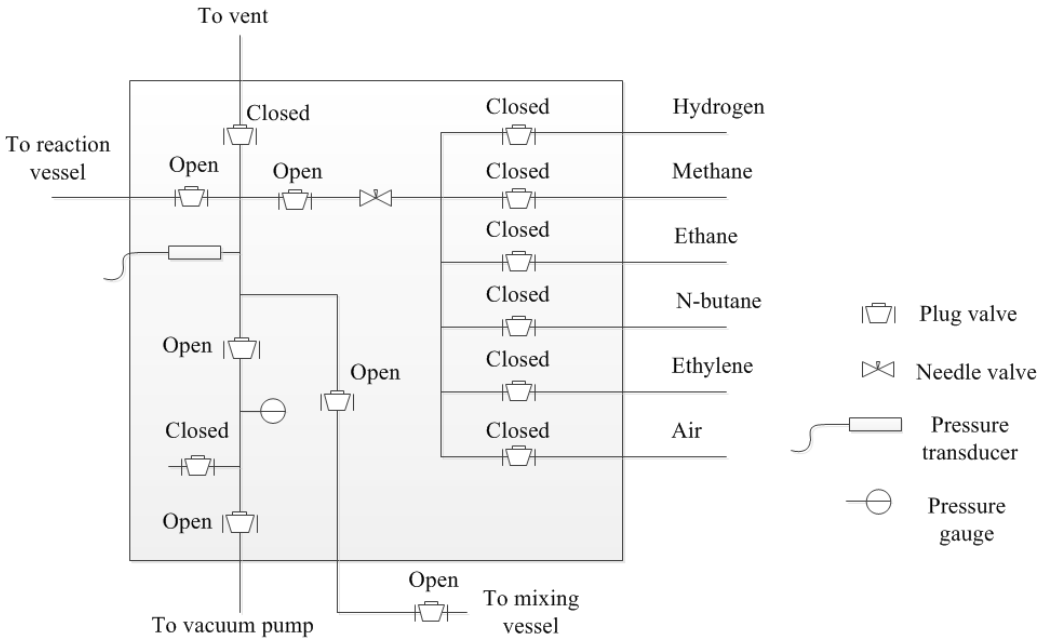

Figure 12: Gas loading manifold: valve configuration for whole system evacuation

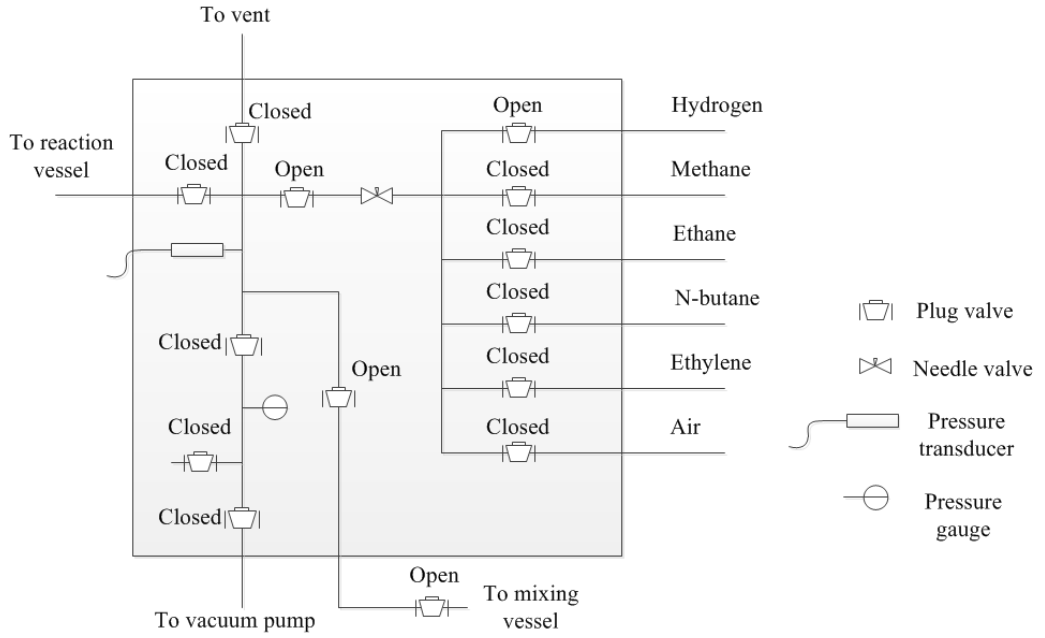

Figure 13: Gas loading manifold: valve configuration for hydrogen loading

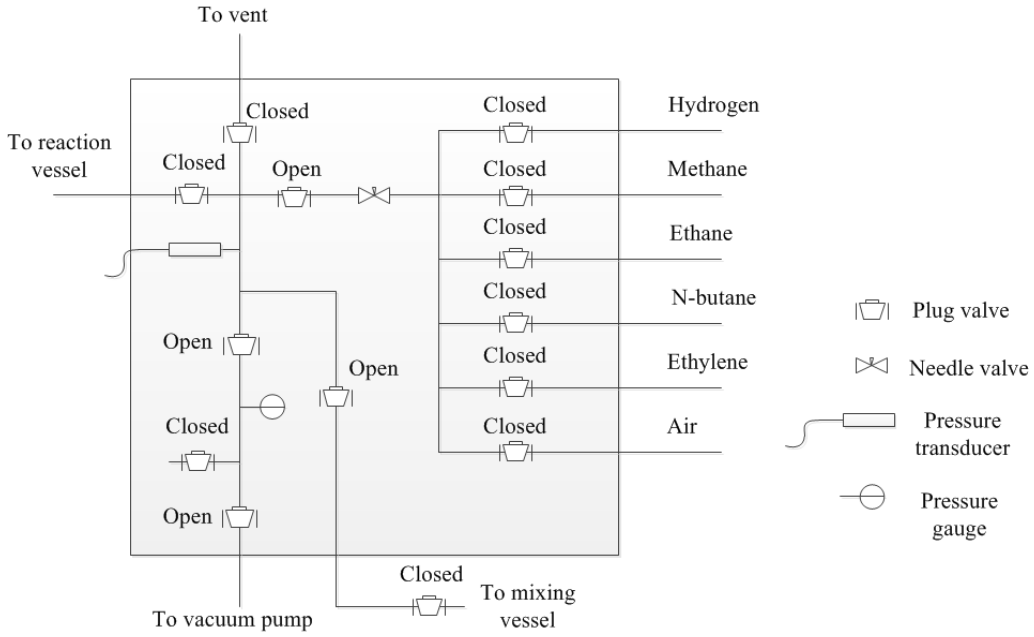

Figure 14: Gas loading manifold: valve configuration for the vacuuming between loading of gases

After the desired gas mixture was loaded into the mixing vessel, the plug valve on the top of the mixing vessel was closed and the vessel was disconnected from the gas loading manifold through the quick connect fitting. The DC motor was activated to rotate the mixing vessel. The vessel was rotated for 5 minutes at 60 inversions a minute to thoroughly mix the gases in the vessel. After the rotation, the mixing vessel was reconnected to the gas loading manifold. The valve on the top of the mixing vessel was still closed. The gas loading manifold was vacuumed to remove air in the system and get ready for the loading of the gas mixture from the mixing vessel to the reaction vessel; refer to Figure 14 for valve configuration in this step.

The gas mixture was then permitted to flow into the reaction vessel; Figure 15 illustrates the valve configuration for this step. When the initial pressure of the reaction vessel reached the desired value, the valve connecting the vessel to the manifold was closed to stop the gas mixture from entering the vessel. Then the gas mixture inside the reaction vessel was allowed to achieve the thermal equilibrium and become quiescent for 5 minutes. After that the igniter was activated by turning the switch on the ignition source. The combustion (or lack of) was detected by the thermistors inside the reaction vessel. Signals from the thermistors were displayed on the computer screen for the determination of the flammability of the mixture which will be discussed in detail in Section 3.3.

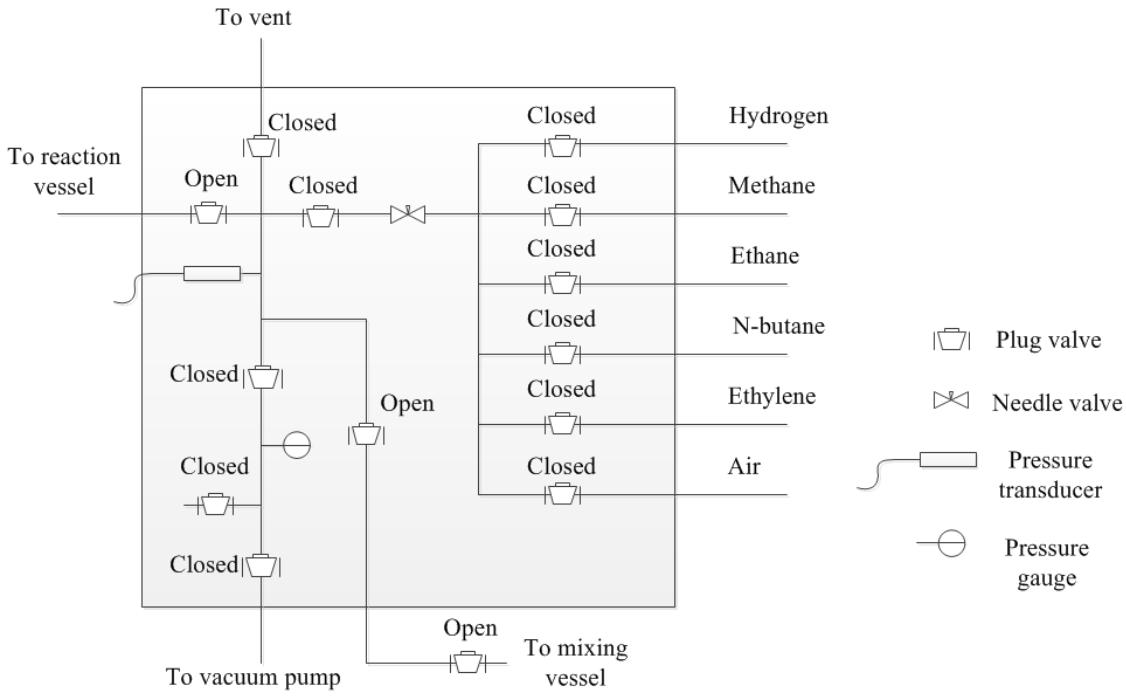

Figure 15: Gas loading manifold: valve configuration for the flowing of test mixture to reaction vessel

After the ignition and combustion, the igniter was removed from the reaction vessel, the combustion products were purged with nitrogen from the vessel by a tube connecting the bottom of the vessel to the fume hood. The igniter was cleaned and fitted with a new fuse wire; then it was inserted into the reaction vessel to get ready for the next experiment.

3.3. Flammability limit determination

The determination of flammability limits depends on three factors: flammability limit definition, flammability criterion and flammability limit selection method from experiments. Each of the factors is discussed in the following sub-sections.

3.3.1. Flammability limit definition

A flammable gas burns over a limited range of concentration bounded by the upper flammability limit (UFL) and lower flammability limit (LFL). UFL is the maximum concentration of fuel in air, and LFL is the minimum concentration of fuel in air capable of propagating flame when ignited. Based on this definition, the flammability criterion and flammability selection method were decided.

3.3.2. Flammability criterion

There are two common flammability criteria used in the literature: i) flame propagation (or flame detachment) by visual observation (or thermal detection), and ii) pressure rise after ignition by pressure measurement. The application of each criterion is described in Section 1.1. Considering the recommendation in Section 1.1 based on the

pros and cons of each criterion, this research used the flame propagation criterion for the determination of flammability limit. Specifically, the flame propagation of mixture in the reaction vessel was detected by the thermistors installed along the length of the vessel (see Figure 5). A mixture is considered flammable if it could propagation flame from the igniter to the top thermistor(s) which is 75 cm away vertically. Such a flame propagation behavior is classified as "continuous flame propagation" indicating the ability of the fuel mixture to sustain combustion indefinitely.[8] Signals from the thermistors were displayed on the computer screen for the determination of the flammability of the test mixture. Figure 16 provides an example of thermistor signals of a flammable mixture, and Figure 17 is an example of a non-flammable mixture whose flame could not reach the top thermistor(s).

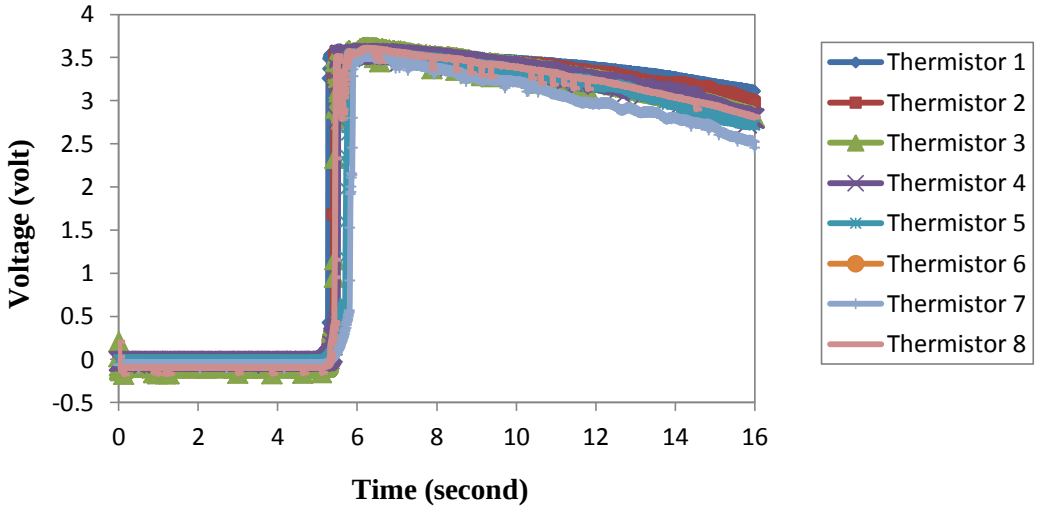

Figure 16: Thermistor output signals of a flammable mixture

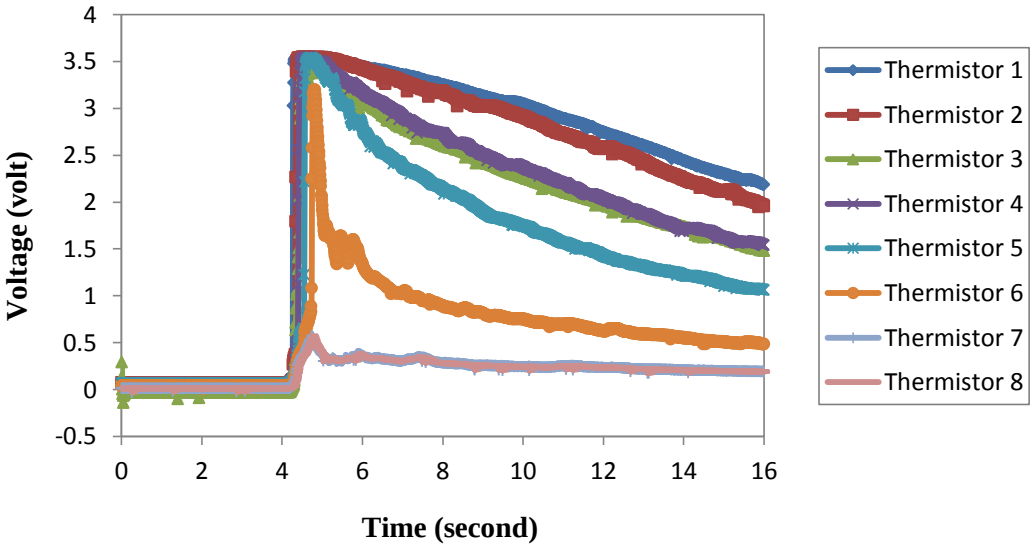

Figure 17: Thermistor output signals of a non-flammable mixture

3.3.3. Flammability limit selection method

Basically, the flammability limit selection method involves guidelines for the experimental step size (step change made in the fuel concentration between experiments), the number of repetitive experiments, and the number of continuous flame propagations (see Figure 16) specified in the flammability limit criterion (section 3.3.2). In this research, a small step size of 0.05 mol% was chosen since such small step sizes are recommended by the European standard and others researchers.[4, 8-9] To ensure the accuracy of the experiment and compensate for the small step size, the number of experiments must be high enough for each mixture concentration.[8] In addition, multiple experiments at the same fuel composition may yield different flame propagation results since flame propagation for a mixture near the flammability limit displays probabilistic behavior due to random errors in composition, fluctuation in mixture conditions and

variation in ignition energy. Therefore, in this research we chose the number of repetitive experiments of 10 times at each concentration.[8] Note that the European standard [4, 9] recommends 3 times; the ASTM standard[1] and the U.S. Bureau of Mines,[2-3] do not provide recommendations on the number of repetitive experiments.

Two fuel compositions within one step size of each other that demonstrate continuous flame propagation over 50% at one composition and less than 50% at the other would indicate that the flammability limit is in between those compositions. In this research, if one composition has 0% propagation occurrences, the next composition with over 50% propagation occurrences is selected as the flammability limit. In all other cases, the mixture composition demonstrating equal or less than 50% propagation occurrences is chosen as the flammability limit. Table 4 presents an example of how the flammability limits were selected.

Table 4: Example of flammability limit selection

	Fuel concentration (mol%)	Number of continuous flame propagation out of 10 experiments	Percent of continuous flame propagation (%)
Hydrogen	3.90	0	0
	3.95*	3	30
	4.00	7	70
Methane	5.30	0	0
	5.35*	6	60

*Concentration selected as flammability limit

4. FLAMMABILITY LIMITS OF PURE HYDROGEN AND LIGHT HYDROCARBONS AT SUB-ATMOSPHERIC PRESSURES[*]

4.1. Lower flammability limits

4.1.1. Lower flammability limit of hydrogen

The obtained LFL of hydrogen in air at atmospheric pressure is presented in Table 5. For comparison, the LFLs of hydrogen at the same condition determined by various researchers with different experimental setups and criteria are also provided in Table 5. Overall, the obtained LFL is similar to the LFLs generated by apparatuses and criteria consistent with the U.S. Bureau of Mines method.[2, 72] The LFLs determined by European methods DIN 51649-1 and EN 1839 (T) are smaller, thus more conservative, since European methods use different measurement criteria and flammability limit definition. According to DIN 51649 and EN 1839 (T), a mixture is considered flammable if upon ignition the resulting flame can propagate a distance of at least 10 cm from the electrodes,[4] whereas our method and the methods similar to that of the U.S. Bureau of Mines require a flame propagation distance of at least 75 cm to be considered

[*] Part of this section is reprinted with permission from "Upper Flammability Limits of Hydrogen and Light Hydrocarbons in Air at Subatmospheric Pressures" by H. Le, S. Nayak, M. S. Mannan, 2012. *Industrial & Engineering Chemistry Research*, 51(27), 9396-9402. DOI: 10.1021/ie300268x. Copyright 2012 American Chemical Society

[*] Part of this section is reprinted with permission from "Lower Flammability Limits of Hydrogen and Light Hydrocarbons in Air at Subatmospheric Pressures" by H. Le, Y.Liu, M. S. Mannan, 2013. *Industrial & Engineering Chemistry Research*, 52(3), 1372-1378. DOI: 10.1021/ie302504h. Copyright 2013 American Chemical Society

flammable. DIN 51649 and EN 1839 (T) define the flammability limit as the concentration where the last non-propagation point occurs, while our method marks the flammability as the concentration which lies between the non-propagation and propagation points.

Table 5: Lower flammability limit of hydrogen in air at atmospheric pressure and room temperature

Fuel	This work (mol %)	Previous work (mol %)	Apparatus type	FL Criteria
H_2	3.95	4.15	Vertical glass tube (ID 7.5 cm, L 150 cm) [2]	visual
		3.90	Vertical stainless steel tube (ID 5.08 cm, L 100 cm) [72]	thermal
		3.75	Glass flask V= 5 dm^3 ASTM E681-01 [4]	visual
		3.80	Vertical glass tube (ID 6 cm, L 30 cm) DIN 51649-1[4]	visual
		3.60	Glass cylinder (ID 8cm, L 30 cm) EN 1839 (T) [4]	visual

When the initial pressure decreased below 1.0 atm, the obtained LFL of hydrogen is shown in Figure 18. Initially, the LFL decreased when the pressure was reduced from 1.0 atm to 0.3 atm; then the LFL began to increase with the further decrease of pressure. The decrease of the LFL implies an increased risk of fire/explosion of hydrogen at sub-atmospheric pressures since a non-flammable mixture at atmospheric pressure becomes flammable at lower pressures. The significance of the increased risk requires a detailed risk analysis and depends on the particular process condition and operation; in this case, the risk may not increase much since the LFL decrease is small.

For example, the maximum change of the LFL under the influence of pressure is within 0.2 mol%, which indicates a small impact of pressure on the LFL of hydrogen. Studies with the LFL of hydrogen at high pressures (larger than 1.0 atm) also show small effect of pressure; for example, Bone et al. showed that the LFL was almost unaffected when the pressure increased from 1.0 atm to 125 atm.[73]

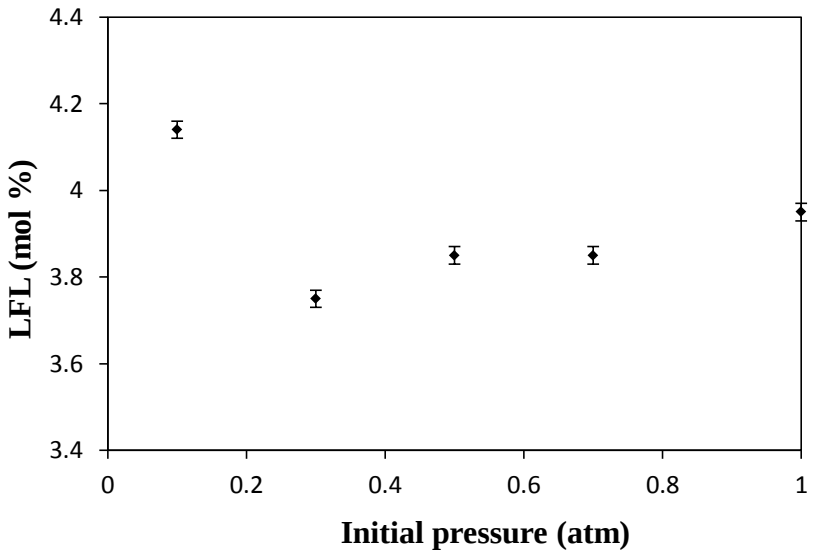

Figure 18: Lower flammability limit of hydrogen at sub-atmospheric pressures and room temperature

With respect to the behavior of the LFL under the influence of pressure, previous studies with the LFL of hydrogen at initial pressures larger than 1.0 atm showed that initially the LFL increased when the initial pressure increased, then the LFL decreased with the further increase of pressure. [23, 73-74] This behavior of the hydrogen LFL at high pressures couples with that at sub-atmospheric pressures described in this study can be

explained by the combustion reaction mechanism of hydrogen in air. In general, combustion reaction involves chain reactions consisting of multiple reaction steps and free radicals.[51] Although the combustion of hydrogen in air involves only two elements, H and O, the chemical reaction mechanism is quite complex with more than 50 elementary reactions including the initiation, chain propagating, chain branching and chain termination steps.[75] When the initial pressure increases, the amount of reactants and the concentration of free radicals increase. This higher density of reactants and free radicals leads to an increase of the overall reaction rate which results in the promotion of the combustion process and the widening of the flammability range. Thus, we found a decrease of the hydrogen LFL when the initial pressure was raised from 0.1 atm to 0.3 atm (Figure 18). However, when the pressure was further increased, the hydrogen LFL started to increase which may be explained by the involvement of a three-body reaction:[51, 75]

$$H + O_2 + M \rightarrow HO_2 + M \qquad (4.1)$$

M can be any third molecule which acts as a stabilizer for the combination of H and O_2. The relatively unstable hydroperoxy molecule HO_2 diffuses to the wall and is consumed there by the following reactions:

$$HO_2 \rightarrow \tfrac{1}{2} H_2 + O_2 \qquad (4.2)$$

$$HO_2 \rightarrow \tfrac{1}{2} H_2O + \tfrac{3}{4} O_2 \qquad (4.3)$$

Reaction (4.1) was considered the dominant chain termination reaction for hydrogen at the flammability limit concentration.[19, 76] As the initial pressure increases,

the probability of the three-body collision reaction (4.1) increases which results in a decreased rate of overall reaction as well as the narrowing of the flammability range.[76] Therefore, we found that the LFL increased when the initial pressure was raised from 0.3 atm (Figure 18) in this study to as much as 15 atm in other studies.[23, 73-74] However, when the initial pressure increases further, HO_2 can react with H_2 to form H_2O_2, H and OH radicals which enhance the chain-branching step;[51, 77] thus increasing the overall reaction rate and widening the flammability zone. Therefore, the LFL started to decrease when the initial pressure was further raised to higher than 15 atm.[23, 73-74]

4.1.2. Lower flammability limits of light hydrocarbons

The obtained LFLs of the hydrocarbons in air at sub-atmospheric pressures and room temperature are presented in Figure 19 and Figure 20 for the alkanes and ethylene, respectively.

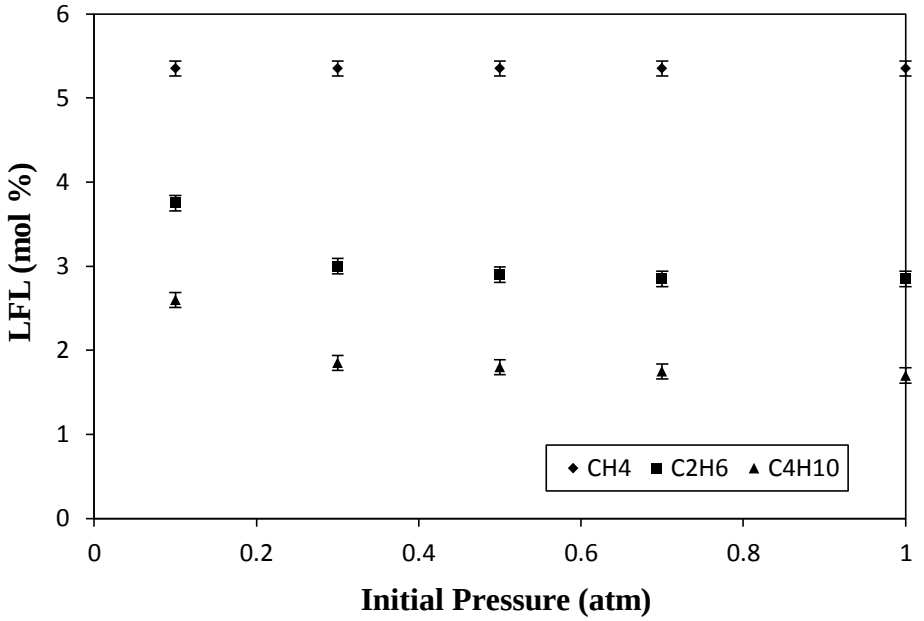

Figure 19: Lower flammability limits of methane, ethane, *n*-butane at sub-atmospheric pressures and room temperature

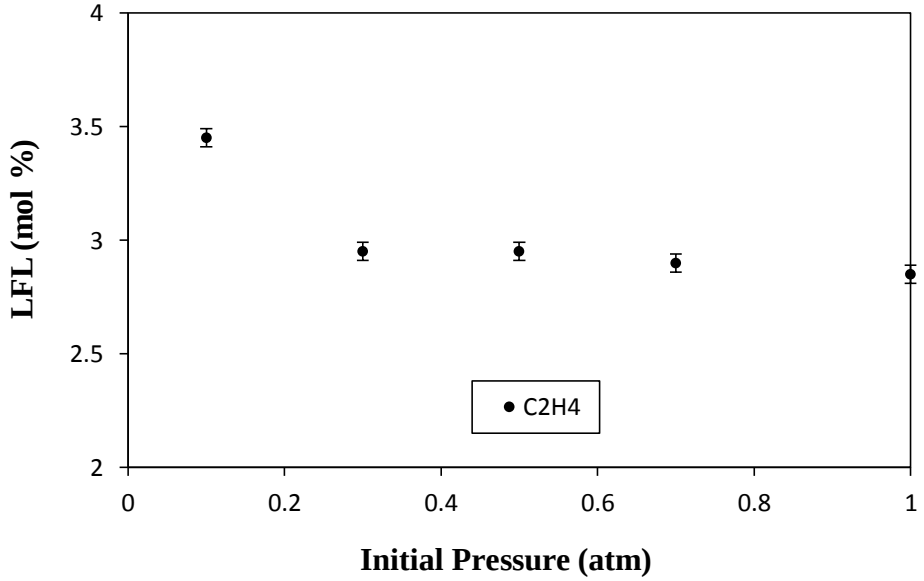

Figure 20: Lower flammability limit of ethylene at sub-atmospheric pressures and room temperature

Overall, the LFLs of the hydrocarbons increased when the initial pressure decreased from 1.0 atm to 0.1 atm; except for methane whose LFL did not change with pressure. This means that the above hydrocarbons pose a lower risk of fire and explosion when the initial pressure decreases. This behavior also implies that the influence of the three body reaction (4.1) on the reaction mechanism of the hydrocarbons at LFL concentration is not as strong as it does for hydrogen. Similar to what is observed with hydrogen LFL, the LFLs of the hydrocarbons change very little with pressure. For example, when the pressure was reduced from 1.0 atm to 0.3 atm, the LFLs of all the hydrocarbons increased within just 0.15 mol%. The LFLs only show appreciable increases when the pressure was further reduced to 0.1 atm; however, the magnitude of increase is still small, within 0.9 mol%. In other words, pressure has little impact on the LFL of the hydrocarbons.

For the alkanes, as shown in Figure 19, *n*-butane has the lowest LFL at all initial pressures followed by ethane and methane; in other words, the higher the carbon number (or molecular weight) the lower the LFL. This molecular weight-LFL relation of alkane hydrocarbons was also observed in other studies at atmospheric pressure.[3]

4.2. Upper flammability limits

4.2.1. Upper flammability limit of hydrogen

At atmospheric pressure, the obtained UFL of hydrogen was similar to those generated with apparatuses whose configurations were consistent to that developed by

the U.S. Bureau of Mines and the apparatuses established by European standards DIN 51649 and EN 1839 (T) (Table 6). The higher values of the upper flammability limits reported by the European methods DIN 51649 and EN 1839 (T) can be explained by their measurement criteria and flammability limit definition as discussed in Section 4.1.1: DIN 51649-1 and EN 1839 (T) require a smaller flame propagation distance (10 cm) for a gas mixture to be considered flammable, and define the flammability limit as the concentration where the mixture just stops to propagate flame.[4, 78]

Table 6: Upper flammability limit of hydrogen in air at atmospheric pressure and room temperature

Fuel	This work (mol %)	Previous work (mol %)	Apparatus type	FL Criteria
H_2	75.73	75.00	Vertical glass tube (ID 7.5 cm, L 150 cm) [2]	visual
		74.70	Vertical stainless steel tube (ID 5 cm, L 100 cm) [72]	thermal
		75.10	Glass flask V= 5 dm^3 ASTM E681-01 [4]	visual
		75.80	Vertical glass tube (ID 6 cm, L 30 cm) DIN 51649-1[4]	visual
		76.60	Glass cylinder (ID 8cm, L 30 cm) EN 1839 (T) [4]	visual

Together with the lower flammability limit (LFL), the flammable region of hydrogen in air at atmospheric pressure and room temperature is 3.95 – 75.73 mol%, which is much wider compared to those of common hydrocarbons, such as methane (5.35 – 15.40 mol%) or ethylene (2.85 – 30.61 mol%).[78] This confirms previous studies

about the high hazard and risk of fire/explosion of hydrogen at atmospheric condition as discussed in Section 1.1.[34, 39]

When the initial pressure decreased below atmospheric pressure, the UFL of hydrogen initially increased as illustrated by Figure 21; the UFL continued increasing until the initial pressure was lowered to about 0.3 atm where the UFL started to decrease. The UFL was still larger than the value at atmospheric pressure until the initial pressure was reduced to 0.1 atm (Figure 21). This means for hydrogen, a mixture that cannot propagate flame at atmospheric pressure, may be able to do so at sub-atmospheric pressures; in other words, hydrogen poses a higher risk of ignition at reduced pressures. However, the risk is not significantly higher since the increase was relatively small which is 2.1 mol%.

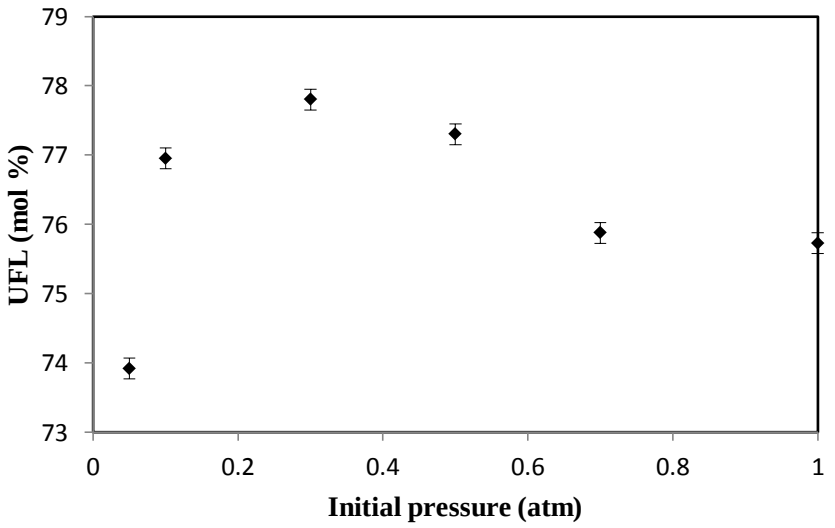

Figure 21: Upper flammability limit of hydrogen at sub-atmospheric pressures and room temperature

Combined with the obtained LFL (Section 4.1.1), the flammable region of hydrogen is presented in Figure 22. The flammability region expands when the initial pressure increases from 0.1 atm to 0.3 atm. The region is the widest at 0.3 atm where the UFL increases by 2.1 mol % and the LFL decreases by 0.2 mol %. The flammable region starts to narrow when the pressure increases from 0.3 atm to 1.0 atm. Studies with hydrogen flammability limit at high pressures showed that the flammable region continued to narrow when the initial pressure increased from 1.0 atm to as much as 10 atm; then the region started to widen again with the further increase of pressure.[19, 23, 73-74, 79] The narrowing of the flammable region of hydrogen at pressures from 0.3 atm to 1.0 atm in our studies and up to 10 atm in others can be explained by hydrogen combustion reaction mechanism where the influence of the 3-body chain termination reaction: $H + O_2 + M \rightarrow HO_2 + M$ becomes stronger when the pressure increases, which results in a decreased rate of the overall combustion reaction thus the narrowing of the flammable region.[19, 51, 75-76, 78] Details about the effect of the 3-body reaction on hydrogen flammable region can be found in Section 4.1.1.

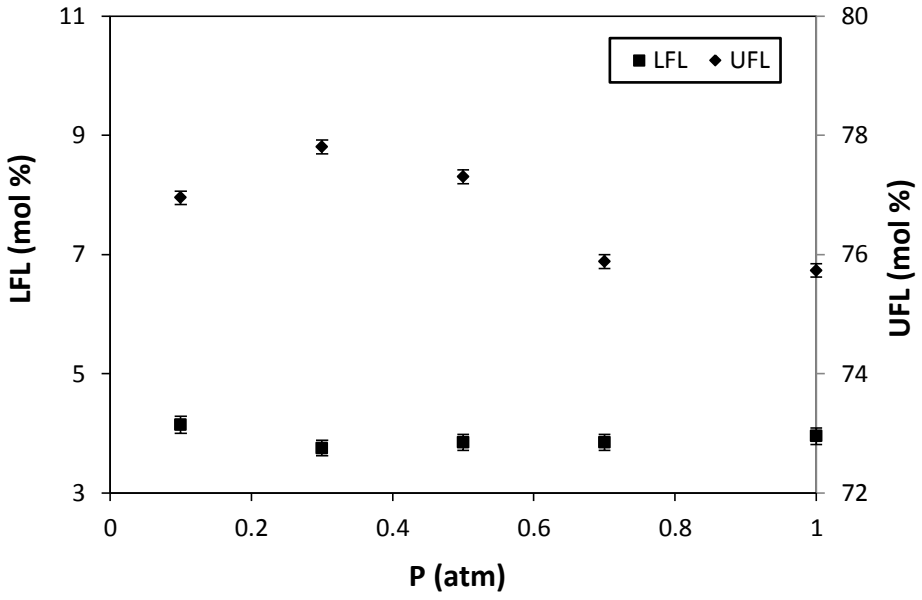

Figure 22: Flammability region of hydrogen at sub-atmospheric pressures and room temperature

Under the influence of pressure, the UFL changes more than the LFL. For example, when the initial pressure decreased from 1.0 atm to 0.1 atm, the maximum change of the LFL was 0.2 mol % which is much smaller than that of the UFL which was 2.1 mol %. Studies on the flammability limit of hydrogen at high pressures (greater than 1.0 atm) also showed the greater impact of pressure on the UFL.[73-74] Terres and Plenz observed that the change of the UFL was 2 times larger than that of the LFL when the pressure increased from 1.0 atm to 10 atm.[74] Experimental results by Bone et al. showed that the LFL was almost unaffected when the pressure increased from 1.0 atm to 125 atm, while the UFL progressively increased with pressure greater than 10 atm.[73] Shebeko et al. also found a negligible influence of pressure on the LFL at high pressure range from 2.0 MPa to 4.0 MPa.[19] The reason for the higher impact of pressure on the

UFL is still unclear; it is assumed that the reaction mechanism of hydrogen at the UFL is more complicated than that at the LFL since more fuel is involved, thus UFL is more susceptible to the influence of pressure than the LFL.

4.2.2. Upper flammability limits of light hydrocarbons

The UFLs of the hydrocarbons in air at sub-atmospheric pressures are shown in Figure 23 and Figure 24. In contrast to the behavior of the UFL of hydrogen, the UFL of methane, ethane, *n*-butane and ethylene decreased when the initial pressure decreased below atmospheric pressure. This means the above hydrocarbons pose a lower risk of fire and explosion when the initial pressure is reduced. In addition, the decrease of the UFLs of the hydrocarbons is larger than the increase of the UFL of hydrogen at reduced pressures which is shown in Figure 25; this suggests that these hydrocarbons present a greater reduction of fire risk compared with the increasing risk of hydrogen at sub-atmospheric pressures.

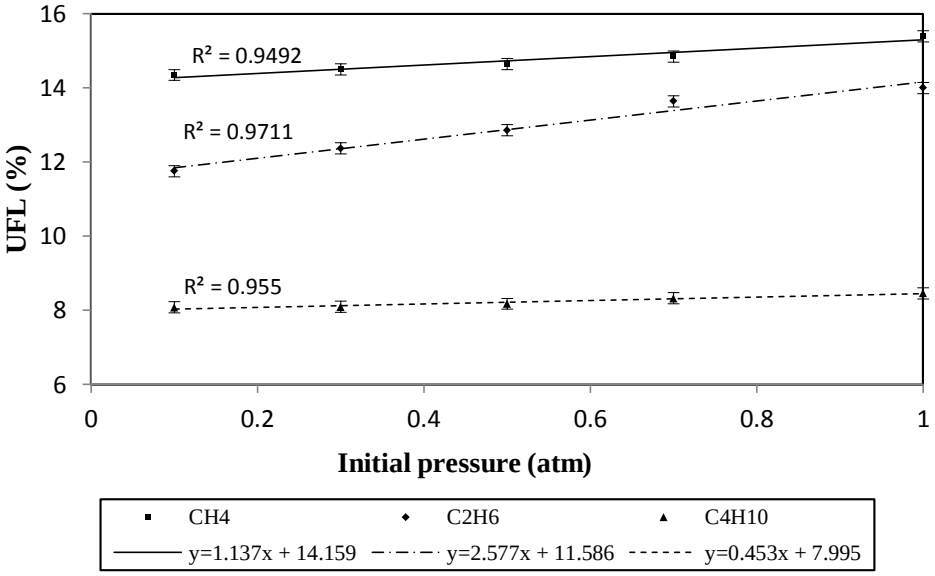

Figure 23: Upper flammability limits of methane, ethane and *n*-butane at sub-atmospheric pressures and room temperature

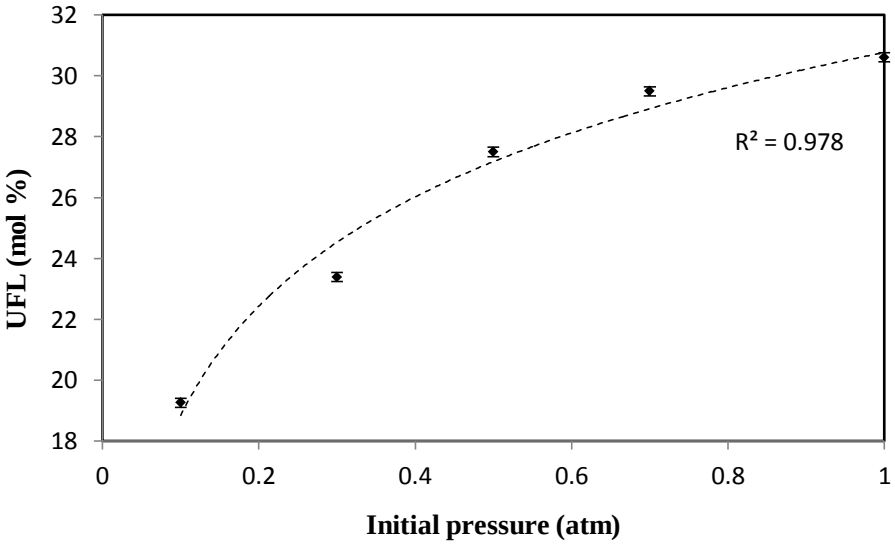

Figure 24: Upper flammability limit of ethylene at sub-atmospheric pressures and room temperature

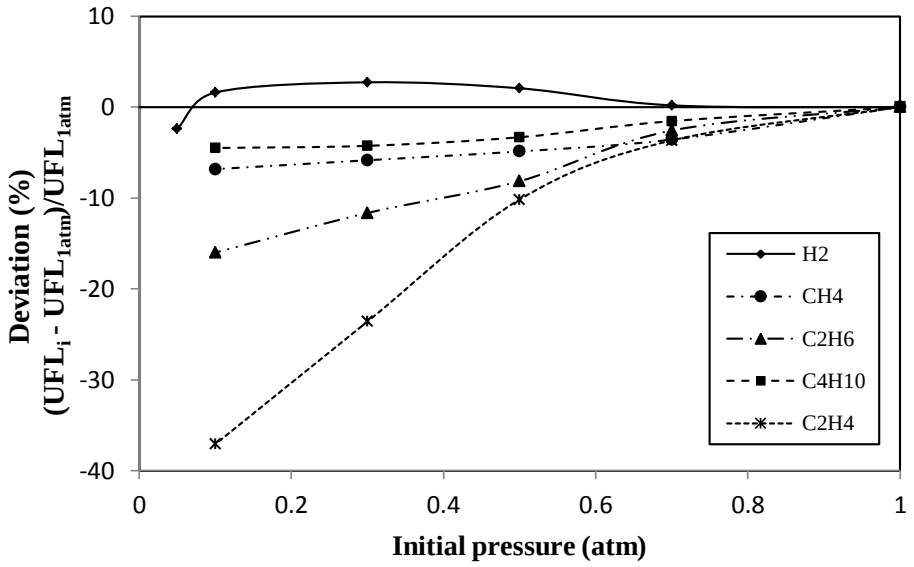

Figure 25: Percentage deviation of UFLs of hydrogen, methane, *n*-butane and ethylene at sub-atmospheric pressures from the UFLs at 1.0 atm

The decrease in the UFLs of the hydrocarbons at reduced pressures is expected since previous studies also showed similar results. For example, Mason and Wheeler [80] observed a decrease in the UFL of methane at pressures less than 1.0 atm in a tube (2 cm diameter, 50 cm length) with downward propagation. Another study with methane in a tube (5 cm diameter, 50 cm length) with upward, horizontal and downward propagation also found a decrease in the UFL at low pressures.[2] In other words, the UFLs of the hydrocarbons increased with pressure; similar behavior was observed at elevated pressures in published studies.[2, 73, 81] There was not a decrease in the UFLs of the hydrocarbons when the pressure increased as observed with the UFL of hydrogen. One possible reason is that the dominant termination reactions of the hydrocarbons at UFL concentration are two-body reactions instead of the three-body reaction (4.1) as

concluded by Law and Egolfopoulos.[76] Two-body termination reactions exert no advantage over the chain branching reactions when the pressure increases as opposed to the three-body reaction (4.1) which becomes more efficient with increasing pressures (as observed with hydrogen).

For the alkanes, while the LFLs did not show any clear pattern of change with pressure (Section 4.1.2), the UFLs decreased linearly with pressure (Figure 23). At initial pressures higher than atmospheric pressure, the UFLs of these lower alkanes increased also linearly as observed by some previous studies.[73, 81] For example, an experimental study with methane using a spherical vessel (7.6 cm diameter) with central ignition at room temperature and initial pressures higher than 1.0 atm found that the UFL of methane increased rapidly and linearly with pressure.[73] Van den Schoor and Verplaetsen [81] experimented on ethane and *n*-butane with a spherical vessel (20 cm diameter) and central ignition discovered that the UFLs of these hydrocarbons increased linearly when the initial pressure was raised up to 20 bar (for ethane) and 10 bar (for *n*-butane). Another study[2] with ethane and *n*-butane at elevated initial pressures using closed tube (20 cm diameter, 40 cm length) also showed a linear increase of the UFLs. It was found in this study that that when the UFLs of the lower alkanes were expressed as equivalence ratios (the actual fuel/air ratio divided by the stoichiometric fuel/air ratio), the higher the carbon number in the series of the observed alkanes, the higher the UFLs as shown in Figure 26. A similar observation was also made by Van den Schoor and Verplaetsen[81] at elevated pressures (up to 55 bar) and elevated temperature (200 ^{o}C).

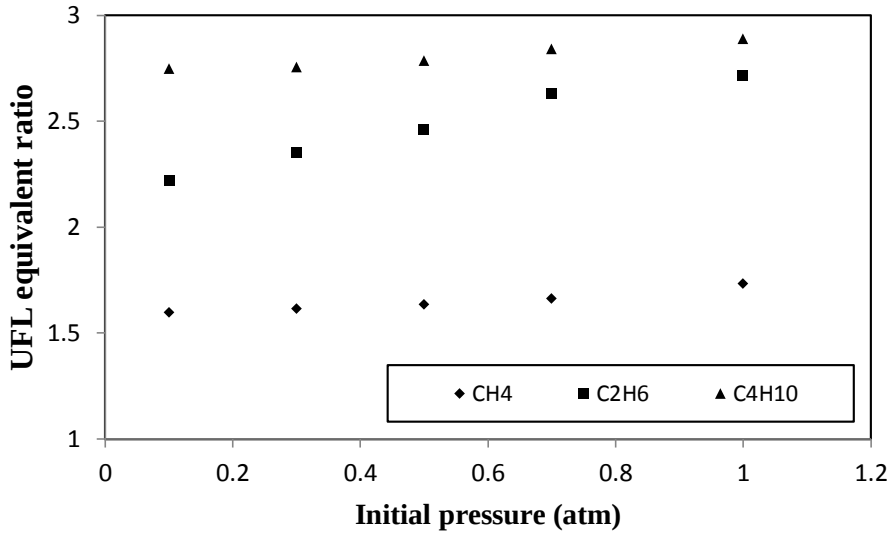

Figure 26: UFLs of methane, ethane and *n*-butane expressed as equivalence ratios at sub-atmospheric pressures and room temperature

The decrease in the UFL of ethylene at sub-atmospheric pressures had two distinct features. First, the decrease was not linear, but more similar to a logarithmic decrease with pressure (Figure 24). The increase in the UFL of ethylene at elevated pressures was also non-linear as determined by Craven & Foster[82] and Hashiguchi et al.[83] Second, the change of the UFL at reduced pressures is much greater for ethylene compared to those of hydrogen and the lower alkanes, particularly when the initial pressure was reduced below 0.5 atm (Figure 25). Larger degrees of change in the UFL of ethylene at elevated pressures compared to those of the lower alkanes was also observed by several researchers,[23, 81-83] for example, Berl and Werner showed that the UFL of ethylene in air increased sharply from 16% at 1.0 atm to 68% at 90 atm.[23] The pronounced effect of pressure on the UFL of ethylene can be attributed to the sensitivity

of the combustion reaction mechanism of ethylene to changes in the pressure. It was shown by Carriere et al.[25] that for fuel-rich mixtures the dominant ethylene consumption pathway and the route to the final oxidation products of the combustion of ethylene changed greatly with pressure. For example, when the pressure increased, the destruction of ethylene changed from abstraction reaction forming C_2H_3 to addition reaction forming $C_2H_{5;}$ consequently, the pathway to the formation of final products via oxygenated species appeared and became more important.[25] Some reactions on this pathway were pressure dependent in a way that an increase in pressure further enhanced the rates of these reactions[25] which promoted the flame propagation and resulted in a large increase of the UFL as observed in this and previous studies.[23, 81-83]

Compared to the changes of the LFLs (Section 4.1.2), the changes of the UFLs are much larger. For example, when the pressure was reduced from 1.0 atm to 0.3 atm, the LFLs of all the hydrocarbons increased within 0.15 mol% while the UFLs decreased much more drastically, for example 11.35 mol% in ethylene case. When the pressure was further reduced to 0.1 atm, the LFLs start to show appreciable increases, but the magnitude of the changes is still smaller than that of the UFLs at the same pressure. Previous studies with flammability limit of the hydrocarbons at pressures higher than 1.0 atm also showed greater impact of pressure on UFL than LFL.[2-3, 53, 81-82, 84-85] For instance, Kondo et al. experimented with methane in a spherical apparatus and observed that the LFL was almost unchanged when the pressure increased from 1 atm to 25 atm while the UFL increased rapidly with pressure.[85] The same observation was made by Hertzberg et al. for methane LFL at pressures from 1 atm to 3 atm.[84] For ethane and *n*-

butane, data from the Bureau of Mines[2] shows greater change in the UFLs compared to the LFLs in the pressure range from 1 atm to 6 atm. For ethylene, it was observed by Craven et al.[82] that the LFL was almost constant while the UFL increased drastically when the pressure increased from 1 atm to 10 atm. Similar to the discussion in the previous section with the LFL of hydrogen, the reason for the greater impact of pressure on the UFLs of the hydrocarbons may be the more complex reaction mechanisms at UFL concentration which are more sensitive to the influence of pressure.

It is worth to note that for ethylene, while the UFL changed significantly with pressure, for example, the UFL decreased by 7.2 mol% when the pressure decreased from 1.0 atm to 0.3 atm, the LFL did not show any appreciable change even at the pressure as low as 0.3 atm (Figure 20). It was explained earlier based on the reaction modeling work of Carriere et al.[25] that the great impact of pressure on the UFL of ethylene was due to the high sensitivity of the combustion reaction mechanism of fuel-rich mixtures of ethylene to changes in the pressure. Therefore, based on the observed behavior of the LFL, it is assumed that pressure does not have much impact on the reaction mechanism of lean mixtures of ethylene; however, to confirm this assumption, a similar research to that of Carriere et al.[25] on the reaction mechanism modeling for lean mixtures of ethylene should be done.

Combined with the obtained LFLs, the flammability regions of the hydrocarbons are shown in Figure 27, Figure 28, Figure 29, and Figure 30 for methane, ethane, *n*-butane and ethylene respectively. It can be seen that the flammable regions of the hydrocarbons narrow when the pressure decreases below 1.0 atm. When the pressure

increases above 1.0 atm, the regions expand as observed in various studies.[2, 82, 85-86] Therefore, it can be concluded that the flammability regions of the hydrocarbons become smaller when the initial pressure decreases, both at low and high pressure regimes. From an inherent safety point of view, considering the flammable region, it is recommended that the operating pressure is reduced as much as possible to decrease the risk of fire and explosion of the hydrocarbons.

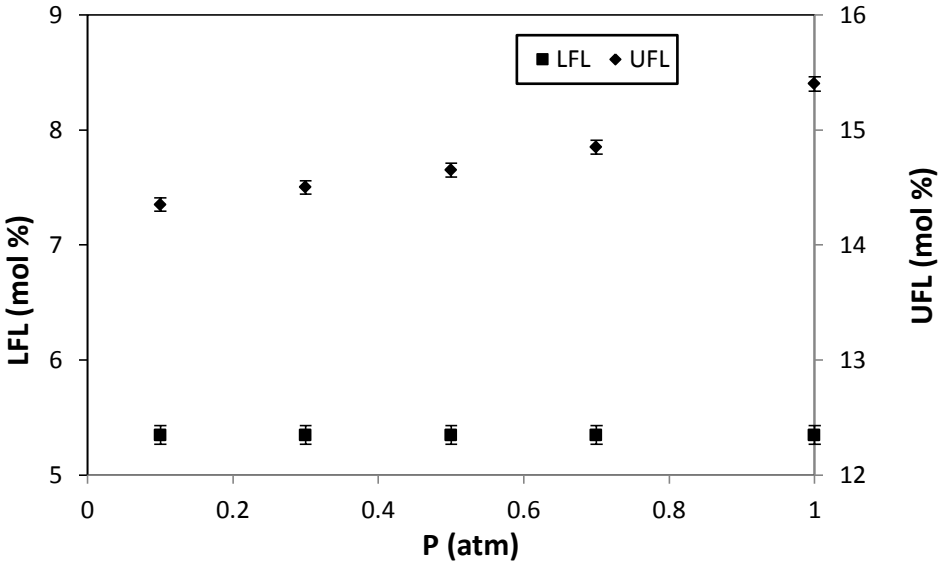

Figure 27: Flammability region of methane at sub-atmospheric pressures and room temperature

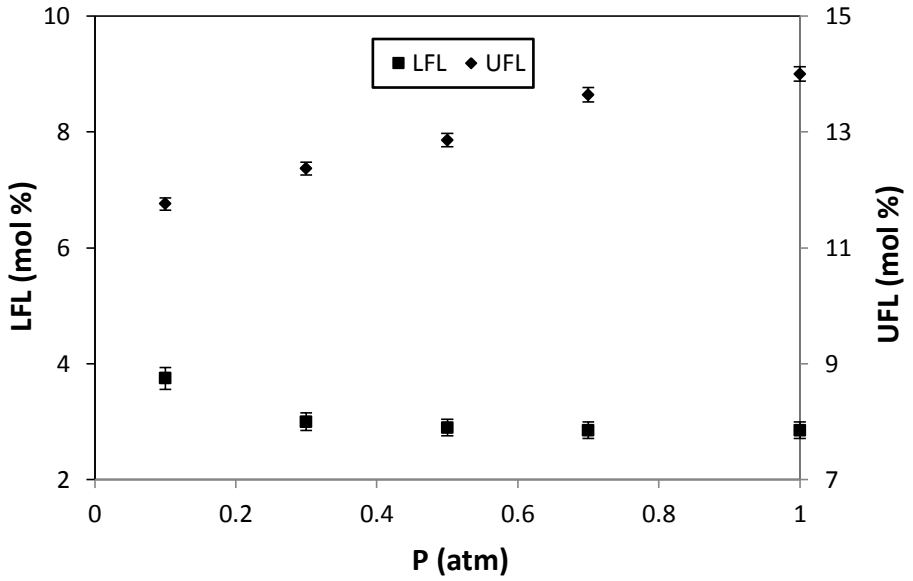

Figure 28: Flammability region of ethane at sub-atmospheric pressures and room temperature

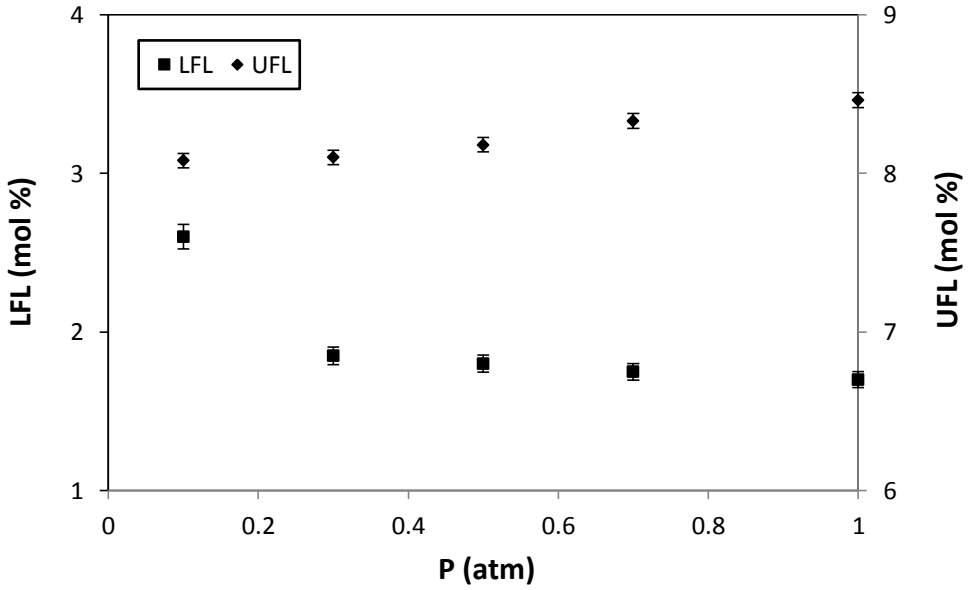

Figure 29: Flammability region of *n*-Butane at sub-atmospheric pressures and room temperature

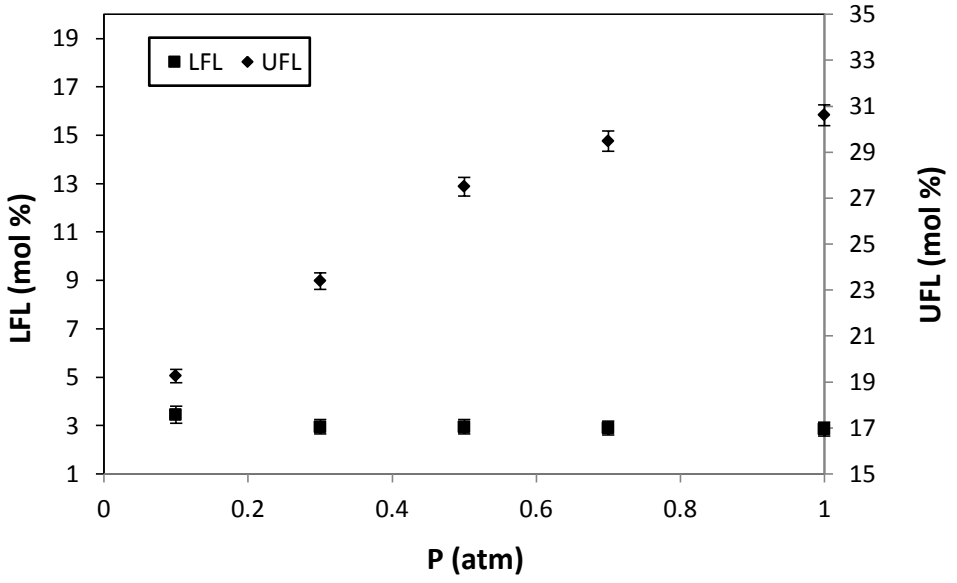

Figure 30: Flammability region of ethylene at sub-atmospheric pressures and room temperature

4.3. Summary

The LFLs and UFLs of hydrogen and light hydrocarbons (methane, ethane, *n*-butane and ethylene) were determined at room temperature and initial pressures ranging from 1.0 atm to 0.1 atm. The obtained LFLs and UFLs are presented in Table 7. Below is a summary of the main findings.

For hydrogen, when the initial pressure decreases below 1.0 atm the flammability region widens (LFL decreases and UFL increases). The region is the widest at 0.3 atm where the LFL decreases by 0.2 mol% and the UFL increases by 2.1 mol%. The region starts to narrow when the pressure decreases below 0.3 atm. The widening of the flammability region when the pressure decreases can be attributed to the reaction mechanism of hydrogen in which the influence of the three body reaction $H + O_2 + M \rightarrow$

HO_2 + M becomes weaker with the decreasing pressure. From the safety point of view, the widening of the flammability region suggests an increased risk of fire and explosion of hydrogen at sub-atmospheric pressures; thus more precaution is recommended when handling hydrogen at low pressure conditions. Under the influence of pressure, the UFL of hydrogen varies more than the LFL; in other words, pressure has more impact on the UFL than the LFL. When the initial pressure decreases from 1.0 atm to 0.1 atm, the maximum change of the UFL is 2.1 mol% which is roughly 10 times that of the LFL (0.2 mol%).

For the hydrocarbons, unlike hydrogen, the flammability regions narrow (the LFLs increase and the UFLs decrease) when the initial pressure decreases from 1.0 atm to 0.1 atm. Therefore, from an inherently safety point of view, it is recommended to handle the hydrocarbons as a pressure as low as possible. It is observed that the UFLs of the alkanes vary linearly with the pressure, while the UFL of ethylene follows a logarithmic pattern. The LFLs of the hydrocarbons do not change much with pressure compared to the UFLs. In other words, it can be concluded that pressure has greater impact on the UFLs and the LFLs.

Table 7: Flammability limits of pure hydrogen and light hydrocarbons at atmospheric and sub-atmospheric pressures and room temperature

		Initial Pressure (atm)				
		1.0	0.7	0.5	0.3	0.1
Hydrogen	LFL (mol%)	3.95	3.85	3.85	3.75	4.14
	UFL (mol%)	75.73	75.88	77.30	77.80	76.95
Methane	LFL (mol%)	5.35	5.35	5.35	5.35	5.35
	UFL (mol%)	15.40	14.85	14.65	14.50	14.35
Ethane	LFL (mol%)	2.85	2.85	2.90	3.00	3.75
	UFL (mol%)	14.00	13.64	12.86	12.37	11.76
n-Butane	LFL (mol%)	1.70	1.75	1.80	1.85	2.60
	UFL (mol%)	8.46	8.33	8.18	8.10	8.08
Ethylene	LFL (mol%)	2.85	2.90	2.95	2.95	3.45
	UFL (mol%)	30.61	29.49	27.50	23.39	19.26

5. ADIABATIC FLAME TEMPERATURES OF HYDROGEN AND LIGHT HYDROCARBONS AT FLAMMABILTIY LIMITS AND SUB-ATMOSPHERIC PRESSURES[*]

5.1. Background

Besides flammability limits, flame temperature is an important parameter in the study of combustion as well as the risk assessment of fire and explosion. Examples of applications of flame temperature can be found in Section 1.3. Adiabatic flame temperature (AFT) is the flame temperature without heat loss to the environment; thus it is often considered the maximum flame temperature. For large vessels, diameter greater 5 cm, heat loss is normally negligible;[2, 51] thus flame temperature can reach adiabatic flame temperature (AFT). In fact, comparisons between calculated AFTs and experimental flame temperatures of various fuels including hydrogen and common hydrocarbons were performed by various researchers[87-89] and it was found that the differences between the calculated AFT and the experimental flame temperature are very small.[87-89] There are two kinds of AFT: constant pressure AFT which is determined at

[*] Part of this section is reprinted with permission from "Upper Flammability Limits of Hydrogen and Light Hydrocarbons in Air at Subatmospheric Pressures" by H. Le, S. Nayak, M. S. Mannan, 2012. *Industrial & Engineering Chemistry Research*, 51(27), 9396-9402. DOI: 10.1021/ie300268x. Copyright 2012 American Chemical Society

[*] Part of this section is reprinted with permission from "Lower Flammability Limits of Hydrogen and Light Hydrocarbons in Air at Subatmospheric Pressures" by H. Le, Y.Liu, M. S. Mannan, 2013. *Industrial & Engineering Chemistry Research*, 52(3), 1372-1378. DOI: 10.1021/ie302504h. Copyright 2013 American Chemical Society

constant pressure condition, and constant volume AFT which is determined at constant volume condition. The calculated AFTs in this research are constant volume ATFs since our experimental setup is at constant volume condition where the combustion happens in a closed cylindrical vessel. Constant volume AFT is generally higher than constant pressure AFT because no energy is utilized to change the volume of the system or to generate work.

The calculation of AFT is based on the assumption of no heat loss and the system reaches chemical equilibrium.[51, 71] First, the composition of combustion products must be obtained. This is performed by solving the chemical equilibrium problem. The chemical equilibrium of a constant volume system is reached if the Helmholtz free energy is minimized (for constant pressure systems, Gibbs free energy is minimized). The Helmholtz free energy of a system is:

$$A = \sum_{j=1}^{s} A_j N_j \qquad [5.1]$$

where A_j is the molar Helmholtz free energy of j^{th} species, N_j is the moles of j^{th} species in the system, s is the total number of species in the system. For ideal gas, the molar Helmholtz free energy is:

$$A_j = G_j(T,P) + RT\ln x_j - RT \qquad [5.2]$$

where G_j is the Gibbs free energy of j^{th} species at the system temperature and pressure, x_j is the molar fraction of j^{th} species, R is the gas constant, and T is the temperature of the system. Substitute equation [5-2] into Equation [5-1], the Helmholtz free energy of the system becomes:

$$A = \sum_{j=1}^{s} (G_j(T,P) + RT \ln x_j - RT) N_j \qquad [5.3]$$

The chemical equilibrium solution is the distribution of N_j that minimizes the Helmholtz free energy, A, subject to the conservation of elements equation:

$$\sum_{j=1}^{s} n_{ij} N_j = a_i \qquad i=1, 2,\ldots p \qquad [5.4]$$

where n_{ij} is the number of i^{th} element, a_i is the moles of i^{th} element, and p is the total number of elements in the system.

Detail about the minimization of the Helmholtz free energy subject to the element conservation constraint can be found elsewhere.[90] Once the equilibrium problem is solved, the composition of the products of combustion is known; next the AFT is calculated by solving the energy conservation law at adiabatic condition and constant volume:

$$\Delta U = 0 \qquad [5.5]$$

where ΔU (J) is the internal energy change of the system.

In this research, the AFTs of hydrogen and the hydrocarbons (methane, ethane, *n*-butane and ethylene) were calculated using the EQUILIBRIUM program of CHEMKIN package; this program is based on the STANJAN – III program which is integrated in CHEMKIN. To obtain the composition of combustion products using the equilibrium program, the required species of the combustion reaction must be provided.[13, 51] For hydrogen and C1-C2 hydrocarbons, GRI Mech 3.0 was used since it contains all the required species (53 species) of the combustion of hydrogen, methane,

ethane and ethylene.[65] For *n*-butane, the Combustion Chemistry Center's *n*-butane mechanism was used since it contains the species of the oxidation of C4.

A simple thermodynamic approach,[71, 91] let us call it CAFT method, could provide an estimate of adiabatic flame temperature. The CAFT method is simple, ready to use and does not require rigorous computational power. However, since CAFT method does not take into account the chemical equilibrium of the system, the accuracy of the method is not as high as those of computational programs available for the calculation of AFTs. For example, CAFT method tends to provide higher, thus conservative, AFTs since it does not consider other products of combustion, such as NOx, free radicals, etc. The accuracy of CAFT method is lower when calculating AFTs of fuels burned at high flame temperature where the dissociation of combustion products takes place, or when significant amount of soot is formed.[51, 58] For the purpose of comparison against the AFTs calculated based on energy balance and chemical equilibrium (obtained using CHEMKIN package), the calculation of the AFTs using CAFT method at constant volume condition was also performed in this research as described in detail in sub-section 5.4.

AFT is a function of various factors including fuel concentration, temperature, and pressure. In general, AFT is the lowest at the flammability limits and the highest at a concentration near stoichiometric as depicted by Figure 31 for hydrogen at atmospheric pressure and room temperature. The lowest AFT at the flammability limits is due to the small amount of fuel or oxygen reacted which results in less heat release, and high amount of inert gas (nitrogen) or unreacted fuel acting as a heat sink in case of LFL and

UFL, respectively. An increase in the temperature of the fuel mixture will increase flame temperature since more energy is available to heat the unburned mixture.[92-93] An increase in the initial pressure of the fuel mixture tends to increase flame temperature; however, the influence of pressure on flame temperature is more complex than that of temperature.[53] This research investigates the effect of pressure on the adiabatic flame temperatures of hydrogen and the light hydrocarbons at the flammability limits; the results are presented later in this Section.

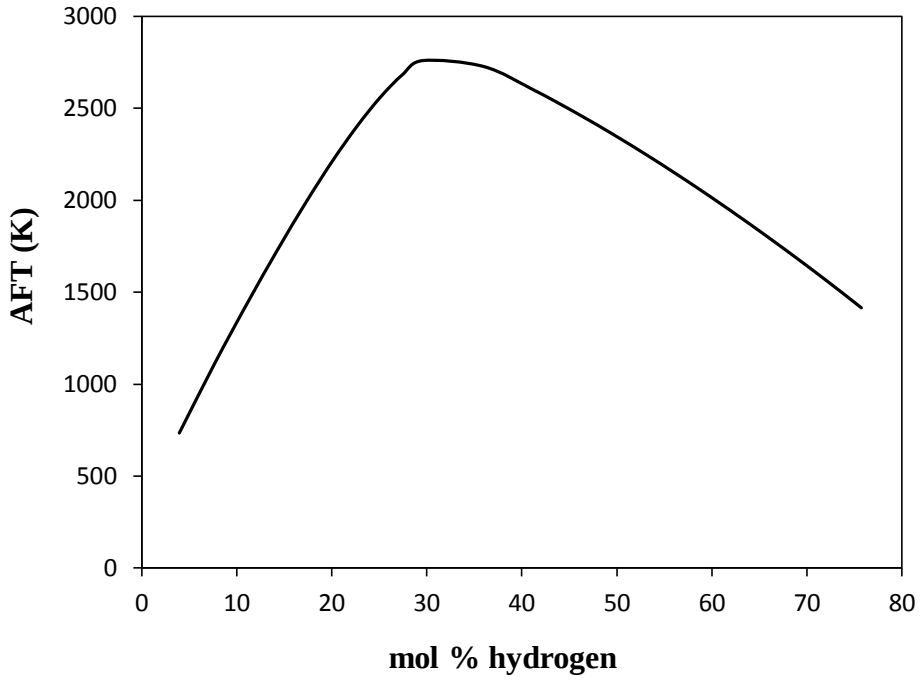

Figure 31: Adiabatic flame temperature of hydrogen in air at room temperature and atmospheric pressure

5.2. AFTs of hydrogen and light hydrocarbons at LFL

The obtained ATFs of hydrogen and the hydrocarbons at the LFL, room temperature and sub-atmospheric pressures are presented in Figure 32 and Figure 33. For hydrogen, the AFT at LFL decreases when the initial pressure decreases from 1.0 atm to 0.3 atm; then the AFT increases with the further decrease of the pressure. For the hydrocarbons, the AFTs at LFL increase when the pressure decreases from 1.0 atm to 0.1 atm, except for methane whose AFT does not change much with pressure.

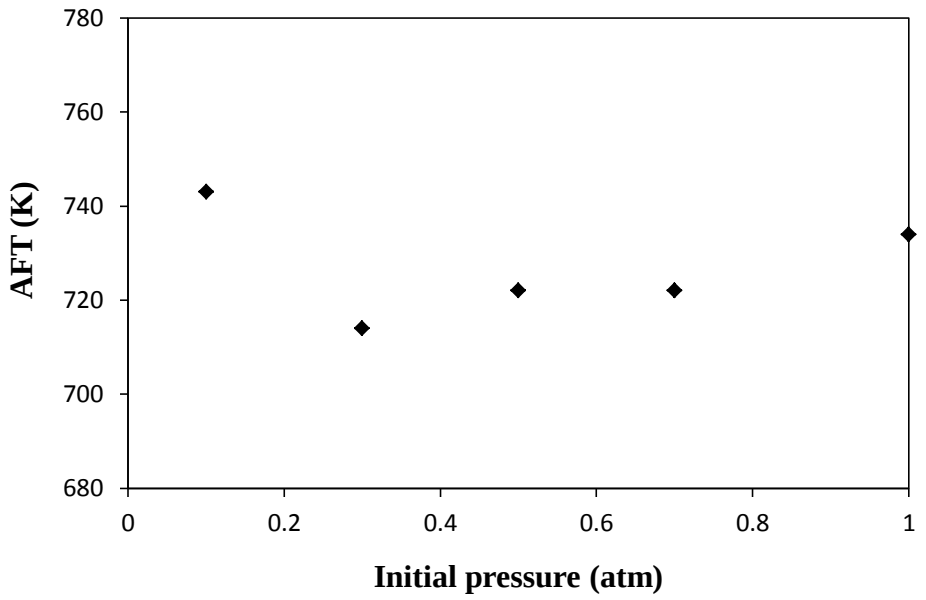

Figure 32: Calculated adiabatic flame temperature of hydrogen at LFL, room temperature and sub-atmospheric pressures

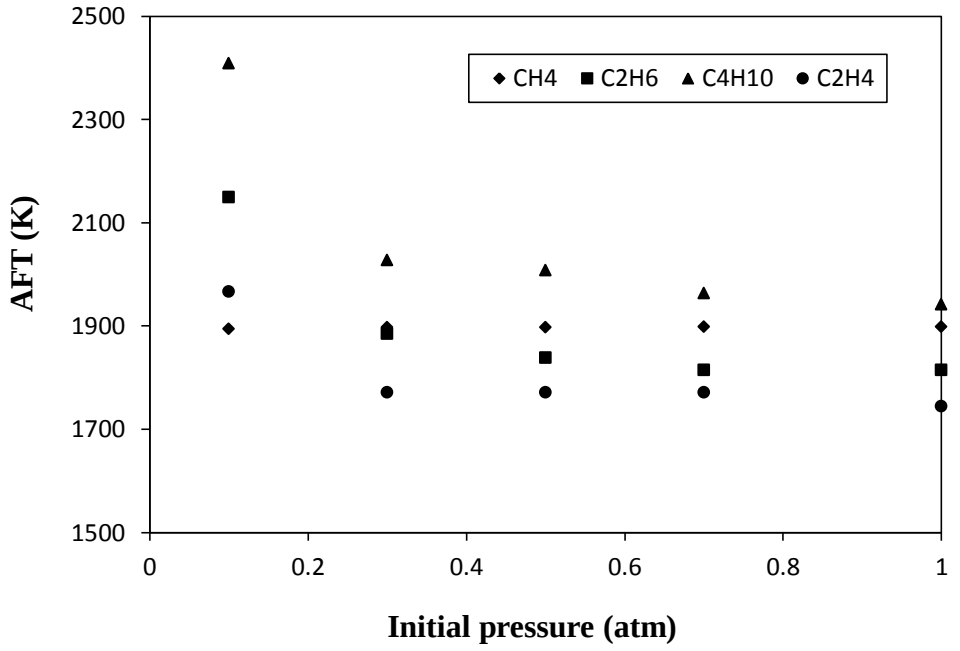

Figure 33: Calculated adiabatic flame temperature of methane, ethane, *n*-butane and ethylene at LFL, room temperature and sub-atmospheric pressures

The behavior of the AFTs at LFL under the influence of pressure is similar to that of the corresponding LFLs. For example, the LFL of hydrogen also decreases with pressure from 1.0 atm to 0.3 atm, then increases with the further decrease of pressure (Section 4.2.1). For both hydrogen and the hydrocarbons, the changes of the AFTs when the pressure decreases from 1.0 atm to 0.3 atm are small as also observed with the LFLs. The AFTs of the fuels start to show appreciable change only when the pressure decreases to 0.1 atm. The similarities between the AFTs at LFL and the corresponding LFLs are understandable since at LFL, fuel is the limiting reactant (oxygen is in excess); therefore, the heat of combustion is proportional to the amount of fuel reacted which is the LFL. The heat of combustion is then consumed to raise the temperature of the

products to its AFT; thus, AFT is proportional to heat of combustion which makes its proportional to the LFL. The proportional relationship between the AFTs and the LFLs can be explained by thermodynamics principles starting with the governing equation [5.5]:

$$\Delta U = 0 \qquad [5.5]$$

The internal energy change ΔU for the closed system under constant volume condition can be divided into two parts: the internal energy change ΔU_c from the combustion reaction at the initial temperature T_i (K); and the internal energy change ΔU_t from the initial temperature T_i to the final flame temperature T_f (K):

$$\Delta U_c = \Delta H_c - \Delta n R T_i \qquad [5.6]$$

$$\Delta U_t = \sum_{\text{products}} n_i \int_{T_i}^{T_f} C_{vi} dT \qquad [5.7]$$

where ΔH_c (J) is the heat of combustion at the initial temperature, Δn (mol) is the total mole number change of the combustion reaction, R is the gas constant (8.31451 J/mol K), n_i is the number of moles of i^{th} component of the combusted products, and C_{vi} (J/mol K) is the heat capacity at constant volume of the i^{th} component.

Combining equations [5.5], [5.6], and [5.7], we have:

$$\Delta H_c - \Delta n R T_i + \sum_{\text{products}} n_i \int_{T_i}^{T_f} C_{vi} dT = 0 \qquad [5.8]$$

At LFL, the total heat of combustion ΔH_c is calculated based on the molar heat of combustion Δh_c (J/mol fuel) and the amount of fuel reacted (LFL) as below:

$$\Delta H_c = LFL\ \Delta h_c \qquad [5.9]$$

The internal energy change $\Delta U_t = \sum_{products} n_i \int_{T_i}^{T_f} C_{vi} dT$ from the initial temperature T_i to the final flame temperature T_f can be approximated by:

$$\Delta U_t = C_{pm}(T_f - T_i) \qquad [5.10]$$

where C_{pm} is the mean heat capacity of the product mixture over the range of temperature of interest, T_f is the adiabatic flame temperature (AFT). Combining equation [5.8], [5.9] and [5.10], we can achieve the linear relationship between AFT and LFL as below:

$$AFT = -\frac{\Delta h_c}{C_{pm}} LFL + C_L \qquad [5.11]$$

where C_L is a constant. The molar heat of combustion Δh_c is negative which makes the slope $-\frac{\Delta h_c}{C_{pm}}$ positive; thus the direct proportional relationship between the AFTs and the LFLs. The linear relationship between AFT and LFL is in fact supported by the experimental data illustrated in Figure 34, Figure 35, Figure 36, and Figure 37 where the AFTs are plotted against the LFLs for hydrogen, ethane, *n*-butane and ethylene, respectively (note that for methane, the LFL and AFT do not change over the range of pressure studied).

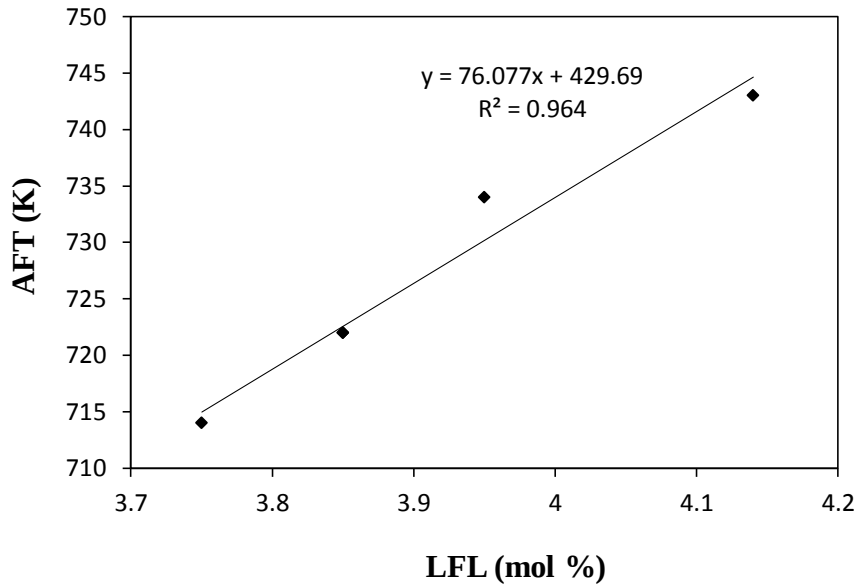

Figure 34: The variation of the calculated AFT with the experimental LFL for hydrogen at room temperature and sub-atmospheric pressures

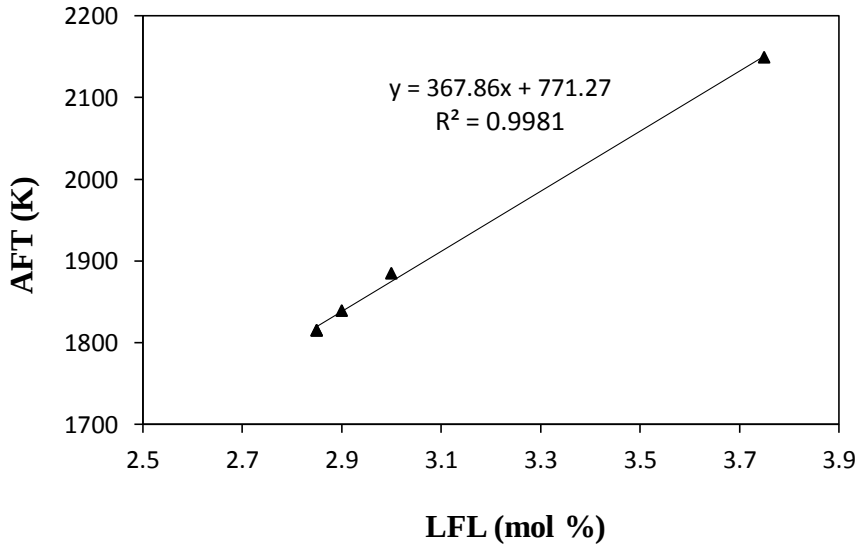

Figure 35: The variation of the calculated AFT with the experimental LFL for ethane at room temperature and sub-atmospheric pressures

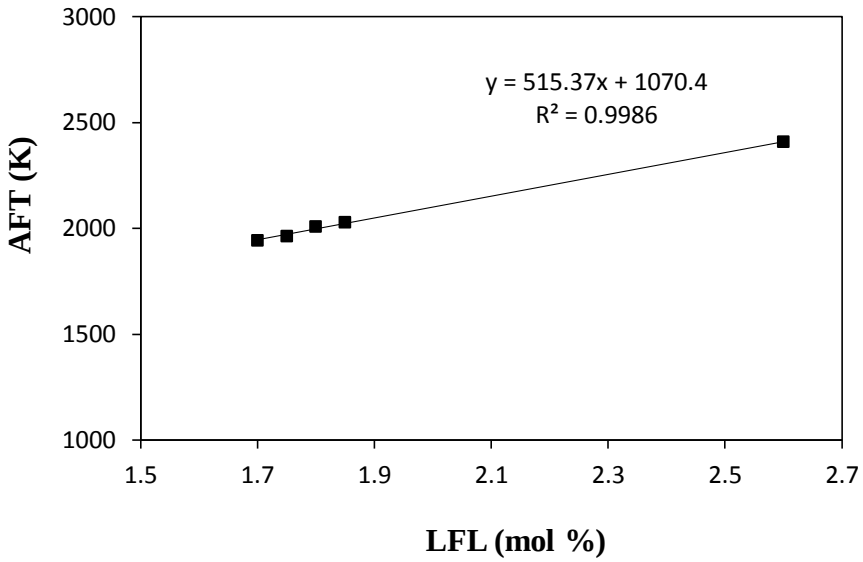

Figure 36: The variation of the calculated AFT with the experimental LFL for *n*-butane at room temperature and sub-atmospheric pressures

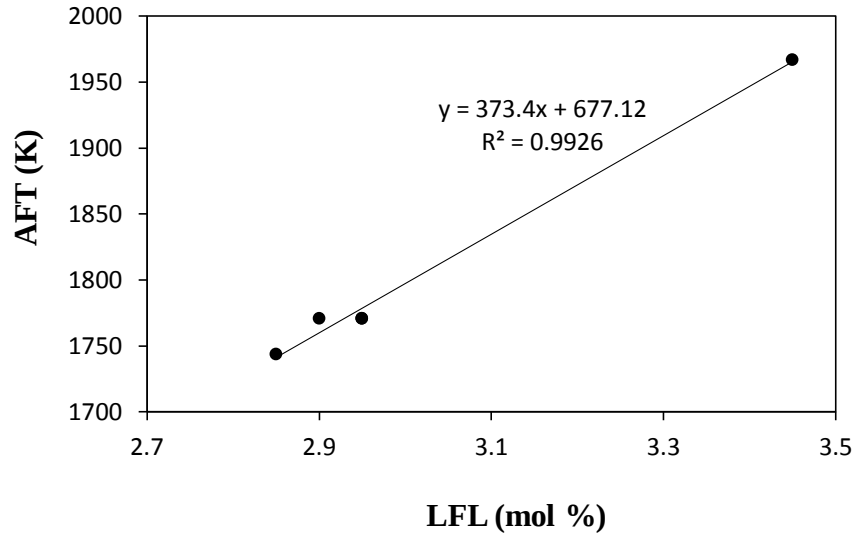

Figure 37: The variation of the calculated AFT with the experimental LFL for ethylene at room temperature and sub-atmospheric pressures

On average, at initial pressure from 1.0 atm to 0.1 atm, the AFT at LFL of hydrogen is about 730 K, and the AFTs at LFL of the alkanes and ethylene are 1900 K and 1800 K, respectively. At each initial pressure, the AFTs of the alkanes are close to each other; therefore, the method of predicting the LFLs of the alkanes using the same threshold flame temperature can be valid in this range of pressure from 1.0 to 0.1 atm. [3, 53, 55] The much smaller AFT at LFL of hydrogen can be explained by its small value of LFL, and more importantly, its small heat of combustion compared to those of the hydrocarbons. From a safety point of view, this much lower AFT at LFL of hydrogen suggests a smaller thermal impact, hence a smaller consequence severity, of a fire involving hydrogen at lean concentration, whereas the impact of a hydrocarbon fire can be significantly higher due to their high AFTs. However, the risk of a hydrogen fire at lean concentration should not be ignored since its thermal radiation could be high enough to ignite other fuels which have low ignition temperatures (e.g., gasoline,[39] acetylene[3]) if the fuels are stored nearby, resulting in a much greater consequence severity. Therefore, the risk of fire/explosion of hydrogen should be carefully analyzed not only based on the concentration of hydrogen, but also on other factors such as the operating condition, proximity to other fuels.

5.3. AFTs of hydrogen and light hydrocarbons at UFL

The obtained AFTs at UFL and sub-atmospheric pressures of hydrogen, the alkanes and ethylene are presented in Figure 38, Figure 39, and Figure 40, respectively. The AFT at UFL of hydrogen decreases when the initial pressure decreases from 1.0 atm to 0.3 atm; then the AFT increases with the further decrease of the pressure. In contrast,

the AFTs at UFL of the hydrocarbons increase when the initial pressure decreases. For the alkanes, the AFTs increase linearly with the decreasing pressure. For ethylene, the AFT increase is not linear, but more like a logarithmic decrease with pressure.

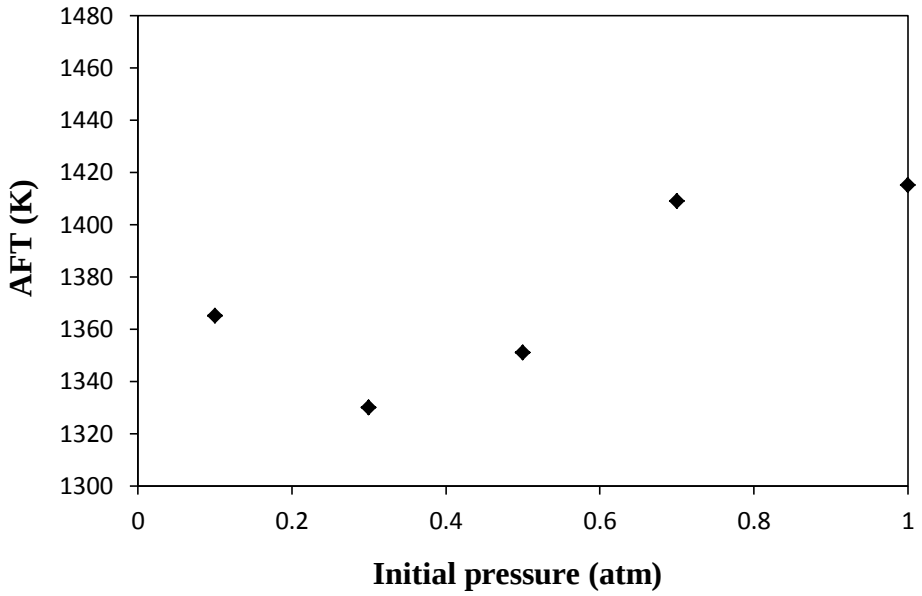

Figure 38: Calculated adiabatic flame temperature of hydrogen at UFL, room temperature and sub-atmospheric pressures

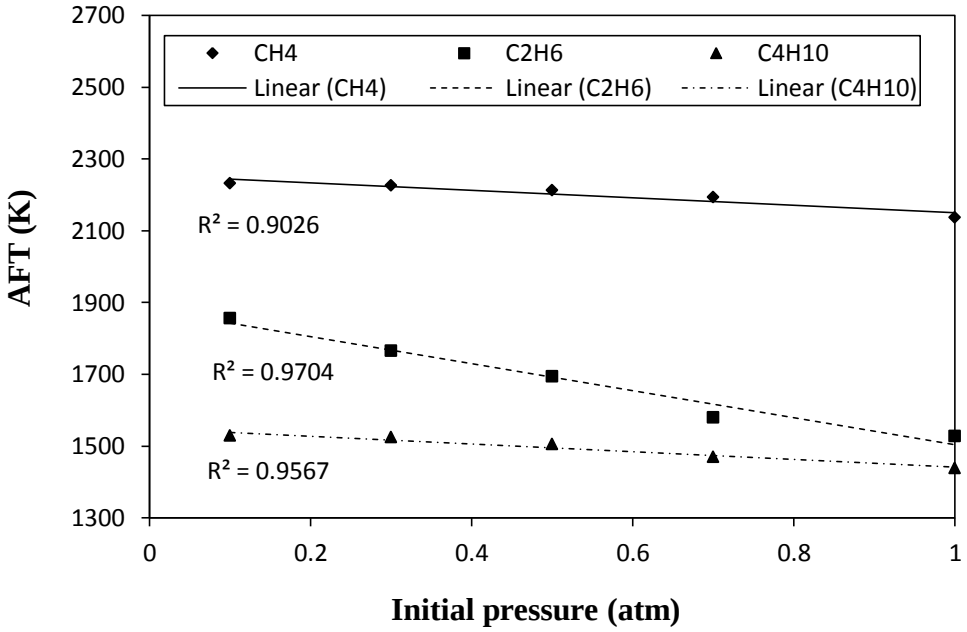

Figure 39: Calculated adiabatic flame temperature of methane, ethane, *n*-butane at UFL, room temperature and sub-atmospheric pressures

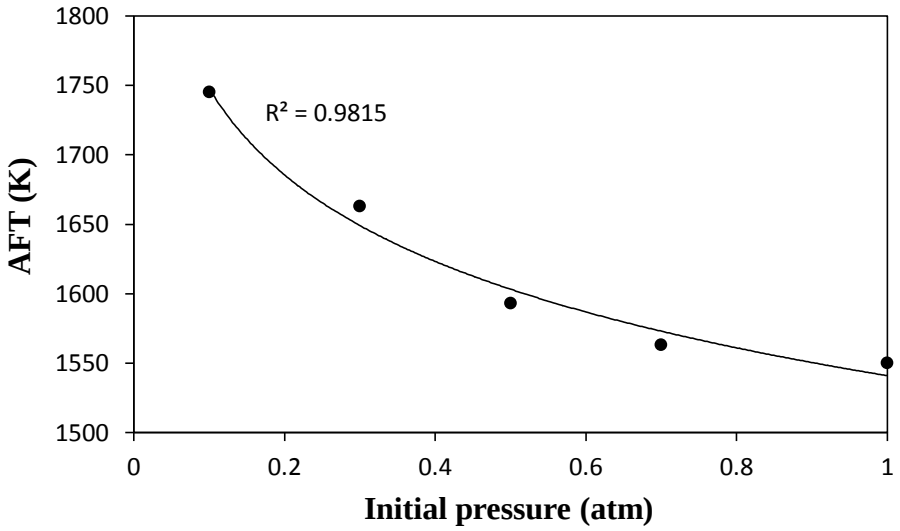

Figure 40: Calculated adiabatic flame temperature of ethylene at UFL, room temperature and sub-atmospheric pressures

Compared to the behaviors of the UFLs of the fuels under the influence of pressure (see Section 4.1), the behaviors of the AFTs at UFL are directly opposite. For example, for hydrogen, the UFL increases while the AFT decrease when the pressure reduces from 1.0 atm to 0.3 atm. For the alkanes, the UFLs decrease linearly with pressure while the AFTs increase linearly. For ethylene, the logarithmic decrease of the UFL with pressure is directly opposite to the logarithmic increase of the AFT. This is understandable since at rich fuel concentration (UFL), the limiting reactant is oxygen; therefore, the heat of reaction is proportional to the amount of oxygen reacting. If the concentration of fuel increases in the fuel mixture, the concentration of oxygen decreases which decreases the heat of combustion and reduces the AFT. In other words, the AFT at UFL is inversely proportional to the UFL.

Similar to the explanation in Section 5.2 about the relationship between the LFLs and the AFTs, the inversely proportional relationship between the AFTs and the UFLs can be explained by thermodynamics principles starting with the governing equation [5.8] (Section 5.2):

$$\Delta H_c - \Delta nRT_i + \sum_{\text{products}} n_i \int_{T_i}^{T_f} C_{vi} dT = 0 \qquad [5.8]$$

The total heat of combustion ΔH_c is calculated based on the molar heat of combustion Δh_c (J/mol fuel) and the amount of fuel reacted, in this case is

$\frac{0.21(1-UFL)}{a+\frac{b}{4}}$ where a, b are the stoichiometric numbers in the overall combustion reaction as below

$$C_aH_b + (a+\frac{b}{4})\,O_2 \rightarrow aCO_2 + \frac{b}{2}\,H_2O \qquad (5.1)$$

Therefore, the total heat of combustion is:

$$\Delta H_c = \frac{0.21(1-UFL)}{a+\frac{b}{4}}\Delta h_c \qquad [5.12]$$

The internal energy change $\Delta U_t = \sum_{products} n_i \int_{T_i}^{T_f} C_{vi}dT$ from the initial temperature T_i to the final flame temperature T_f can be approximated by equation [5.10] (Section 5.2) as below:

$$\Delta U_t = C_{pm}(T_f - T_i) \qquad [5.10]$$

where C_{pm} is the mean heat capacity of the product mixture over the range of temperature of interest, T_f is the adiabatic flame temperature (AFT), T_i is the initial temperature (298K). Combining equation [5.8], [5.10] and [5.12], we can achieve the linear relationship between AFT and UFL as below:

$$AFT = \frac{0.21\Delta h_c}{(a+b/4)C_{pm}}UFL + C_U \qquad [5.13]$$

where C_U is a constant:

$$C_U = -\frac{0.21\Delta h_C}{(a+b/4)C_{pm}} + \frac{\Delta nRT_i}{C_{pm}} + T_i \qquad [5.14]$$

The slope $\frac{0.21\Delta h_c}{(a+b/4)C_{pm}}$ of the linear relationship in equation [5.13] is negative since Δh_c is negative; thus the inversely proportional relationship between the UFLs and the AFTs.

The linear relationship between the AFTs and the UFLs is confirmed by the experimental data illustrated clearly when the UFLs are plotted against the corresponding AFTs in Figure 41, Figure 42, Figure 43, Figure 44 and Figure 45 for hydrogen, methane, ethane, *n*-butane and ethylene, respectively.

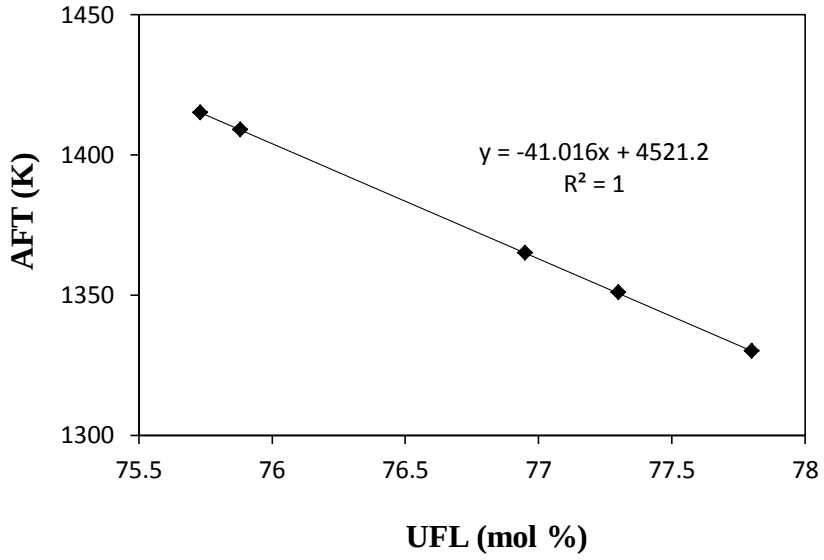

Figure 41: The variation of the calculated AFT with the experimental UFL for hydrogen at room temperature and sub-atmospheric pressures

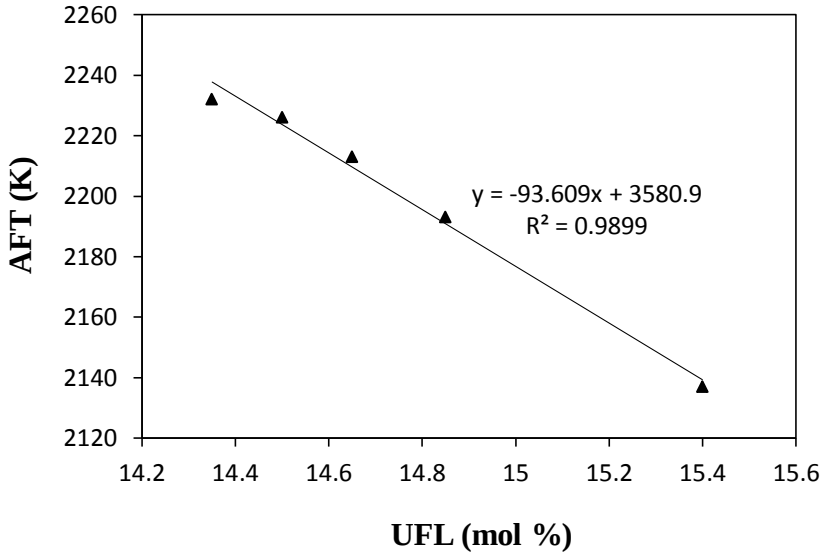

Figure 42: The variation of the calculated AFT with the experimental UFL for methane at room temperature and sub-atmospheric pressures

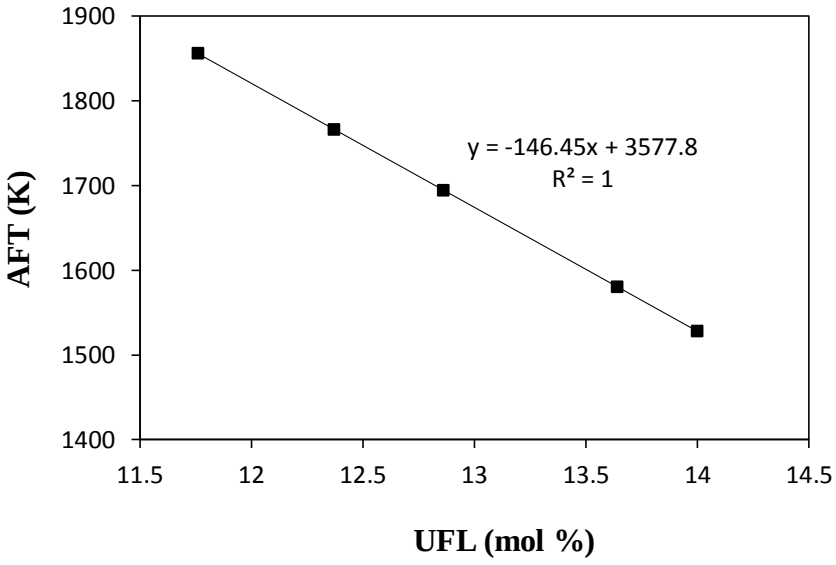

Figure 43: The variation of the calculated AFT with the experimental UFL for ethane at room temperature and sub-atmospheric pressures

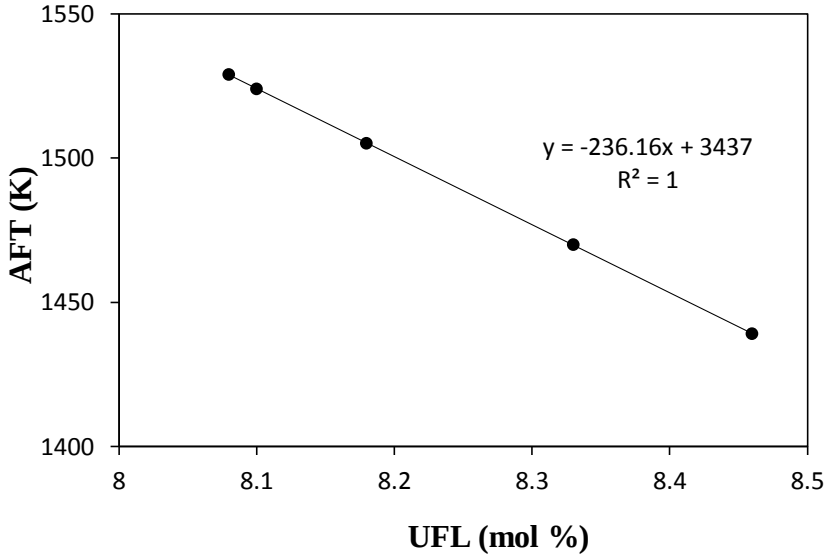

Figure 44: The variation of the calculated AFT with the experimental UFL for *n*-butane at room temperature and sub-atmospheric pressures

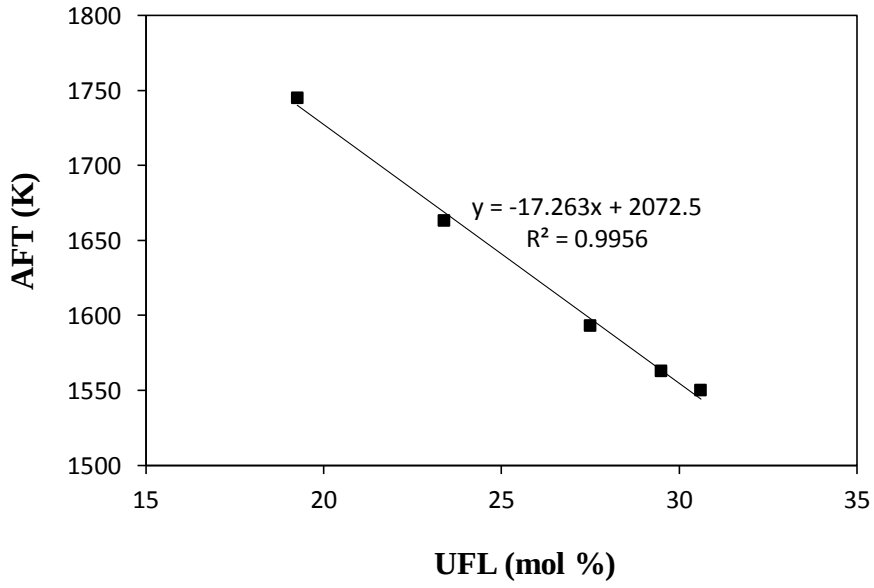

Figure 45: The variation of the calculated AFT with the experimental UFL for ethylene at room temperature and sub-atmospheric pressures

Comparing the variation of the AFT at UFL with the AFT at LFL under the influence of pressure, the AFT at UFL is more sensitive to the change in pressure. In other words, pressure has a higher impact on the AFT at UFL than on the AFT at LFL. It is understandable since pressure also has a much higher impact on the UFL than on the LFL (Section 4).

For the alkanes, the AFTs at UFL are very different from each other, whereas the AFTs at LFL are close to each other (Section 5.2: approximately 1900 K among methane, ethane and *n*-butane). For example, the average AFT of methane at UFL in the range of pressure studied is 2200 K which is 500 K and 700 K higher than that of ethane and *n*-butane, respectively. These large flame temperature differences at the UFLs of the alkanes explain the inaccurate prediction of the UFLs of these hydrocarbons using the constant threshold flame temperature method performed by various researchers.[3, 53, 55]

For hydrogen, at all initial pressures studied, the AFT at UFL is much larger than the AFT at LFL: the AFT at UFL is roughly 2 times the AFL at LFL. The much higher AFT at UFL is due to the much less inert gas (nitrogen) in the UFL mixture than in the LFL mixture. Inert gas acts as a heat sink which absorbs heat, thus reduces the flame temperature. Furthermore, the amount of fuel combusted in the LFL mixture is much less than that in the UFL mixture, which results in less heat released; thus lower flame temperature at LFL. From the safety point of view, the much higher flame temperature at UFL implies a higher thermal radiation which results in a more severe consequence from a rich hydrogen flame compared to a lean hydrogen flame. However, as mentioned in Section 5.2, the risk of fire/explosion of hydrogen should be carefully analyzed not only

based on the concentration, but also on other factors such as the operating condition, proximity to other fuels.

5.4. Adiabatic flame temperature calculated by CAFT method

As mentioned in sub-section 5.1, a simple thermodynamic approach, CAFT method, could provide an estimate of adiabatic flame temperature. The CAFT method is simple, ready to use and does not require rigorous computational power since the method does not take into account the chemical equilibrium calculation.

The principle of CAFT method is based on the total energy balance dictated by the first law of thermodynamics:

$$\Delta U = W + Q \qquad [5.15]$$

where ΔU (J) is the internal energy change of the system, W (J) is work acting on the system or by the system, and Q (J) is the total amount of heat exchanged between the system and its surroundings. Since no work is done on the system and the system does not perform any work, W is zero. And the assumption of no heat losses gives Q =0. Equation [5.6] then becomes

$$\Delta U = 0 \qquad [5.5]$$

Then, the internal energy change ΔU for the closed system under constant volume condition can be divided into two parts: the internal energy change ΔU_c from the combustion reaction at the initial temperature T_i (K); and the internal energy change ΔU_t from the initial temperature T_i to the final flame temperature T_f (K)

$$\Delta U_c = \Delta H_c - \Delta nRT_i \qquad [5.6]$$

$$\Delta U_t = \sum_{\text{products}} n_i \int_{T_i}^{T_f} C_{vi} dT \qquad [5.7]$$

where ΔH_c (J) is the heat of combustion at the initial temperature, Δn (mol) is the total mole number change of the combustion reaction, R is the gas constant (8.31451 J/mol K), n_i is the number of moles of i^{th} component of the combusted products, and C_{vi} (J/mol K) is the heat capacity at constant volume of the i^{th} component which is commonly represented in the form:

$$C_v = a + bT + cT^2 + dT^3 \qquad [5.16]$$

where a, b, c, d are constants. The values of the constants (a, b, c, d) for the gases in this research are provided in Table 8.

Table 8: Heat capacities at constant volumes of the gases used in this research[94]

Gas	$C_v = a + bT + cT^2 + dT^3$ (J/mol K)			
	a	b x 10^2	c x 10^5	d x 10^9
H_2	18.565	0.435	-0.033	0
CH_4	11.561	5.021	1.268	-11.004
C_2H_6	-1.419	17.255	-6.402	7.28
C_4H_{10}	-4.36	37.126	-18.326	34.979
C_2H_4	-4.364	15.628	-8.339	17.657

Combining equations [5.5], [5.6] and [5.7], the final governing equation for the calculation of AFT is obtained as below:

$$\Delta H_c - \Delta n R T_i + \sum_{\text{products}} n_i \int_{T_i}^{T_f} C_{vi} dT = 0 \qquad [5.8]$$

The overall combustion reaction of fuel in air is represented by reaction:

$$C_aH_b + (a + \frac{b}{4})\, O_2 \rightarrow aCO_2 + \frac{b}{2} H_2O \qquad (5.1)$$

In this case, the total mole number change of the combustion reaction (Δn), and the number of moles of the i^{th} component (n_i) are calculated based on the stoichiometric numbers in reaction (5.1) and the original mole or volume percent of the fuel in air. The above assumption that the combustion products are only CO_2 and H_2O is usually used to obtain an estimate of the AFT easily and quickly. The AFTs calculated in this way are accurate if the flame temperature of the combustion reaction is low. If the flame temperature is high, above 1700 K, dissociation of the combustion products can occur.[51] Then the final products are a complex mixture of various compounds and radicals such as CO_2, CO, H_2, H, O, O_2, OH, etc. In addition, the dissociation and ionization of combustion products absorb great amount of energy which reduce the flame temperature appreciably. This is confirmed in sub-sections 5.2 and 5.3 when the comparison between the CAFT AFTs and CHEMKIN AFTs are presented.

The composition of the combustion products at LFL and UFL concentrations are listed in Table 9 and Table 10, respectively.

Table 9: Composition of combustion products at LFL concentration

Compounds	Number of moles before burning	Number of moles after burning (n_i)	The total mole number change (Δn)
C_aH_b	LFL	0	
O_2	0.21(1-LFL)	$0.21(1-LFL)-(a+\frac{b}{4})$ LFL	
N_2	0.79(1-LFL)	0.79(1-LFL)	$(\frac{b}{4}-1)$ LFL
CO_2	0	aLFL	
H_2O	0	$\frac{b}{2}$ LFL	

Table 10: Composition of combustion products at UFL concentration

Compounds	Number of moles before burning	Number of moles after burning (n_i)	The total mole number change (Δn)
C_aH_b	UFL	$UFL-\frac{0.21(1-UFL)}{a+b/4}$	
O_2	0.21(1-UFL)	0	
N_2	0.79(1-UFL)	0.79(1-UFL)	
CO_2	0	$0.21(1-UFL)\left(\frac{a}{a+b/4}\right)$	$0.21(1-UFL)\left(\frac{b/4-1}{a+b/4}\right)$
H_2O	0	$0.21(1-UFL)\left(\frac{b/2}{a+b/4}\right)$	

The heat of combustion ΔH_c at LFL and UFL concentrations are calculated based on equations [5.9] and [5.12], respectively:

$$\Delta H_c = LFL\Delta h_c \qquad [5.9]$$

$$\Delta H_c = \frac{0.21(1-UFL)}{a + b/4} \Delta h_c \qquad [5.12]$$

where Δh_c is the molar heat of combustion of the fuel which is presented in Table 11 for the fuels studied in this research.

Table 11: Molar heat of combustion of the fuels at T_i = 298K [94]

Fuel	Molar heat of combustion, Δh_c (kJ/mol fuel)
H_2	-241.826
CH_4	-802.32
C_2H_6	-1427.84
n-C_4H_{10}	-2658.45
C_2H_4	-1322.96

The heat capacity constants for the products of combustion are listed in Table 12.

Table 12: Heat capacities at constant volume for combustion products [94]

Products	$C_v = a + bT + cT^2 + dT^3$ (J/mol K)			
	a	b x 10^2	c x 10^5	d x 10^9
O_2	17.146	1.519	-0.715	1.311
N_2	20.569	-0.157	0.808	-2.971
CO_2	13.929	5.977	-3.499	7.464
H_2O	23.904	0.192	1.055	-3.593
H_2	18.565	0.435	-0.033	0

Combining final governing equation [5.8]; the composition of combustion products (n_i, Δn) provided by Table 9 and Table 10 for LFL and UFL, respectively; the

heat of combustion ΔH_c calculated by equations [5.9] and [5.12] for LFL and UFL, respectively; the heat capacities at constant volume for combustion products (C_{vi}) given by Table 8 and Table 12, the AFTs of the fuels (T_f) at LFL and UFL concentrations and can be obtained.

The AFTs calculated by CAFT method for hydrogen and the hydrocarbons at LFL concentration are presented in Table 13 along with the AFTs calculated by the CHEMKIN package for comparison. As expected, CAFT method provides higher AFTs since the method does not take into account the chemical equilibrium of the system; thus, the heat effects of other combustion products such as NOx, radicals are not considered. For *n*-butane which burns at high flame temperatures, CAFT method returns much higher AFTs since the method ignores the dissociation of combustion products which occurs at high flame temperature. At 0.1 atm, the chemistry of the combustion is complex and active species (e.g., free radicals) tend to remain since the collision frequency is much less at this low pressure, the accuracy of CAFT method is significantly reduced for all fuels as can be seen in Table 13. Therefore, CAFT method should be limited to a rough estimation of adiabatic flame temperatures; for a more accurate calculation of AFTs, computational methods (e.g., CHEMKIN package) which consider both the thermodynamics and chemical equilibrium of the combustion system should be used.

Table 13: AFTs (K) at LFL of hydrogen and the hydrocarbons calculated by CAFT method and CHEMKIN package

P (atm)	H_2		CH_4		C_2H_6		C_4H_{10}		C_2H_4	
	CAFT	CHEM	CAFT	CHEM	CAFT	CHEM	CAFT	CHEM	CAFT	CHEM
1.0	737	734	1911	1898	1824	1815	1949	1942	1750	1744
0.7	726	722	1911	1898	1824	1815	1989	1964	1772	1771
0.5	726	722	1911	1897	1846	1839	2029	2008	1793	1771
0.3	715	714	1911	1897	1890	1885	2068	2028	1793	1771
0.1	757	743	1911	1894	2215	2149	2675	2409	2004	1967

At UFL concentration, the AFTs calculated by CAFT method for hydrogen and the hydrocarbons are presented in Table 14 along with the AFTs calculated by the CHEMKIN package for comparison. Except for hydrogen, the differences between the AFTs calculated by CAFT method and those by CHEMKIN package are much larger at UFL concentration than at LFL concentration. This is understandable since at UFL concentration, the chemistry of the combustion reaction gets more complicated which is not taken into account by CAFT method. For example, larger amount of carbon monoxide is formed due to incomplete combustion and significant amount of soot is also formed [51, 58] which consume significant heat. This explain the much higher AFTs calculated by CAFT method compared to CHEMKIN package at UFL concentration.

Table 14: AFTs (K) at UFL of hydrogen and the hydrocarbons calculated by CAFT method and CHEMKIN package

P (atm)	H_2		CH_4		C_2H_6		C_4H_{10}		C_2H_4	
	CAFT	CHEM	CAFT	CHEM	CAFT	CHEM	CAFT	CHEM	CAFT	CHEM
1.0	1409	1415	2614	2137	2272	1528	2224	1439	1818	1550
0.7	1403	1409	2650	2193	2296	1580	2238	1470	1858	1563
0.5	1345	1351	2663	2213	2350	1694	2253	1505	1932	1593
0.3	1324	1330	2672	2226	2386	1766	2262	1524	2101	1663
0.1	1359	1365	2682	2232	2432	1856	2264	1529	2298	1745

5.5. Summary

The adiabatic flame temperatures (AFTs) of hydrogen and light hydrocarbons at the flammability limits, room temperature and sub-atmospheric pressures were calculated using CHEMKIN package[62] with thermochemical and transport properties from the database compiled by Kee et al.[63-64] and reaction mechanism from GRI Mech 3.0[65] and the Combustion Chemistry Center.[66] The obtained AFTs are summarized in Table 15. Below are a summary of the main findings.

Table 15: Adiabatic flame temperatures at flammability limit concentration, room temperature and sub-atmospheric pressures of hydrogen and light hydrocarbons

		Initial Pressure (atm)				
		1.0	0.7	0.5	0.3	0.1
Hydrogen	AFT at LFL (K)	734	722	722	714	743
	AFT at UFL (K)	1415	1409	1351	1330	1365
Methane	AFT at LFL (K)	1898	1898	1897	1897	1894
	AFT at UFL (K)	2137	2193	2213	2226	2232
Ethane	AFT at LFL (K)	1815	1815	1839	1885	2149
	AFT at UFL (K)	1528	1580	1694	1766	1856
n-Butane	AFT at LFL (K)	1942	1964	2008	2028	2409
	AFT at UFL (K)	1439	1470	1505	1524	1529
Ethylene	AFT at LFL (K)	1744	1771	1771	1771	1967
	AFT at UFL (K)	1550	1563	1593	1663	1745

Overall, when the initial pressure decreases from 1.0 atm to 0.1 atm, the AFT at LFL and the AFT at UFL behave similarly. For hydrogen, the AFTs at both flammability limits initial decrease when the pressure decrease from 1.0 atm to 0.3 atm, then the AFTs increase with the further decrease with pressure. For the hydrocarbons, the AFTs at both flammability limits increase when the pressure decreases, except for methane whose AFT at LFL does not change much with pressure.

Under the influence of pressure from 1.0 – 0.1 atm, the AFTs at LFL are proportional to the LFLs whereas the AFTs at UFL are inversely proportional to the

UFLs. The AFTs at LFL and at UFL varies linearly with the corresponding LFLs and UFLs.

Pressure has higher impact on the AFT at UFL than on the AFT at LFL. The AFT at LFL varies very little when the pressure decrease from 1.0 atm to 0.1 atm which suggests that the method of the constant threshold flame temperature to predict the LFL is valid. On the other hand, the great variation of the AFT at UFL with pressure and the large differences among the AFTs at the UFL of the alkanes imply that the method of constant threshold flame temperature is not accurate to predict UFLs.

For hydrogen, at all initial pressures studied, the AFT at UFL is roughly 2 times the AFL at LFL which means that the AFT at UFL is much higher than the AFT at LFL. This suggests that the thermal impact of a flame at UFL is higher than that at LFL; thus, on the safety point of view, the consequence of a hydrogen flame at UFL is more severe than that at LFL. However, the risk of hydrogen flame, whether at lean or rich concentration, should be carefully analyzed holistically based on many other factors, such as the operating condition, proximity to other fuels.

For comparison, CAFT method, a thermodynamic approach which does not consider the reaction equilibrium calculation, was used to calculate the AFTs. Compared to the AFTs calculated using the CHEMKIN package, this method could provide very good estimates of the AFTs of hydrogen at all initial pressures studied. The same is not true for the AFTs of the hydrocarbons where there are large differences between the AFTs calculated by two methods. The differences are larger for the AFTs at UFLs than for the AFTs at LFLs. At all initial pressure, CAFT method provides higher AFTs. This

is because CAFT method does not take into account the complex chemistry of the combustion reaction including the product dissociation and the formation of complex product mixtures (NO_x, radicals, soot…) which consume energy.

6. FLAMMABILITY LIMITS OF MIXTURES OF HYDROGEN AND HYDROCARBONS AT SUB-ATMOSPHERIC PRESSURES

6.1. Background

The knowledge of the flammability limits of mixtures of hydrogen and hydrocarbons is important since hydrogen is present in various mixtures with hydrocarbons in many processes and applications. Examples of such mixtures are refinery gas streams which contain various percentages of hydrogen (up to 90%) and hydrocarbons (methane, ethane, C_3, C_{4+}.).[95] Hydrogen is also added to natural gas, consisting mostly methane, to reduce CO, CO_2 and NO_x emissions[96-98], improve flame stability,[97-98] and extend the lean operating limit of spark ignited engines.[99] Therefore, it is critical to understanding the flammability limits of these hydrogen mixtures in order to handle them safely.

A number of studies on the flammability limits of hydrogen mixtures with hydrocarbons have been carried out at atmospheric and non-atmospheric conditions. The effect temperature, from very low temperature (-60 ºC) to very high temperature (350 ºC), on the flammability limits of various mixtures of hydrogen and hydrocarbons (e.g., methane, propane, ethylene) has been investigated extensively by many researchers. In general, it was found that the flammable zone of the mixtures increases with the increase of temperature.[72, 100-102] The effect of pressure on the flammability limits of mixtures of hydrogen and hydrocarbons was much less studied than that of temperature. Van den

Schoor and Verplaetsen[100] investigated the impact of high pressure, up to 10 bar, on the UFLs of mixtures of 20% and 40% of hydrogen with methane, and found that the UFLs of the mixtures increase with the initial pressure, and the increase was linear in the pressure range from 1 bar to 6 bar. However, it is unclear how the flammability limits of hydrogen mixtures with hydrocarbons behave at low pressures. In addition, the role of hydrogen in the flammability limits of its mixtures with hydrocarbons at sub-atmospheric pressures is not clearly understood. To address the above limitations and to further enhance the understanding of flammability limits of mixtures of hydrogen and hydrocarbons, this research experimentally determines the LFLs and UFLs of various binary mixtures of hydrogen with hydrocarbons, such as methane, ethane, *n*-butane, ethylene, at room temperature and initial pressures of 1.0 atm, 0.5 atm, and 0.1 atm. The influence of low pressure and of the concentration of hydrogen in the fuel mixtures will be investigated. In addition, the very popular method for the prediction of flammability limits of mixtures of fuels, the Le Chatelier's rule, is verified for the mixtures of hydrogen and the hydrocarbons at atmospheric and sub-atmospheric pressures. Another method called Calculated Adiabatic Flame Temperature (CAFT) model is also tested and compared with Le Chatelier's rule.

6.1.1. Le Chatelier's rule

Le Chatelier's rule is basically an empirical formula which is the most widely used to calculate flammability limits of fuel mixtures. Algebraically, Le Chatelier's rule states that the mixture flammability limit has a value between the maximum and minimum of the pure component flammability limits.

$$LFL_{mix} = \frac{1}{\sum_{1}^{n} \frac{y_i}{LFL_i}} \quad [6.1]$$

$$UFL_{mix} = \frac{1}{\sum_{1}^{n} \frac{y_i}{UFL_i}} \quad [6.2]$$

where y_i is the mole fraction of the i^{th} component considering only the combustible species, and LFL_i and UFL_i are the lower flammability limit and upper flammability limit of the i^{th} component in mole percent, LFL_{mix} and UFL_{mix} are the lower flammability limit and upper flammability limit of the gas mixtures.

Originally, Le Chatelier's rule was developed based on experiment data with lower flammability limits of gas mixtures of methane and other hydrocarbons, and it generally predicts the LFL of mixtures quite well. The proof for Le Chatelier's rule at LFL was provided by Mashuga and Crowl [71] with the assumptions of: i) constant adiabatic flame temperature rise at the lower flammability limit for all species, ii) constant product heat capacities, and iii) same number of moles for the initial mixture and final products. At the upper flammability limit, fuel no longer represents a small percentage of the mixture. These mixtures can contain a complex mixture of fuel, oxygen and nitrogen resulting in a wide variation from the initial to final heat capacities and molar quantities. So the application of Le Chatelier's rule to predict the UFL of mixtures can be accurate for some fuel mixtures and inaccurate for others; in other words, the application of the rule depends upon the individual mixtures.[71, 100, 103-107]

The accuracy of Le Chatelier's rule has been tested carefully for many mixtures containing hydrogen. It was found that Le Chatelier's rule can predict the LFL of various

mixtures of hydrogen and hydrocarbons including methane, propane and ethylene very well at either ambient or non-ambient condition (e.g., low temperature, high temperature, high pressure) if the corresponding LFLs generated at the same condition of the fuel components are used. For UFL, the rule can predict quite well for various mixtures of hydrogen and methane, hydrogen and propane, hydrogen and methane and carbon monoxide at atmospheric pressure and ambient or elevated temperatures.[72, 101]

At sub-atmospheric pressure condition, the application of Le Chatelier's rule to binary mixtures of hydrogen and hydrocarbons is unclear. Whether this rule can predict the flammability limits of the mixtures well or not is investigated in this research using comprehensive experimental data of different mixtures of hydrogen and hydrocarbons at room temperature and sub-atmospheric pressures.

6.1.2. Calculated Adiabatic Flame Temperature (CAFT) model

Another method being used to predict the flammability limits of mixtures of fuels is the Calculated Adiabatic Flame Temperature (CAFT) model. The CAFT model assumes that the flammability limits are mostly thermal in behavior, and does not take into account the chemical equilibrium of combustion reaction.[58, 108] The principle of CAFT is based on the total energy balance dictated by the first law of thermodynamics

$$\Delta U = W + Q \qquad [6.3]$$

where ΔU (J) is the internal energy change of the system, W (J) is work acting on the system or by the system, and Q (J) is the total amount of heat exchanged between the system and its surroundings. Since no work is done on the system and the system does

not perform any work, W is zero. And the assumption of no heat losses gives Q =0. Equation [6.3] then becomes

$$\Delta U = 0 \qquad [6.4]$$

The internal energy change ΔU (J) for the closed system under constant volume condition can be divided into two parts: the internal energy change ΔU_c (J) from the combustion reaction at the initial temperature T_i (K); and the internal energy change ΔU_t (J) from the initial temperature T_i (K) to the final flame temperature T_f (K) of the mixture of fuels

$$\Delta U_c = \Delta H_c - \Delta n R T_i \qquad [6.5]$$

$$\Delta U_t = \sum_{\text{products}} n_i \int_{T_i}^{T_f} C_{vi} dT \qquad [6.6]$$

where ΔH_c (J) is the heat of combustion at the initial temperature, Δn (mol) is the total mole number change of the combustion reaction, R is the gas constant (8.31451 J/mol K), n_i is the number of moles of i^{th} component of the combusted products, and C_{vi} (J/mol K) is the heat capacity at constant volume of the i^{th} component which is commonly represented in the form:

$$C_v = a + bT + cT^2 + dT^3 \qquad [6.7]$$

where a, b, c, d are constants.

Combining equation [6.4], [6.5] and [6.6], the final governing equation for the CAFT modeling is obtained as equation [6.8]

$$\Delta H_c - \Delta n R T_i + \sum_{\text{products}} n_i \int_{T_i}^{T_f} C_{vi} dT = 0 \qquad [6.8]$$

In general, the CAFT modeling for fuel mixtures involves four steps [54]:

1. Collect the flammability limits of the pure fuels
2. Estimate the AFTs of the pure fuels
3. Estimate the AFT of the mixture of fuels (T_f)
4. Calculate the flammability limit of the mixture of fuels

In step 1, the experimental flammability limits of the pure fuels (refer to Section 4) are used for the prediction of the flammability limits of the mixtures of the corresponding fuels. In step 2, the AFTs of the pure fuels calculated earlier in Section 5 are used. In step 3, the AFT of the mixture of fuels T_f is calculated as below:[54]

$$T_f = y_1 T_{f,1} + y_2 T_{f,2} \qquad [6.9]$$

where $T_{f,1}$ and $T_{f,2}$ are the adiabatic flame temperatures of fuel 1 and fuel 2, respectively (Section 5); y_1 and y_2 are the molar fractions of fuel 1 and fuel 2 in the fuel mixture. The calculated T_f for various mixtures of hydrogen and the hydrocarbons at LFL and UFL and different initial pressures are presented in Table 16

Table 16: Calculated adiabatic flame temperatures for mixtures of hydrogen and hydrocarbons at room temperature and initial pressures of 1.0 atm, 0.5 atm, and 0.1 atm

H_2 molar fraction in the fuel mixture		P = 1.0 atm		P = 0.5 atm		P = 0.1 atm	
		T_f at LFL (K)	T_f at UFL (K)	T_f at LFL (K)	T_f at UFL (K)	T_f at LFL (K)	T_f at UFL (K)
$H_2 + CH_4$	1	737	1409	726	1345	757	1359
	0.75	1031	1710	1022	1675	1046	1690
	0.5	1324	2012	1319	2004	1334	2021
	0.25	1618	2313	1615	2334	1623	2351
	0	1911	2614	1911	2663	1911	2682
$H_2 + C_2H_6$	1	737	1409	726	1345	757	1359
	0.75	1009	1625	1006	1596	1122	1627
	0.5	1281	1841	1286	1848	1486	1896
	0.25	1552	2056	1566	2099	1851	2164
	0	1824	2272	1846	2350	2215	2432
$H_2 + C_4H_{10}$	1	737	1409	726	1345	757	1359
	0.75	1040	1613	1052	1572	1237	1585
	0.5	1343	1817	1378	1799	1716	1812
	0.25	1646	2020	1703	2026	2196	2038
	0	1949	2224	2029	2253	2675	2264
$H_2 + C_2H_4$	1	737	1409	726	1345	757	1359
	0.75	990	1511	993	1492	1069	1594
	0.5	1244	1614	1260	1639	1381	1829
	0.25	1497	1716	1526	1785	1692	2063
	0	1750	1818	1793	1932	2004	2298

In step 4, the flammability limit of the mixture of fuels is calculated based on the governing equation [6.8] where T_i = 298K, T_f is calculated based on equation [6.9], ΔH_c, Δn, n_i, C_{vi} are calculated using the flammability limits of the pure fuels, the fractions of

the fuels in the mixture, and the amount of each product of the combustion. The calculation of ΔH_c, Δn, n_i, C_{vi} is specific for LFL and UFL, and is presented below.

a) CAFT model for the lower flammability limit (LFL)

For LFL, the amount of oxygen is in excess, it can be assumed that fuel reacts completely. Another assumption is that there is no dissociation of the combustion products.[51] The overall combustion reaction of the fuels in air at LFL is represented by reaction (6.1) and the numbers of moles of the products is detailed in Table 17

$$y_1H_2 + y_2C_aH_b + (\frac{y_1}{2} + ay_2 + \frac{by_2}{4})\,O_2 \rightarrow ay_2CO_2 + (y_1 + \frac{by_2}{2})\,H_2O \qquad (6.1)$$

where y_1, y_2 are the molar fractions of fuel 1 and fuel 2 in the fuel mixture, respectively.

Table 17: Amount of combustion products for binary mixtures of hydrogen and hydrocarbons at LFL

Compounds	Number of moles before burning	Number of moles after burning (n_i)	The total mole number change (Δn)
H_2	y_1LFL_{mix}*	0	
C_aH_b	y_2LFL_{mix}	0	
O_2	$0.21(1\text{-}LFL_{mix})$	$0.21(1\text{-}LFL_{mix}) - (\frac{y_1}{2} + ay_2 + \frac{by_2}{4})LFL_{mix}$	$(-\frac{y_1}{2} + \frac{by_2}{4} - y_2)\,LFL_{mix}$
N_2	$0.79(1\text{-}LFL_{mix})$	$0.79(1\text{-}LFL_{mix})$	
CO_2	0	ay_2LFL_{mix}	
H_2O	0	$(y_1 + \frac{by_2}{2})LFL_{mix}$	

*LFL_{mix} is the LFL of the mixture of fuels

The overall heat of combustion ΔH_c (J) of reaction (6.1) and in equation [6.8] can be estimated based on Hess's law of chemical reaction which states that for the conversion from reactants to products, the change of energy is the same whether the reaction takes place in one step or in a series of steps

$$\Delta H_c = y_1 LFL_{mix} \Delta h_{c,H_2} + y_2 LFL_{mix} \Delta h_{c,C_aH_b} \quad [6.10]$$

where $\Delta h_{c,\,H2}$ and $\Delta h_{c,\,CaHb}$ are the molar heats of combustion of H_2 (J/mol H_2) and of the hydrocarbon C_aH_b (J/mol C_aH_b), respectively, at the initial temperature T_i = 298K. The values of $\Delta h_{c,\,H2}$ and $\Delta h_{c,\,CaHb}$ can be obtained from the physical-chemical data of hydrogen and the corresponding hydrocarbon, and are presented in Table 18.[94]

Table 18: Molar heat of combustion of the fuels[94]

Fuel	Molar heat of combustion, Δh_c (kJ/mol fuel)
H_2	-241.826
CH_4	-802.32
C_2H_6	-1427.84
n-C_4H_{10}	-2658.45
C_2H_4	-1322.96

Combining equation [6.9], [6.10] with the numbers of moles of products (n_i) and the total mole number change (Δn) as provided in Table 17, the heat capacities at constant volume for combustion products (C_{vi}) as given by Table 19, and the governing equation [6.8], the LFL_{mix} of the binary fuel mixtures can be estimated. The calculated LFL_{mix} of various binary mixtures of hydrogen and hydrocarbons at atmospheric and

sub-atmospheric pressures are compared with the experimental data to verify the application of CAFT model to the prediction of the LFL of the mixtures.

Table 19: Heat capacities at constant volume for combustion products [94]

Products	$C_v = a + bT + cT^2 + dT^3$ (J/mol K)			
	A	b x 10^2	c x 10^5	d x 10^9
O_2	17.146	1.519	-0.715	1.311
N_2	20.569	-0.157	0.808	-2.971
CO_2	13.929	5.977	-3.499	7.464
H_2O	23.904	0.192	1.055	-3.593
H_2	18.565	0.435	-0.033	0

b) CAFT model for the upper flammability limit (UFL)

For UFL, the amount of fuels is in excess, it can be assumed that oxygen reacts completely. For simplicity, it is also assumed that there is negligible dissociation of combustion products. The overall combustion reaction of the fuels in air at UFL is represented by reaction (6.2) and the numbers of moles of the products is detailed in Table 20

$$y_1H_2 + y_2C_aH_b + (ay_2 + \frac{y_1}{2} + \frac{y_2b}{4})O_2 \rightarrow ay_2CO_2 + (y_1 + \frac{y_2b}{2})H_2O \qquad (6.2)$$

where y_1, y_2 are the molar fractions of hydrogen and C_aH_b in the fuel mixture, respectively.

Table 20: Amount of combustion products for binary mixtures of hydrogen and hydrocarbons at UFL

Compounds	Number of moles before burning	Number of moles after burning (n_i)	The total mole number change (Δn)
H_2	$y_1 UFL_{mix}^*$	$y_1 UFL_{mix} - 0.21(1-UFL_{mix})k_1$	$0.21\ (1-UFL_{mix})\ k_5$
C_aH_b	$y_2 UFL_{mix}$	$y_2 UFL_{mix} - 0.21(1-UFL_{mix})k_2$	
O_2	$0.21(1-UFL_{mix})$	0	
N_2	$0.79(1-UFL_{mix})$	$0.79(1-UFL_{mix})$	
CO_2	0	$0.21(1-UFL_{mix})k_3$	
H_2O	0	$0.21(1-UFL_{mix})k_4$	

*UFL_{mix} is the UFL of the mixture of fuels

where:

$$k_1 = \frac{y_1}{ay_2 + \frac{y_1}{2} + b\frac{y_2}{4}} \qquad k_2 = \frac{y_2}{ay_2 + \frac{y_1}{2} + b\frac{y_2}{4}} \qquad k_3 = \frac{ay_2}{ay_2 + \frac{y_1}{2} + b\frac{y_2}{4}}$$

$$k_4 = \frac{y_1 + \frac{y_2 b}{2}}{ay_2 + \frac{y_1}{2} + b\frac{y_2}{4}} \qquad k_5 = \frac{ay_2 + \frac{y_2 b}{2} - y_2}{ay_2 + \frac{y_1}{2} + b\frac{y_2}{4}} - 1$$

The overall heat of combustion ΔH_c (J) of reaction (6.2) and in equation [6.8] can be estimated based on Hess's law of chemical reaction which states that for the conversion from reactants to products, the change of energy is the same whether the reaction takes place in one step or in a series of steps

$$\Delta H_c = 0.21(1\text{-}UFL_{mix})k_1\,\Delta h_{c,H_2} + 0.21(1\text{-}UFL_{mix})k_2\,\Delta h_{c,C_aH_b} \qquad [6.11]$$

where $\Delta h_{c,\,H2}$ and $\Delta h_{c,\,CaHb}$ are the molar heats of combustion of H_2 (J/mol H_2) and of the hydrocarbon C_aH_b (J/mol C_aH_b), respectively, at the initial temperature T_i = 298K. The value of $\Delta h_{c,\,H2}$ and $\Delta h_{c,\,CaHb}$ can be obtained from the physical-chemical data of hydrogen and the corresponding hydrocarbon (Table 18).[94]

Combining equation [6.9], [6.11] with the numbers of moles of products (ni) and the total mole number change (Δn) as provided in Table 10, the heat capacities at constant volume for combustion products (Cvi) as given by Table 21, and the governing equation [6.8], the UFLmix of the binary fuel mixtures can be estimated. The calculated UFLmix of various binary mixtures of hydrogen and hydrocarbons at atmospheric and sub-atmospheric pressures are compared with the experimental data to verify the application of CAFT model to the prediction of the UFL of the mixtures.

Table 21: Heat capacities at constant volume for combustion products [94]

Products	$C_v = a + bT + cT^2 + dT^3$ (J/mol K)			
	a	b x 10^2	c x 10^5	d x 10^9
O_2	17.146	1.519	-0.715	1.311
N_2	20.569	-0.157	0.808	-2.971
CO_2	13.929	5.977	-3.499	7.464
H_2O	23.904	0.192	1.055	-3.593
H_2	18.565	0.435	-0.033	0
CH_4	11.561	5.021	1.268	-11.004
C_2H_6	-1.419	17.255	-6.402	7.28
C_4H_{10}	-4.36	37.126	-18.326	34.979
C_2H_4	-4.364	15.628	-8.339	17.657

6.2. Results and discussion

6.2.1. UFLs and LFLs of mixtures of hydrogen and hydrocarbons

a) Mixtures of hydrogen and methane

The LFLs of mixtures of hydrogen and methane at room temperature and initial pressures of 1.0 atm, 0.5 atm and 0.1 atm are presented in Figure 46. Overall, the LFL of the mixture decreases when the fraction of hydrogen in the fuel composition increases. Pressure shows little effect on the LFLs of the mixtures since the LFLs do not change much when the pressure decreases from 1.0 atm to 0.1 atm. The maximum absolute deviation of the LFLs from each other is 0.2 mol%. This can be explained by the little impact of pressure on the LFLs of pure hydrogen and pure methane as described in Section 4.1. The change of the LFLs with pressure increases when the fraction of hydrogen in the fuel composition increases. This is understandable since hydrogen LFL varies more with pressure than methane LFL which does not change when the pressure decreases from 1.0 atm to 0.1 atm as observed in Section 4.1.2. The LFLs of the mixtures is the lowest at 0.5 atm.

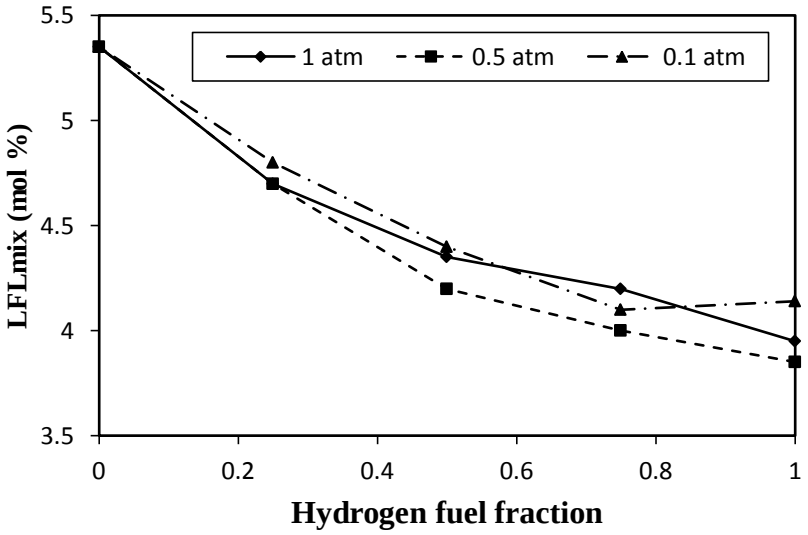

Figure 46: LFLs of mixtures of hydrogen and methane at room temperature and initial pressures of 1.0 atm, 0.5 atm, and 0.1 atm

The UFLs of mixtures of hydrogen and methane at room temperature and initial pressures of 1.0 atm, 0.5 atm, and 0.1 atm are presented in Figure 47. Overall, the UFL of the mixture increases when the fraction of hydrogen in the fuel composition increases. This is understandable since hydrogen has much higher UFLs than methane (Section 4); therefore, the more hydrogen in the mixture, the higher the UFL and the more risk of fire and explosion. With respect to the influence of pressure, the UFLs of the mixtures change much more with pressure compared to the LFLs. The higher the fraction of hydrogen, the more change of the UFLs with pressure. For example, the maximum absolute deviations of the UFL from 1.0 atm is 3.3 mol% at 0.5 atm (0.2 mol% for the LFL), and 7.4 mol% at 0.1 atm (0.2 mol% for the LFL). The larger influence of pressure on the UFLs of the mixtures can be explained by the higher impact of pressure on the

UFLs of the pure components (Section 4.2). The UFLs of the mixtures are the highest at 1.0 atm, followed by 0.5 atm and 0.1 atm. This means at rich fuel concentration, that the higher the initial pressure, the higher hazard/risk of fire for the mixtures.

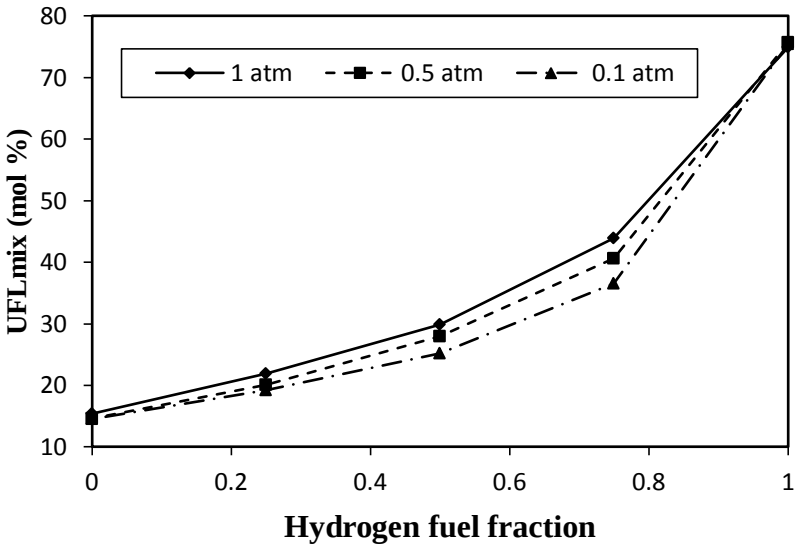

Figure 47: UFLs of mixtures of hydrogen and methane at room temperature and initial pressures of 1.0 atm, 0.5 atm, and 0.1 atm

Combining the LFLs and the UFLs, the flammable range of mixtures of hydrogen and methane at 1.0 atm, 0.5 atm, and 0.1 atm are presented in Figure 48. As can be seen in Figure 48, the flammable region of the mixture widens when the fraction of hydrogen in the mixture increases. With respect to the influence of pressure, when the initial pressure decreases, the flammable region narrows, which is understandable since the UFL of the mixture decreases more significantly with decreasing pressure while the LFL does not vary much with pressure.

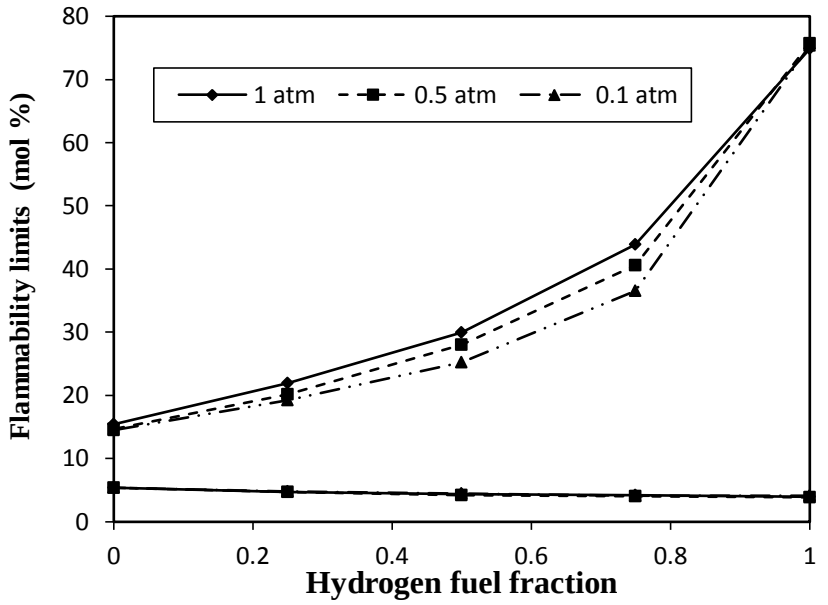

Figure 48: The flammability region of mixtures of hydrogen and methane at room temperature and initial pressure of 1.0 atm, 0.5 atm, and 0.1 atm

b) Mixtures of hydrogen and ethane

The LFLs of mixtures of hydrogen and ethane at room temperature and pressures of 1.0 atm, 0.5 atm, and 0.1 atm is shown in Figure 49. In general, the LFL of the mixture increases with the increasing fraction of hydrogen. It is found that pressure has little impact on the LFL of the mixtures since there is not much difference among the LFLs at 1.0 atm, 0.5 atm, and 0.1 atm. The LFL only shows appreciable difference when the pressure change from 1.0 atm to 0.1 atm and when the hydrogen fraction is 0 (pure ethane). The LFL is the lowest at 1 atm when the fraction of hydrogen is equal or less than 0.25, and at 0.5 atm when the fraction of hydrogen is equal or larger than 0.5.

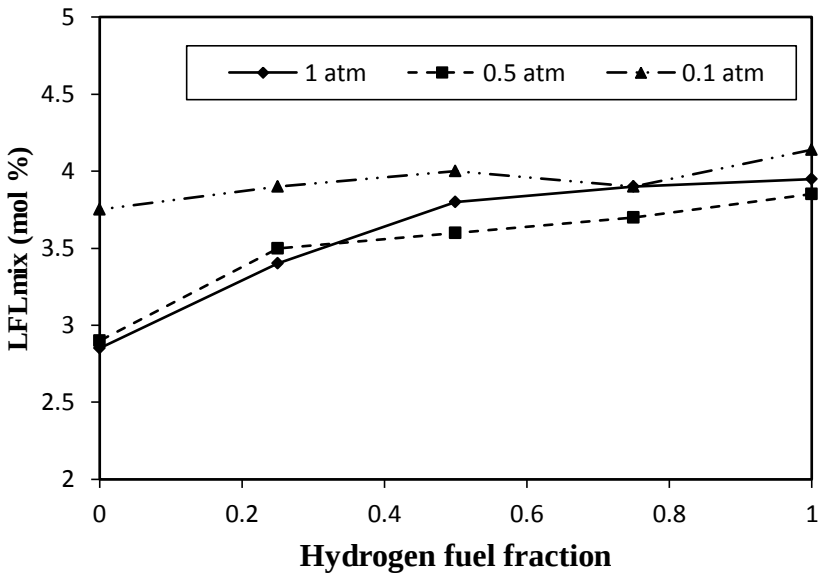

Figure 49: LFLs of mixtures of hydrogen and ethane at room temperature and initial pressures of 1.0 atm, 0.5 atm, and 0.1 atm

The UFLs of mixtures of hydrogen and ethane at room temperature and initial pressures of 1.0 atm, 0.5 atm, and 0.1 atm are presented in Figure 50. Similar to the observation of the LFLs, the UFL of the mixture increases when the fraction of hydrogen in the fuel composition increases. With respect to the influence of pressure, the UFLs of the mixtures vary slightly less than the UFLs of mixtures with methane; however, compared to the LFLs of the same mixtures with ethane, the UFLs are still affected much more with pressure. For example, the maximum absolute deviations of the UFL from 1.0 atm is 2.4 mol% at 0.5 atm (0.2 mol% for the LFL), and 5.5 mol % at 0.1 atm (0.9 mol% for the LFL). The larger influence of pressure on the UFLs of the mixtures can be explained by the higher impact of pressure on the UFLs of the pure components

(Section 4.2). And the higher the fraction of hydrogen, the more change of the UFLs with pressure. The UFLs of the mixtures are the highest at 1.0 atm, followed by 0.5 atm and 0.1 atm. This means at rich fuel concentration, that the higher the initial pressure, the higher hazard/risk of fire for the mixtures.

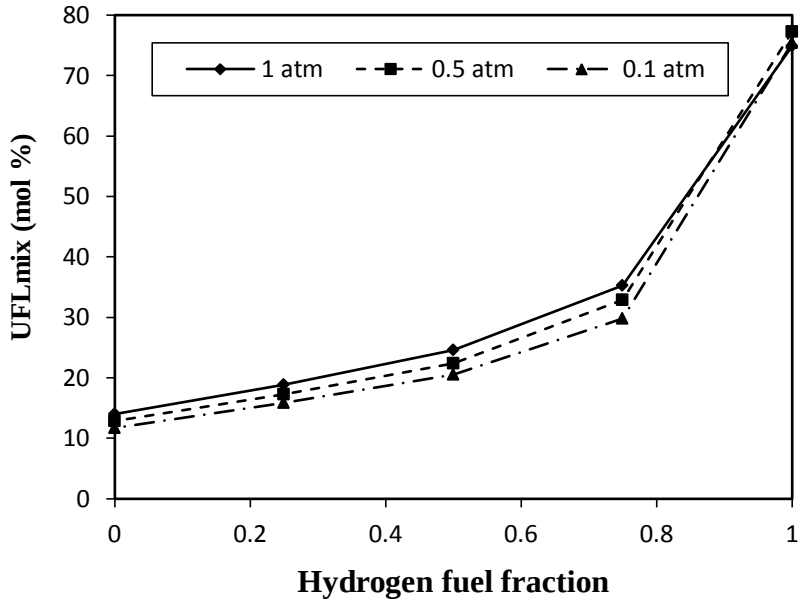

Figure 50: UFLs of mixtures of hydrogen and ethane at room temperature and initial pressures of 1.0 atm, 0.5 atm, and 0.1 atm

Combining the LFLs and the UFLs, the flammable range of mixtures of hydrogen and ethane at 1.0 atm, 0.5 atm, and 0.1 atm are presented in Figure 51. As can be seen in Figure 51, the flammable region of the mixture widens when the fraction of hydrogen in the mixture increases. With respect to the influence of pressure, when the initial pressure decreases, the flammable region narrows, which is understandable since

the UFL of the mixture decreases more significantly with decreasing pressure while the LFL does not vary much with pressure.

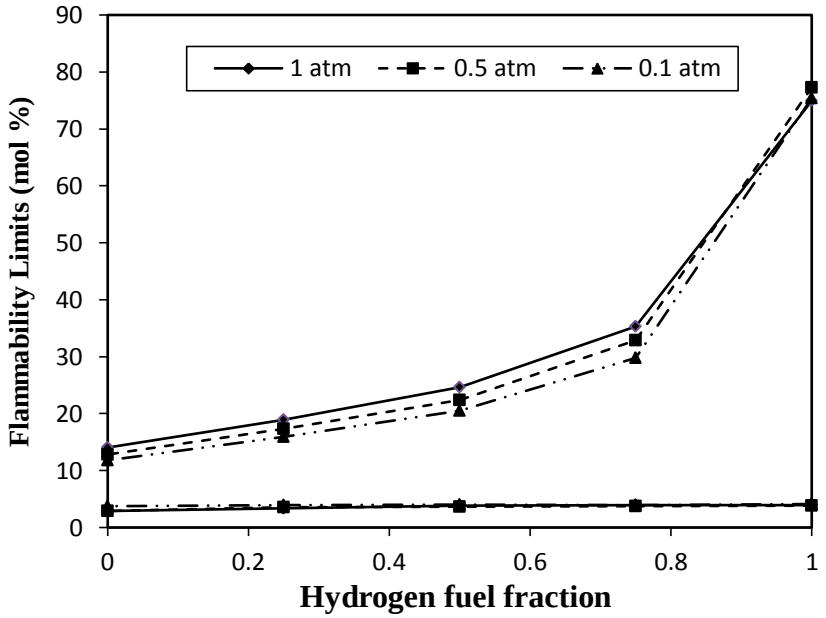

Figure 51: The flammability region of mixtures of hydrogen and ethane at room temperature and initial pressure of 1.0 atm, 0.5 atm, and 0.1 atm

c) Mixtures of hydrogen and *n*-butane

The LFLs of mixtures of hydrogen and *n*-butane at room temperature and pressures of 1.0 atm, 0.5 atm, and 0.1 atm is shown in Figure 52. Overall, the LFL of the fuel mixture increases when the fraction of hydrogen increases. With respect to the influence of pressure, the LFL of the mixture does not show any appreciable change when the initial pressure decrease from 1.0 atm to 0.5 atm. The LFLs of the mixture of

hydrogen and *n*-butane only show noticeable changes when the pressure decreases to 0.1 atm; however, the changes are still small, within 0.9 mol%.

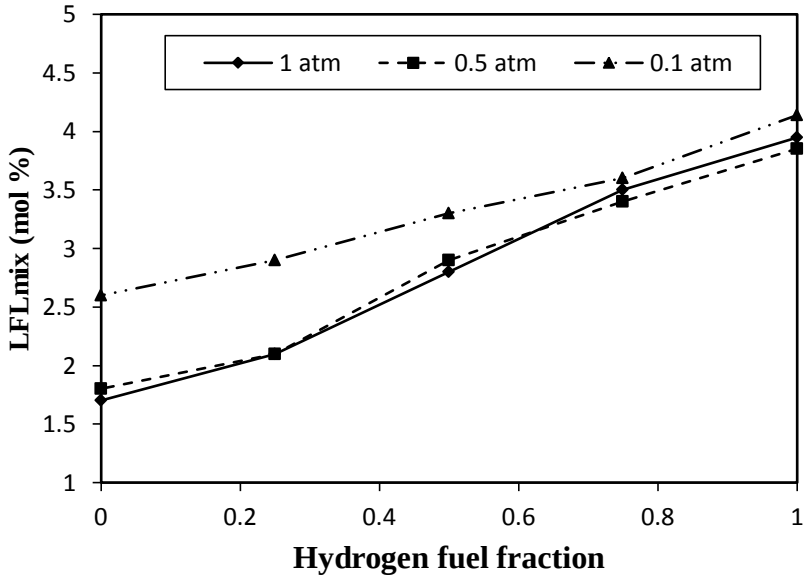

Figure 52: LFLs of mixtures of hydrogen and *n*-butane at room temperature and initial pressures of 1.0 atm, 0.5 atm, and 0.1 atm

The UFLs of mixtures of hydrogen and *n*-butane at room temperature and initial pressures of 1.0 atm, 0.5 atm, and 0.1 atm are presented in Figure 53. Overall, the UFL of the mixture increases when the fraction of hydrogen in the fuel composition increases; thus, the more hydrogen in the mixture, the higher the UFL and the more risk of fire and explosion. Similar to what is observed with mixtures with methane and with ethane, the UFLs of the mixtures with *n*-butane are the highest at 1.0 atm, followed by 0.5 atm and 0.1 atm. This means that the higher the initial pressure, the higher hazard/risk of fire for

the mixtures. With respect to the influence of pressure, the UFLs of the mixtures vary less than the UFLs of mixtures with methane and with ethane; however, compared to the LFLs of the same mixtures with *n*-butane, the UFLs are impacted much more with pressure. For example, the maximum absolute deviations of the UFL from 1.0 atm is 2.3 mol% at 0.5 atm (0.1 mol% for the LFL), and 3.6 mol% at 0.1 atm (0.9 mol% for the LFL). And the higher the fraction of hydrogen, the more change of the UFLs with pressure.

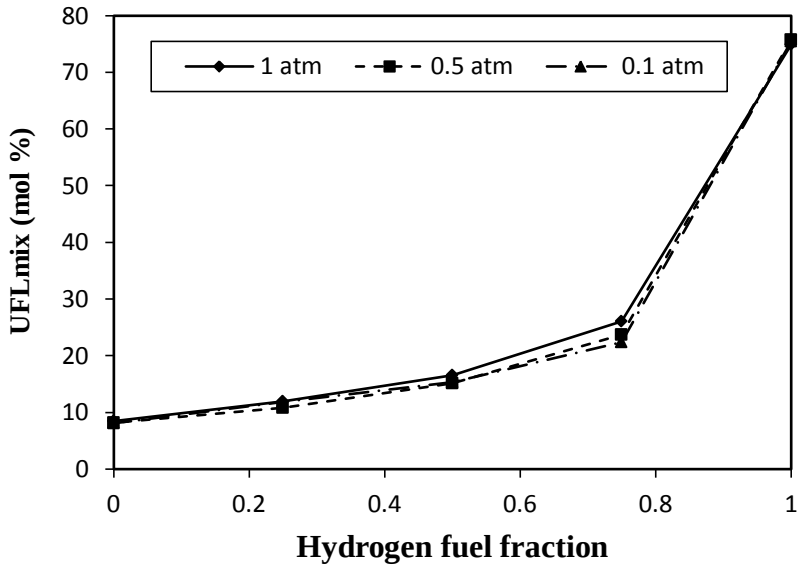

Figure 53: UFLs of mixtures of hydrogen and *n*-butane at room temperature and initial pressures of 1.0 atm, 0.5 atm, and 0.1 atm

Combining the LFLs and the UFLs, the flammable range of mixtures of hydrogen and *n*-butane at 1.0 atm, 0.5 atm, and 0.1 atm are presented in Figure 54. As can be seen in Figure 54, the flammable region of the mixture widens when the fraction

of hydrogen in the mixture increases. With respect to the influence of pressure, when the initial pressure decreases, the flammable region narrows, which is understandable since the UFL of the mixture decreases more significantly with decreasing pressure while the LFL does not vary much with pressure.

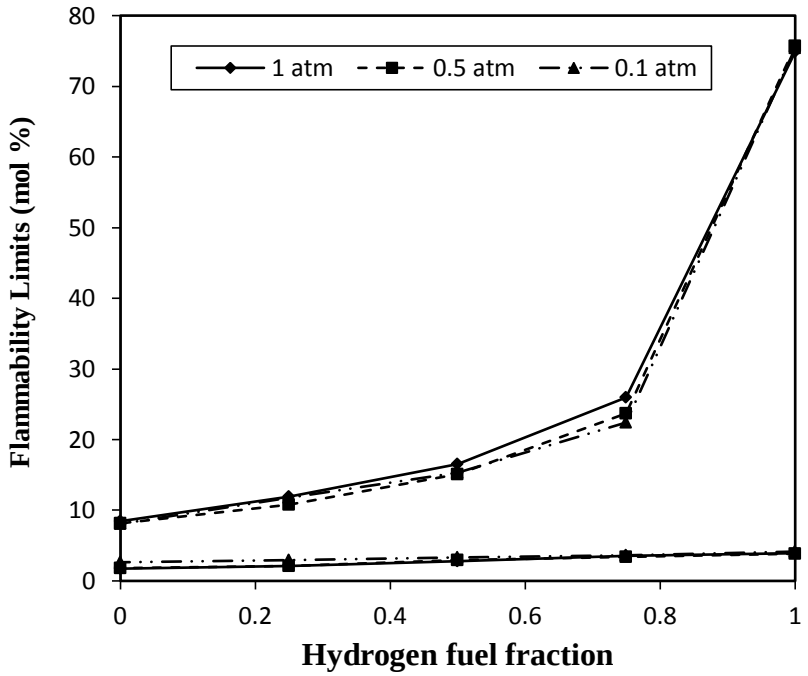

Figure 54: The flammability region of mixtures of hydrogen and *n*-butane at room temperature and initial pressure of 1.0 atm, 0.5 atm, and 0.1 atm

d) Mixtures of hydrogen and ethylene

The LFLs of mixtures of hydrogen and ethylene at room temperature and pressures of 1.0 atm, 0.5 atm, and 0.1 atm is shown in Figure 55. Overall, the LFL of the mixture increase with the increasing fraction of hydrogen. Similar to what is observed

for the mixtures of hydrogen and the alkanes, the LFLs of the mixtures of hydrogen and ethylene are not much affected by the pressure since the LFLs do not change much when the pressure decreases from 1.0 atm to 0.1 atm. The largest change in the LFLs is when the pressure decreases to 0.1 atm and when the fraction of hydrogen is 0 (pure ethylene).

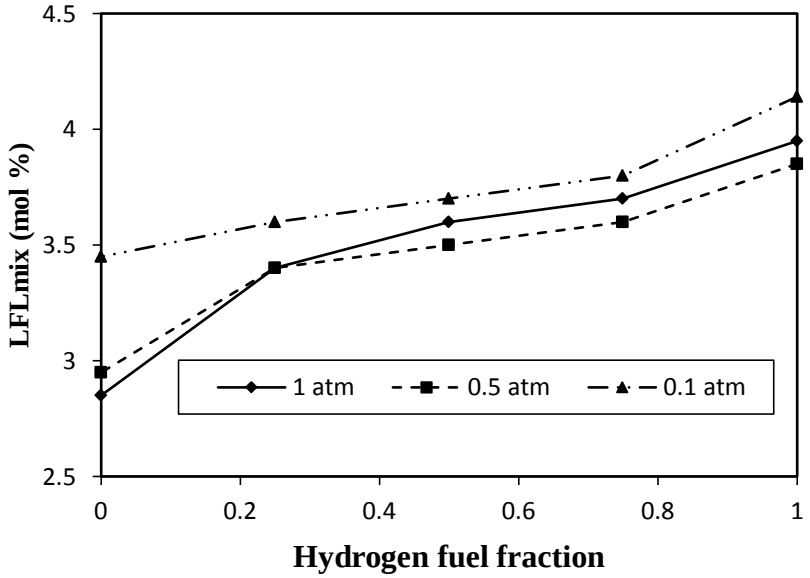

Figure 55: LFLs of mixtures of hydrogen and ethylene at room temperature and initial pressures of 1.0 atm, 0.5 atm, and 0.1 atm

The UFLs of mixtures of hydrogen and ethylene at room temperature and initial pressures of 1.0 atm, 0.5 atm, and 0.1 atm are presented in Figure 56. Overall, the UFL of the mixture increases when the fraction of hydrogen in the fuel composition increases; thus, the more hydrogen in the mixture, the higher the UFL and the more risk of fire and explosion. Similar to what is observed with mixtures of hydrogen and the alkanes, the

UFLs of mixtures with ethylene are the highest at 1.0 atm, followed by 0.5 atm and 0.1 atm. This means that the higher the initial pressure, the higher hazard/risk of fire for the mixtures at rich fuel concentration. With respect to the influence of pressure, the UFLs of the mixtures of hydrogen and ethylene are much more affected by pressure than mixtures of hydrogen and the alkanes. In contrast to what is observed with mixtures with the alkanes, the UFLs of mixtures with ethylene change more with pressure when the fraction of hydrogen in the fuel composition decreases. This can be explained by the huge impact of pressure on the UFL of pure ethylene compared with others. Therefore, the more ethylene (the less hydrogen) in the fuel, the more sensitive the UFL is to the influence of pressure. Compared with the LFLs of the same mixtures of hydrogen and ethylene, the UFLs are affected much more by pressure. For example, the maximum absolute deviations of the UFL of the mixtures from 1.0 atm is 3.8 mol% at 0.5 atm (0.1 mol% for the LFL), and 12.6 mol% at 0.1 atm (0.6 mol% for the LFL).

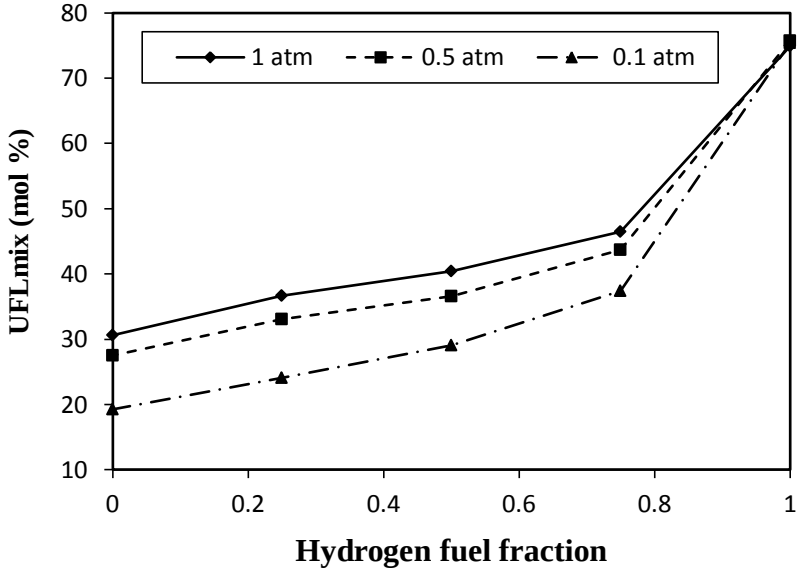

Figure 56: UFLs of mixtures of hydrogen and ethylene at room temperature and initial pressures of 1.0 atm, 0.5 atm, and 0.1 atm

Combining the LFLs and the UFLs, the flammable range of mixtures of hydrogen and ethylene at 1.0 atm, 0.5 atm, and 0.1 atm are presented in Figure 57. Similar to the observation made for mixtures of hydrogen and the alkanes, the flammable region of the mixture widens when the fraction of hydrogen in the mixture increases. Compared to mixtures of hydrogen and the alkanes, the flammable region of the mixture of hydrogen and ethylene is much more affected by pressure which can be seen clearly in Figure 57. When the initial pressure decreases below 1.0 atm, the flammable region narrows due to the significant decrease of the UFL with pressure; especially when there is more ethylene in the fuel mixture.

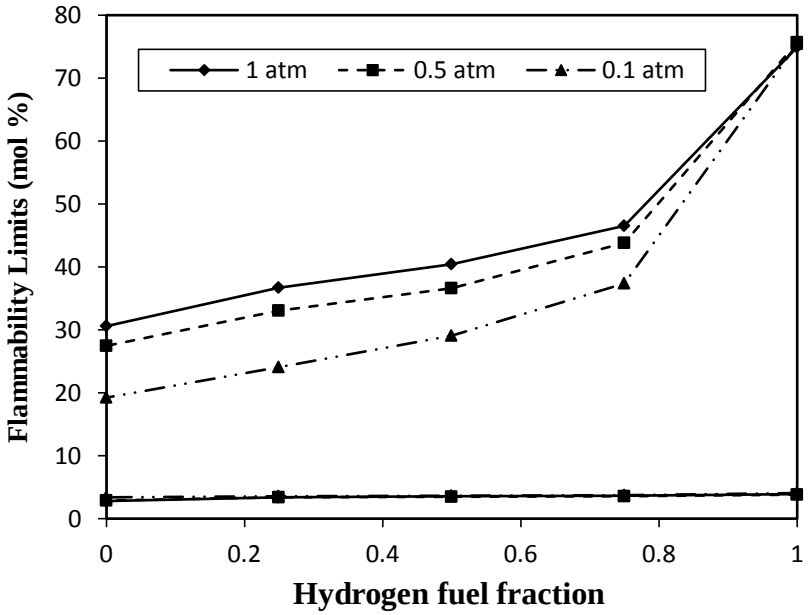

Figure 57: The flammability region of mixtures of hydrogen and ethylene at room temperature and initial pressure of 1.0 atm, 0.5 atm, and 0.1 atm

6.2.2. The application of Le Chatelier's rule and CAFT model

a) Mixtures of hydrogen and methane

The application of the Le Chatelier's rule and CAFT model for the LFLs of mixtures of hydrogen and methane at room temperature and initial pressures of 1.0 atm, 0.5 atm and 0.1 atm is presented by Figure 58, Figure 59 and Figure 60, respectively.

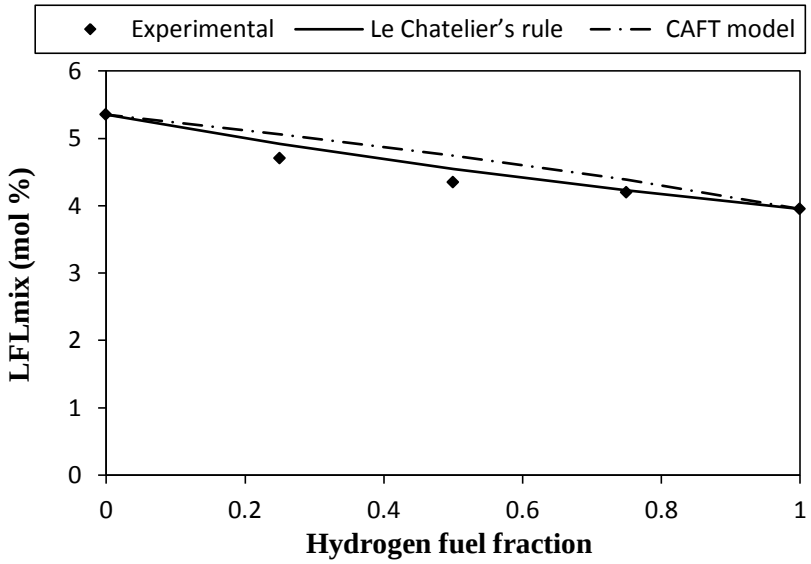

Figure 58: Application of Le Chatelier's rule and CAFT model to the LFLs of mixtures of hydrogen and methane at room temperature and 1.0 atm

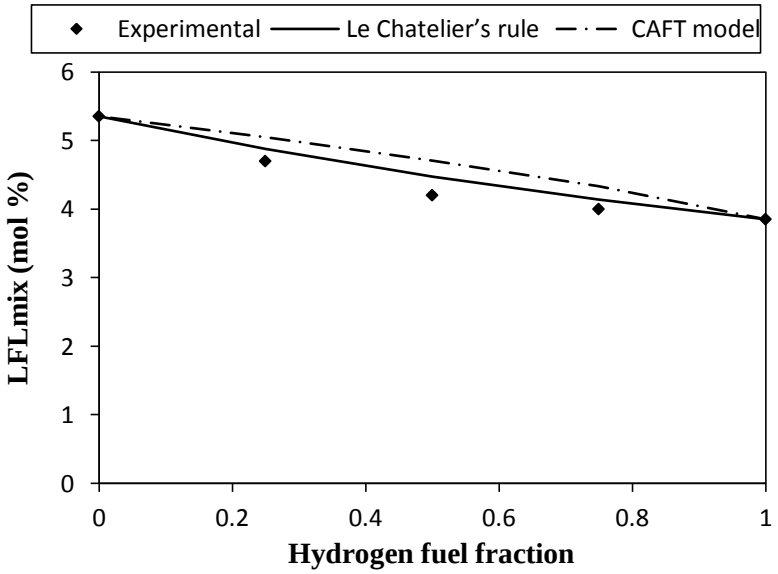

Figure 59: Application of Le Chatelier's rule and CAFT model to the LFLs of mixtures of hydrogen and methane at room temperature and 0.5 atm

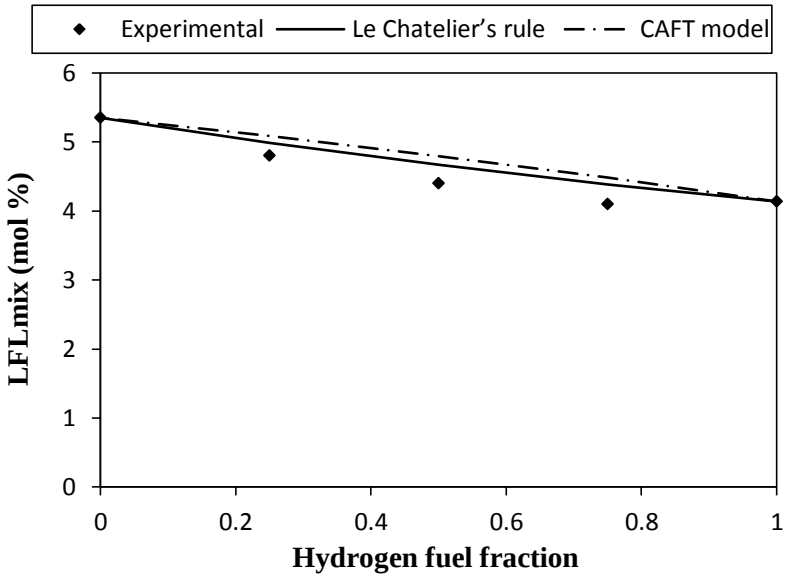

Figure 60: Application of Le Chatelier's rule and CAFT model to the LFLs of mixtures of hydrogen and methane at room temperature and 0.1 atm

Overall, Le Chatelier' rule could predict the LFLs of mixtures very well at all initial pressures. The relative difference between the experimental LFLs and the calculated LFLs is within 7.0% (0.3 mol% absolute difference), and the average relative difference is 4.5% (0.2 mol% absolute difference. With respect to the application of CAFT model, it is found that CAFT model can also predict the LFLs of the mixtures relatively well with the maximum relative difference is 12.2% (0.5 mol% absolute difference), and the average relative difference between experimental and calculated LFLs is 8.1% (0.4 mol% absolute difference). At all initial pressure, the maximum deviations from the experimental LFLs at all initial pressures occur when there are equal fractions of hydrogen and methane in the fuel mixture (fuel fraction of hydrogen is 0.5).

This may be attributed to the increased level of interaction between the fuels which is not taken in account by CAFT model.

For the UFLs, the application of the Le Chatelier's rule and CAFT model for mixtures at room temperature and initial pressures of 1.0 atm, 0.5 atm and 0.1 atm is presented by Figure 61, Figure 62, and Figure 63, respectively.

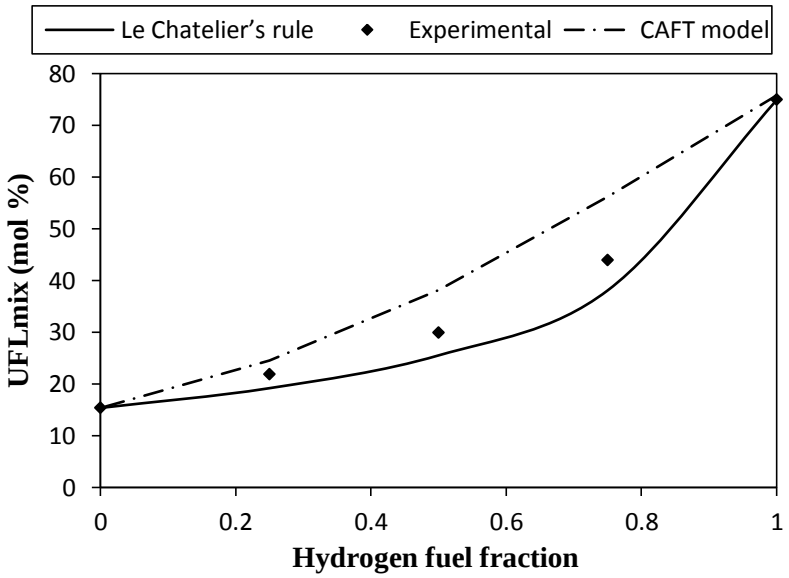

Figure 61: Application of Le Chatelier's rule and CAFT model to the UFLs of mixtures of hydrogen and methane at room temperature and 1.0 atm

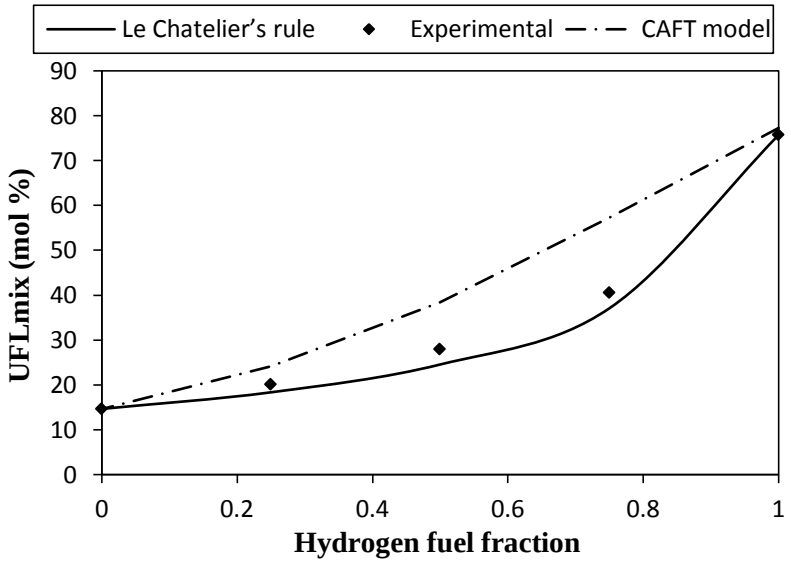

Figure 62: Application of Le Chatelier's rule and CAFT model to the UFLs of mixtures of hydrogen and methane at room temperature and 0.5 atm

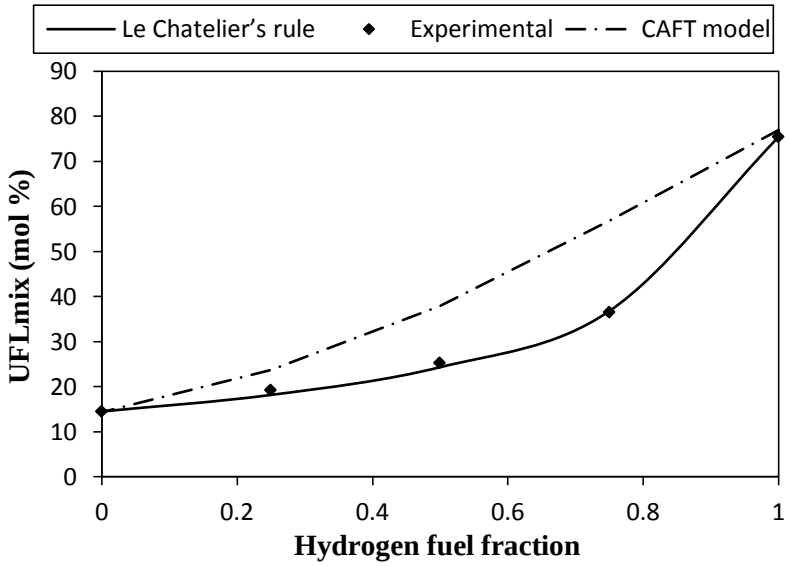

Figure 63: Application of Le Chatelier's rule and CAFT model to the UFLs of mixtures of hydrogen and methane at room temperature and 0.1 atm

Overall, Le Chatelier's rule could also predict the UFLs of the mixtures quite well. The level of prediction increases when the initial pressure decreases from 1.0 atm to 0.1 atm. This is understandable since there is less fuel interaction at lower pressure. The relative difference between the experimental and the calculated UFLs is within 14.6% (5.8 mol% absolute difference), and the average relative difference is 8.8% (2.6 mol% absolute difference). Compared to the LFLs, the differences between the experimental and calculated values for the UFLs are larger; which means that Le Chatelier's rule could predict the LFLs better than the UFLs. This is agreeable with observations in other studies when comparing the application of Le Chatelier's rule to LFL and UFL for mixtures of various fuels.[72, 106] The possible reason for the less accurate prediction of Le Chatelier's rule for UFL than for the LFL is discussed in sub-section 6.1.1 which is at the upper flammability limit, fuel no longer represents a small percentage of the mixture which contains a complex mixture of fuel, oxygen and nitrogen resulting in a wide variation from the initial to final heat capacities and molar quantities; therefore, the simple mixing rule of Le Chatlier's rule could not predict the UFL as good as it does for the LFL.

With respect to the application of the CAFT model, it is found that the CAFT model does not apply well to the UFLs of the mixtures. There are large deviations between the experimental and calculated UFLs. The maximum difference is as high as 55.8% (20.4 mol% absolute difference), and the average relative difference is 32.9% (10.2 mol% absolute difference). Compared to the application to the LFLs, the application to the UFLs shows much larger deviation. These can be explained by the

much more complex reaction mechanism at UFL which is not considered by the model. At UFL, fuel is in excess; therefore, the combustion is not complete.[58, 91] In addition, the flame temperature of hydrogen and methane is much higher at UFL (around 1400 K for hydrogen, 2200K for methane) which promote further dissociation of combustion products.[92] Thus, as shown by CHEMKIN simulation, the products of combustion include a wide variety of species such as H_2O, CO_2, CO, H_2, CH_4, NO, NO_2, H_2O_2, H, OH, HO_2, solid C, etc. Actual experiments also showed a lot of soot (solid C) from the combustion; the more methane in the mixture, the more amount of soot found. The product dissociation and soot absorb a lot of energy from combustion which is not taken into account my CAFT model. This explains the large deviation from experimental data, especially when the fraction of methane in the fuel composition increases. This also explains the over-estimation of the UFLs by CAFT model. Therefore, for the purpose of predicting the flammability limits (LFLs and UFLs) of the mixtures, it is recommended to apply the Le Chatlier's rule, not the CAFT model.

b) Mixtures of hydrogen and ethane

The application of Le Chatelier's rule and CAFT model to the predict the LFLs of mixtures of hydrogen and ethane at room temperature and initial pressures of 1.0 atm, 0.5 atm and 0.1 atm is presented by Figure 64, Figure 65 and Figure 66, respectively.

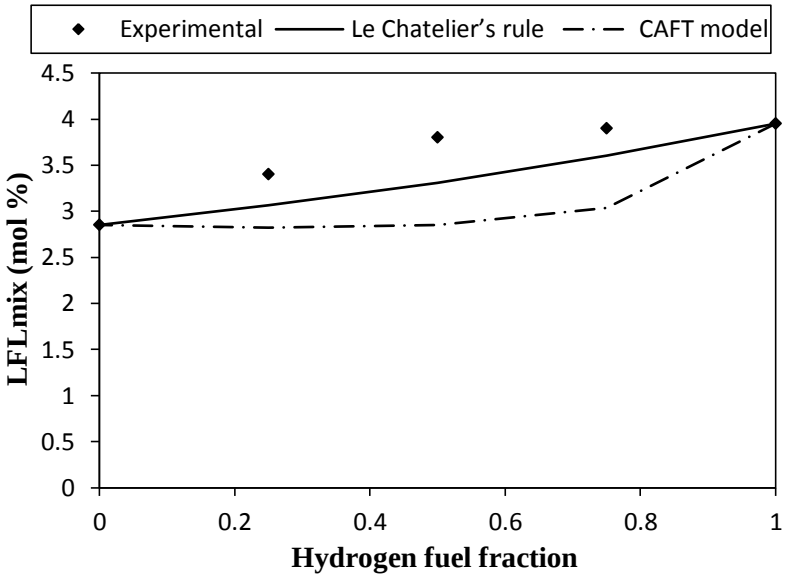

Figure 64: Application of Le Chatelier's rule and CAFT model to the LFLs of mixtures of hydrogen and ethane at room temperature and 1 atm

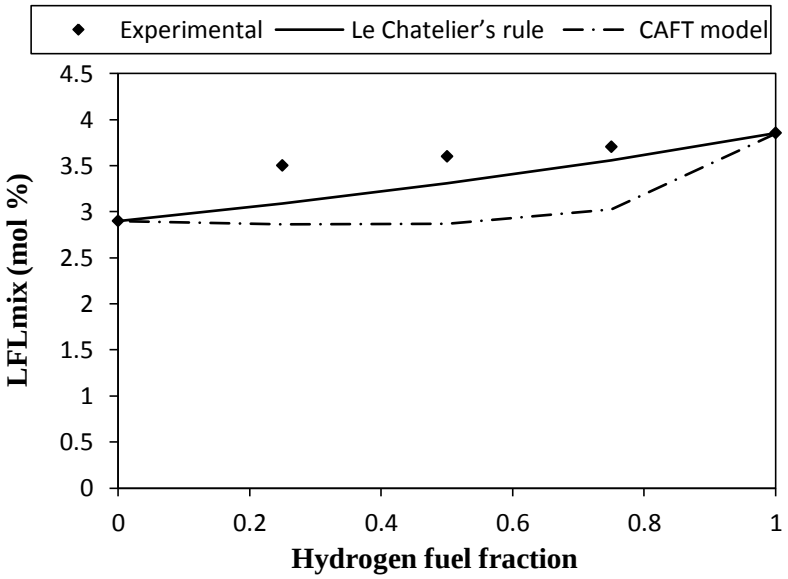

Figure 65: Application of Le Chatelier's rule and CAFT model to the LFLs of mixtures of hydrogen and ethane at room temperature and 0.5 atm

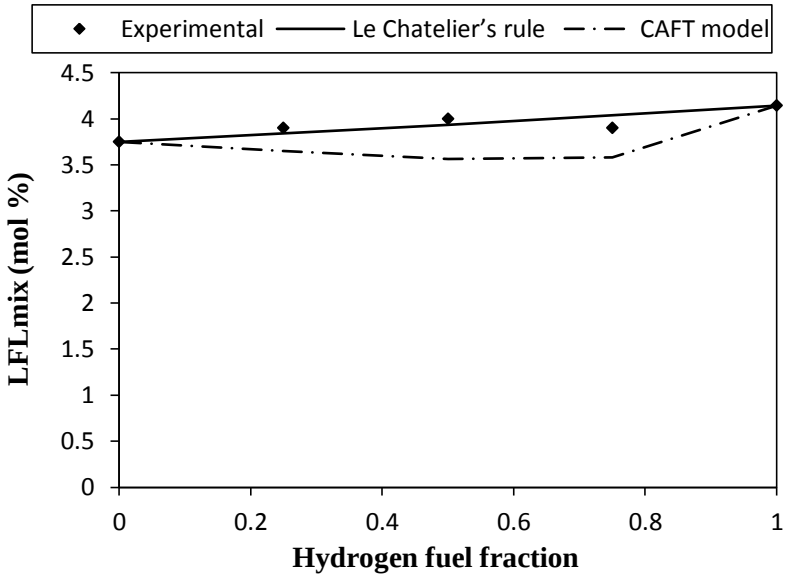

Figure 66: Application of Le Chatelier's rule and CAFT model to the LFLs of mixtures of hydrogen and ethane at room temperature and 0.1 atm

Overall, Le Chatelier's rule could predict the LFLs of the mixtures quite well. The relative difference between the experimental and the calculated LFLs is within 12.9% (0.5 mol% absolute difference), and the average relative difference is 6.7% (0.2 mol% absolute difference). The level of prediction of the rule increases when the initial pressure decreases from 1.0 atm to 0.1 atm. This is because of less fuel interaction at lower pressure. At all initial pressures, Le Chatelier's rule provides more conservative prediction of the LFLs (lower LFLs). Therefore, from a safety point of view, the application of Le Chatelier's rule for these mixtures is acceptable since it is both accurate and conservative. With respect to the application of CAFT model, there are

large deviations between the experimental and calculated LFLs. The maximum difference is 24.9% (1.0 mol% absolute difference), and average relative difference is 16.3% (0.6 mol% absolute difference). The deviation is the largest at 1.0 atm followed by 0.5 atm and 0.1 atm. With the same initial pressure, the deviation is the largest when there are equal fractions of hydrogen and ethane in the fuel mixture (hydrogen fraction is 0.5). The deviation can be explained by several reasons. First, there is a level of product dissociation which leads to more species not taken into account by CAFT model. CHEMKIN[62] simulation shows a noticeable amount of NO, and OH in the products of combustion. Second, the interaction of the fuels (hydrogen and ethane) could be a factor which disturbs the combustion reaction; the interaction is the largest when there are equal fractions of the fuel (this is also observed with mixtures of hydrogen and methane).[107] For these reasons, the application of CAFT for mixtures of hydrogen and ethane is even less accurate than a simple empirical mixing rule by Le Chatelier.

For the UFLs, the application of the Le Chatelier's rule and CAFT to the mixtures at room temperature and initial pressures of 1.0 atm, 0.5 atm and 0.1 atm is presented by Figure 67, Figure 68 and Figure 69, respectively.

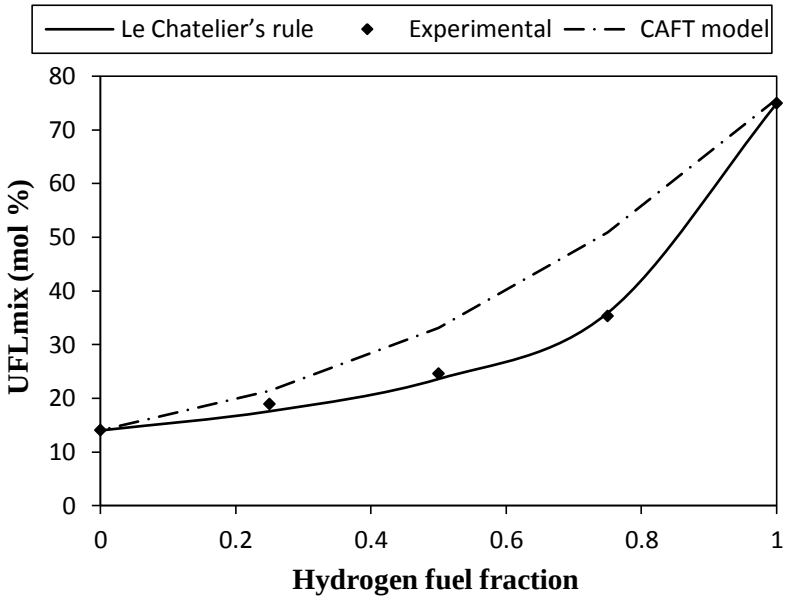

Figure 67: Application of Le Chatelier's rule and CAFT model to the UFLs of mixtures of hydrogen and ethane at room temperature and 1.0 atm

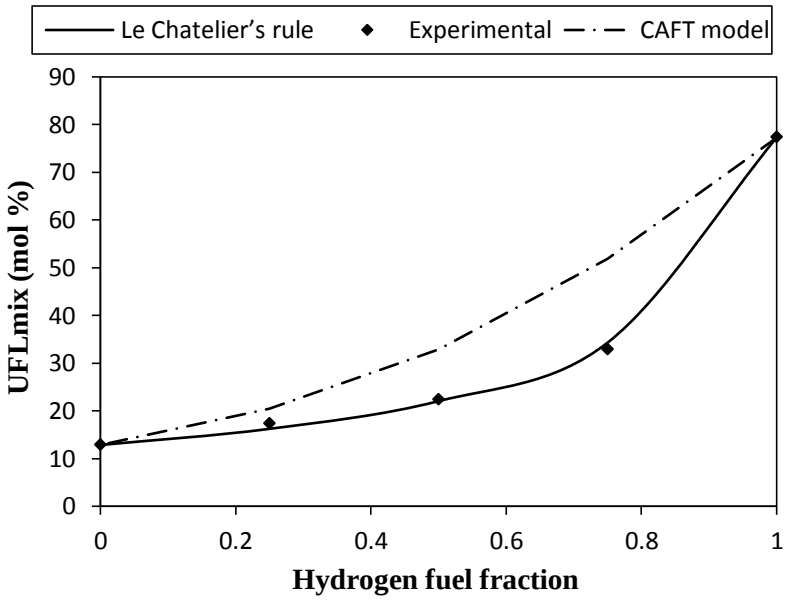

Figure 68: Application of Le Chatelier's rule and CAFT model to the UFLs of mixtures of hydrogen and ethane at room temperature and 0.5 atm

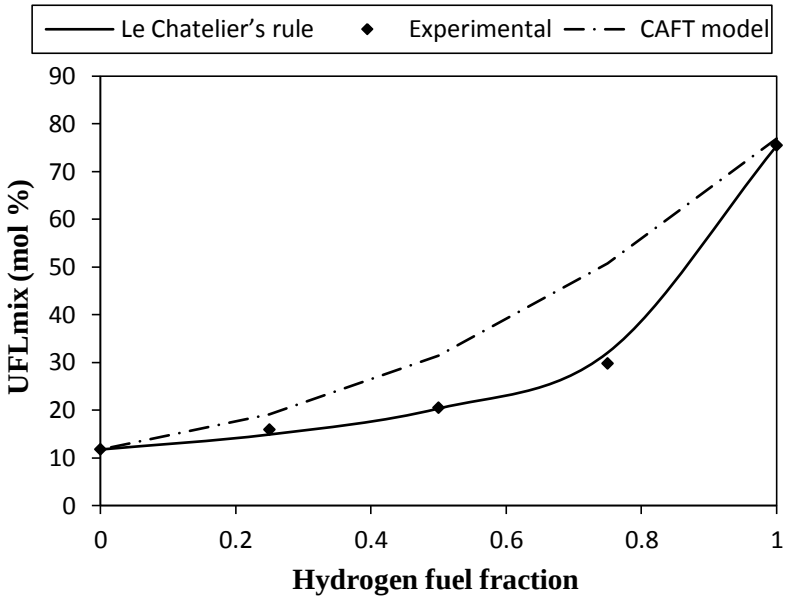

Figure 69: Application of Le Chatelier's rule and CAFT model to the UFLs of mixtures of hydrogen and ethane at room temperature and 0.1 atm

Overall, Le Chatlier's rule could predict the UFLs of the mixtures of hydrogen and ethane very well at all initial pressures. The maximum relative difference between the experimental and calculated UFLs is 7.5% (2.2 mol% absolute difference), and the average relative difference is 4.4% (1.0 mol% absolute difference). With respect to the application of CAFT model, large deviations from experimental data are observed. The maximum relative deviation from experimental UFLs is as much as 70.4% (21.0 mol% absolute deviation), and the average relative deviation is 39.9% (10.5% absolute deviation). The reasons for the deviation are the same as those explained for mixtures of hydrogen and methane. Therefore, it is recommended to apply Le Chatelier's rule for the

purpose of predicting the flammability limits (LFLs and UFLs) of the mixtures not the CAFT model.

c) Mixtures of hydrogen and *n*-butane

The application of Le Chatelier's rule and CAFT model to the LFLs of the mixtures at room temperature and initial pressures of 1.0 atm, 0.5 atm and 0.1 atm, is illustrated by Figure 70, Figure 71, and Figure 72, respectively.

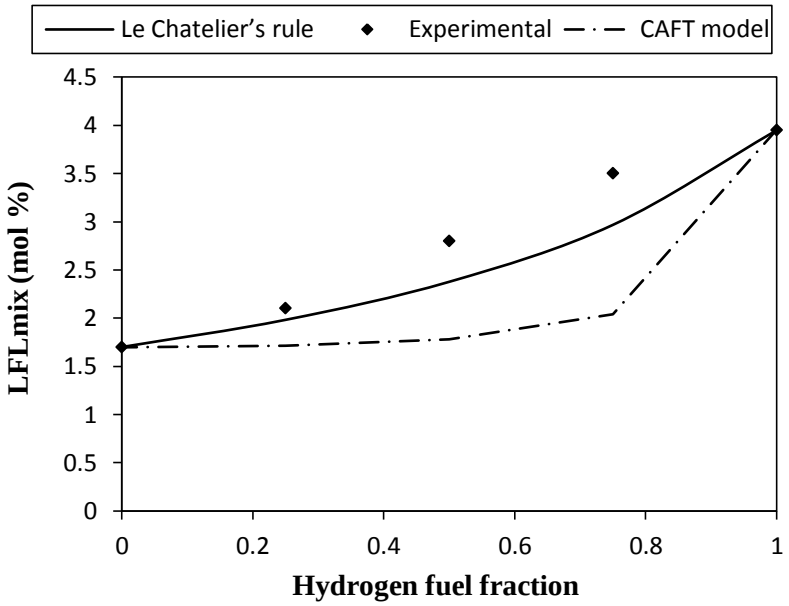

Figure 70: Application of Le Chatelier's rule and CAFT model to the LFLs of mixtures of hydrogen and *n*-butane at room temperature and 1.0 atm

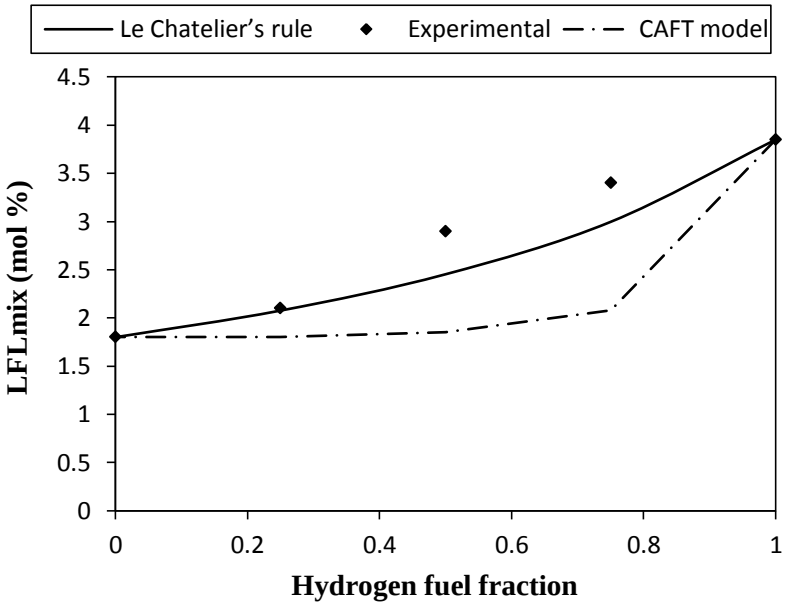

Figure 71: Application of Le Chatelier's rule and CAFT model to the LFLs of mixtures of hydrogen and *n*-butane at room temperature and 0.5 atm

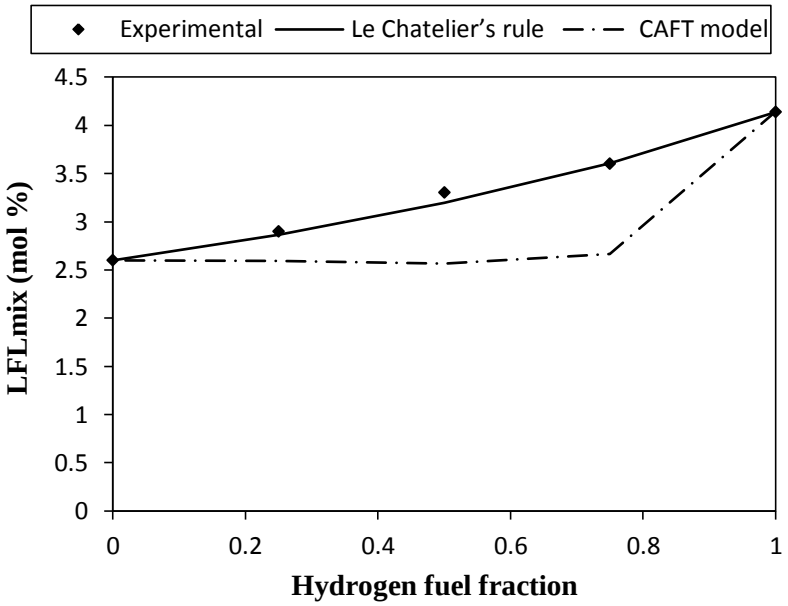

Figure 72: Application of Le Chatelier's rule and CAFT model to the LFLs of mixtures of hydrogen and *n*-butane at room temperature and 0.1 atm

Overall, Le Chatelier's rule could predict the LFLs of the mixtures quite well, though the level of prediction is not as good as those observed for mixtures of hydrogen and methane, hydrogen and ethane. The relative difference between the experimental and the calculated LFLs is within 15.4% (0.5 mol% absolute difference), and the average relative difference is 7.6% (0.2 mol% absolute difference). The level of prediction of the rule increases when the initial pressure decreases from 1.0 atm to 0.1 atm. This is because there is less effect of fuel interaction at lower pressure. At all initial pressures, Le Chatelier's rule provides more conservative prediction of the LFLs (lower LFLs). Therefore, from a safety point of view, the application of Le Chatelier's rule for these mixtures is acceptable since it is both accurate and conservative.

On the application of CAFT model, there are large differences between the experimental and calculated LFLs. The maximum relative difference is 41.6% (1.5 mol% absolute difference), and the average relative difference is 27.2% (0.8 mol% absolute difference). The deviation decreases slightly when the pressure decreases from 1.0 atm to 0.1 atm. At the same initial pressure, the deviation increases with increasing fraction of hydrogen in the fuel mixture, except for pure hydrogen. The reasons for the deviation are the same as those described for mixtures of hydrogen and ethane. For mixtures of hydrogen and butane, the deviation is even larger since the degree of dissociation of combustion products is greater due to the large flame temperature of *n*-butane (AFT is 1940K at 1.0 atm, 2409K at 0.1 atm, Section 5) which is not taken into account by the CAFT model. [91]

For the UFLs, the application of the Le Chatelier's rule and CAFT model for the mixtures at room temperature and initial pressures of 1.0 atm, 0.5 atm and 0.1 atm is presented by Figure 73, Figure 74 and Figure 75, respectively.

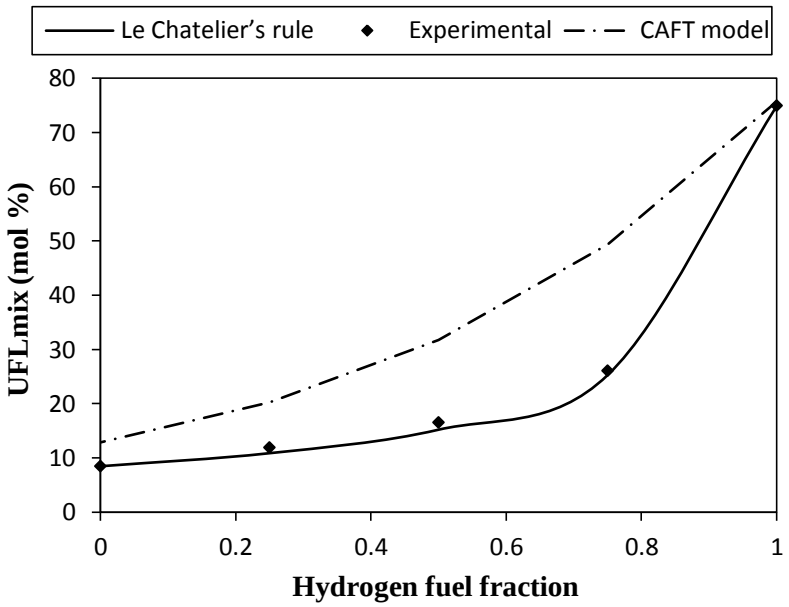

Figure 73: Application of Le Chatelier's rule and CAFT model to the UFLs of mixtures of hydrogen and *n*-butane at room temperature and 1.0 atm

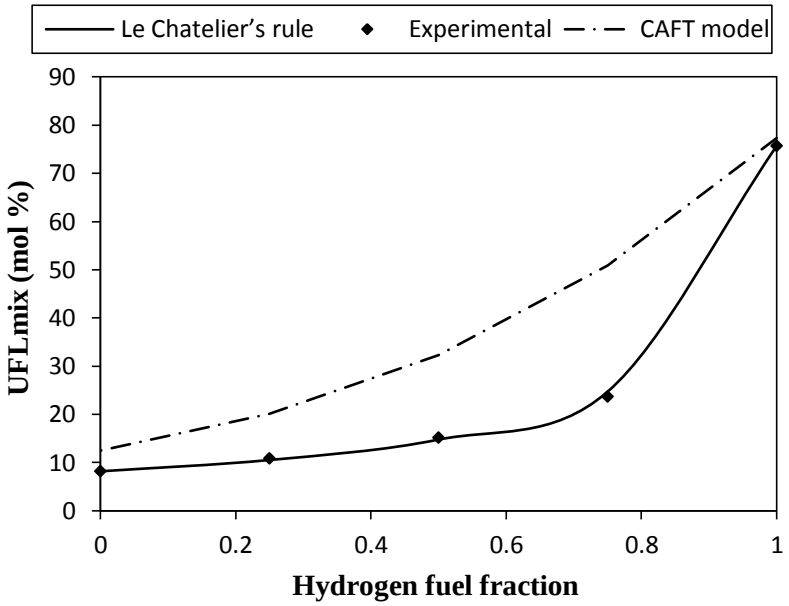

Figure 74: Application of Le Chatelier's rule and CAFT model to the UFLs of mixtures of hydrogen and *n*-butane at room temperature and 0.5 atm

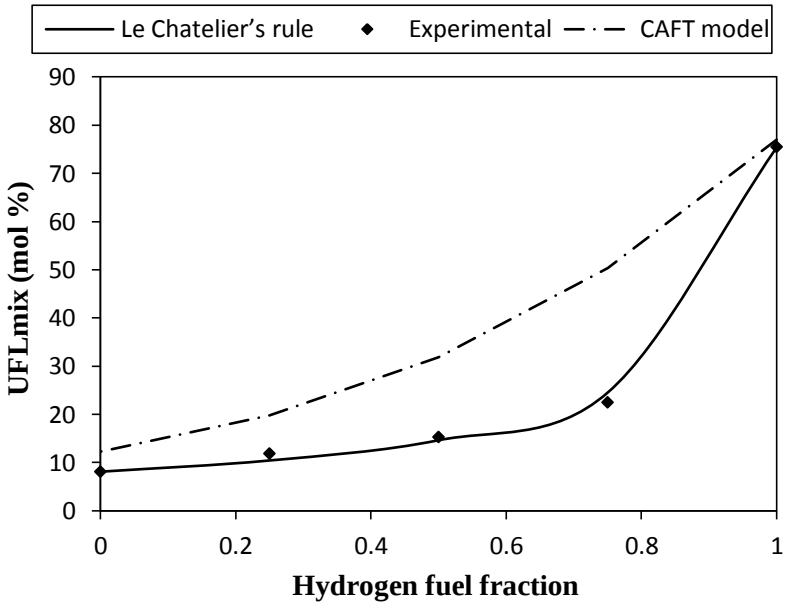

Figure 75: Application of Le Chatelier's rule and CAFT model to the UFLs of mixtures of hydrogen and *n*-butane at room temperature and 0.1 atm

As can be seen from Figure 73, Figure 74, and Figure 75, Le Chatlier's rule could predict the UFLs of the mixtures of hydrogen and butane quite well at all initial pressures. The maximum relative difference between the experimental and calculated UFLs is 11.6% (2.1 mol% absolute difference), and the average relative difference is 6.0% (1.0 mol% absolute difference). On the application of CAFT model, large deviations from experimental data are also observed. The maximum relative deviation from experimental UFLs is 124.8% (28.0% absolute deviation), and the average relative deviation is as much as 96.4% (17.0 mol% absolute deviation). The reasons for the deviation are the same as those explained for mixtures of hydrogen and methane.

d) Mixtures of hydrogen and ethylene

The application of the Le Chatelier's rule and CAFT model to the LFLs of the mixtures at room temperature and initial pressures of 1.0 atm, 0.5 atm and 0.1 atm is presented by Figure 76, Figure 77, and Figure 78, respectively.

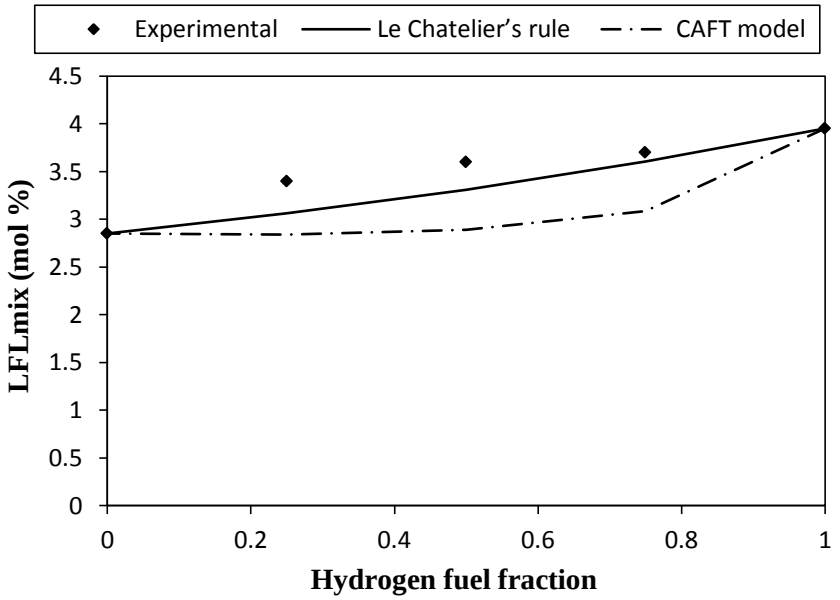

Figure 76: Application of Le Chatelier's rule and CAFT model to the LFLs of mixtures of hydrogen and ethylene at room temperature and 1.0 atm

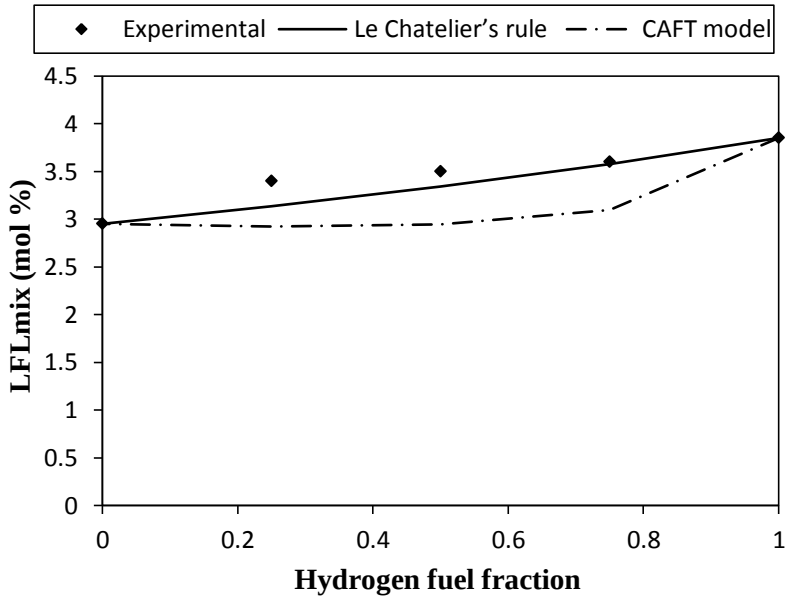

Figure 77: Application of Le Chatelier's rule and CAFT model to the LFLs of mixtures of hydrogen and ethylene at room temperature and 0.5 atm

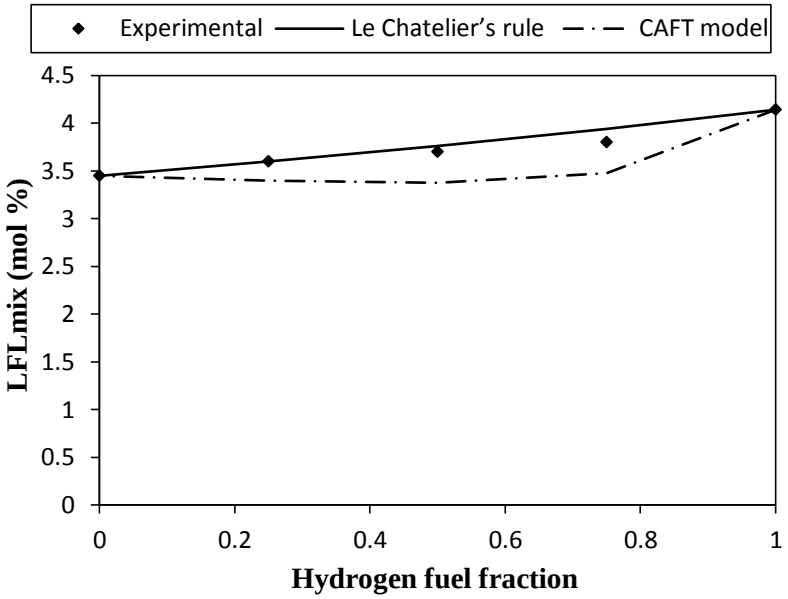

Figure 78: Application of Le Chatelier's rule and CAFT model to the LFLs of mixtures of hydrogen and ethylene at room temperature and 0.1 atm

Overall, Le Chatelier's rule could predict the LFLs of the mixtures very well. The relative difference between the experimental and the calculated LFLs is within 9.9% (0.3 mol% absolute difference), and the average relative difference is 4.3% (0.2 mol% absolute difference). The level of prediction of the rule increases when the initial pressure decreases from 1.0 atm to 0.1 atm. At all initial pressures, Le Chatelier's rule provides more conservative prediction of the LFLs (lower LFLs). Therefore, from a safety point of view, the application of Le Chatelier's rule for these mixtures is acceptable since the rule is both accurate and conservative.

The application of CAFT model is less accurate than that of Le Chatelier's rule since there are larger differences between the experimental and calculated LFLs. The maximum relative difference is 19.8% (0.7 mol% absolute difference), and the average relative difference is 13.3% (0.5 mol% absolute difference). The deviation decreases when the initial pressure is reduced from 1.0 atm to 0.1 atm. With the same initial pressure, the deviation is the largest at equal fractions of hydrogen and ethylene (hydrogen fraction is 0.5). The reasons for the deviation are the same as those described for mixtures of hydrogen and ethane.

For the UFLs, the application of the Le Chatelier's rule and CAFT model at room temperature and initial pressures of 1.0 atm, 0.5 atm and 0.1 atm is presented by Figure 79, Figure 80 and Figure 81, respectively.

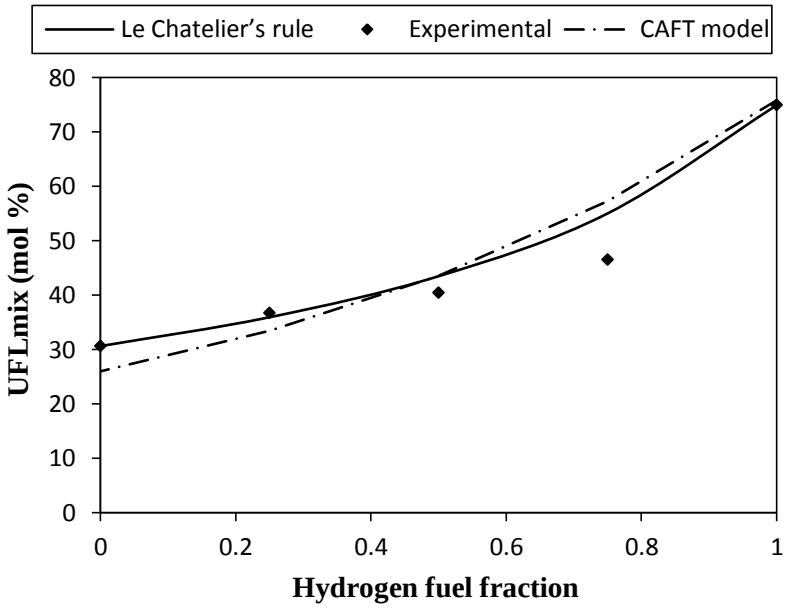

Figure 79: Application of Le Chatelier's rule and CAFT model to the UFLs of mixtures of hydrogen and ethylene at room temperature and 1.0 atm

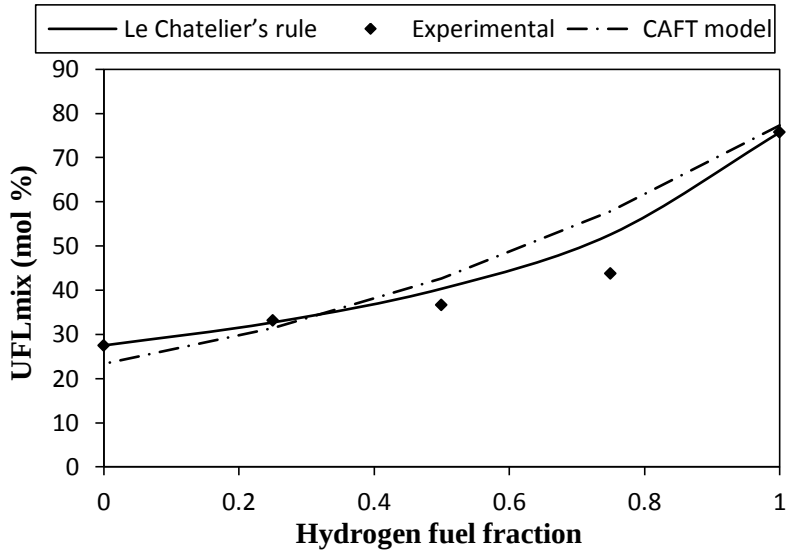

Figure 80: Application of Le Chatelier's rule and CAFT model to the UFLs of mixtures of hydrogen and ethylene at room temperature and 0.5 atm

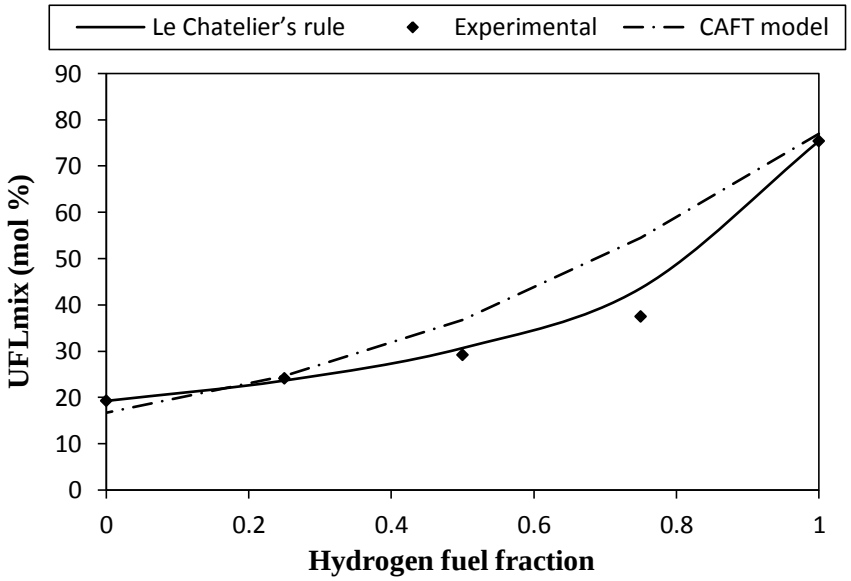

Figure 81: Application of Le Chatelier's rule and CAFT model to the UFLs of mixtures of hydrogen and ethylene at room temperature and 0.1 atm

The UFLs of mixtures of hydrogen and ethylene do not obey Le Chatelier as well as the UFLs of mixtures of hydrogen and the alkanes. The maximum relative deviation is 20.2% (8.8 mol% absolute deviation), and the average relative deviation is 9.3% (3.7 mol% absolute deviation). At all initial pressures, the rule could predict the UFLs quite well when the fraction of hydrogen is equal or less than 0.5; at higher fraction of hydrogen, significant deviation occurs. The same observation was made by Wierzba and Ale[101] when they studied the UFLs of mixtures of hydrogen and ethylene at room temperature and atmospheric pressure. The reason for the deviation can be explained by the chemical interaction between hydrogen and ethylene within the propagating flame which strongly affects the UFLs of the mixtures and not presented by the simple mixing rule of Le Chatelier.[101, 109]

With respect to the application of CAFT model, there are large deviations between the experimental and calculated UFLs. The maximum relative deviation is 45.6% (17.1 mol% absolute deviation), and the average relative deviation is 15.6% (6.0 mol% absolute deviation). The reasons for the deviation are the same as those explained for mixtures of hydrogen and the alkanes.

6.3. Summary

6.3.1. UFLs and LFLs of mixtures of hydrogen and hydrocarbons

The LFLs and UFLs of binary mixtures of hydrogen and light hydrocarbons (methane, ethane, *n*-butane, and ethylene) were determined at room temperature and

initial pressures of 1.0 atm, 0.5 atm, and 0.1 atm. Table 26 summarizes the LFLs and UFLs of the mixtures.

The LFLs of mixtures of hydrogen and the hydrocarbons do not change much when the initial pressure decreases from 1.0 atm to 0.1 atm. For all studied mixtures, the maximum absolute change in the LFLs when the pressure decreases from 1.0 atm to 0.5 atm is 0.2 mol%, and from 1.0 atm to 0.1 atm is 0.9 mol%. Therefore, it can be concluded that low pressure (from 1.0 atm to 0.1 atm) has little effect on the LFLs of mixtures of hydrogen and the hydrocarbons. In contrast, the UFLs of the mixtures are much more influenced by pressure. For example, the maximum absolute deviations from 1.0 atm of the UFLs is 3.8 mol% at 0.5 atm (0.1 mol% for the LFL), and 12.6 mol% at 0.1 atm (0.9 mol% for the LFL). The impact of pressure is the greatest for mixtures of hydrogen and ethylene. For mixtures of hydrogen and the alkanes, the impact of pressure is the highest with methane, followed ethane and *n*-butane.

Table 22: Flammability limits of mixtures of hydrogen and light hydrocarbons at room temperature and initial pressures of 1.0 atm, 0.5 atm, and 0.1 atm

H_2 molar fraction in the fuel mixture		P = 1.0 atm		P = 0.5 atm		P = 0.1 atm	
		LFL (mol%)	UFL (mol %)	LFL (mol%)	UFL (mol%)	LFL (mol%)	UFL (mol%)
$H_2 + CH_4$	1	3.95	74.90	3.85	75.70	4.14	75.40
	0.75	4.20	43.90	4.00	40.60	4.10	36.50
	0.5	4.35	29.90	4.20	28.00	4.40	25.20
	0.25	4.70	21.89	4.70	20.10	4.80	19.20
	0	5.35	15.40	5.35	14.65	5.35	14.50
$H_2 + C_2H_6$	1	3.95	74.90	3.85	77.30	4.14	75.40
	0.75	3.90	35.30	3.70	32.90	3.90	29.80
	0.5	3.80	24.60	3.60	22.40	4.00	20.50
	0.25	3.40	18.90	3.50	17.30	3.90	15.90
	0	2.85	14.00	2.90	12.86	3.75	11.76
$H_2 + C_4H_{10}$	1	3.95	74.90	3.85	75.70	4.14	75.40
	0.75	3.50	26.00	3.40	23.70	3.60	22.40
	0.5	2.80	16.50	2.90	15.10	3.30	15.30
	0.25	2.10	11.90	2.10	10.80	2.90	11.80
	0	1.70	8.46	1.80	8.18	2.60	8.10
$H_2 + C_2H_4$	1	3.95	74.90	3.85	75.70	4.14	75.4
	0.75	3.70	46.50	3.60	43.80	3.8	37.4
	0.5	3.60	40.40	3.5	36.60	3.7	29.1
	0.25	3.40	36.70	3.40	33.10	3.6	24.1
	0	2.85	30.61	2.95	27.50	3.45	19.26

With respect to the role of hydrogen in the fuel mixture, the LFLs of all mixtures increase when the fraction of hydrogen increases; except for mixtures with methane whose LFLs decrease with increasing hydrogen fraction. The LFLs of the mixtures are less impacted by the pressure with increasing fraction of hydrogen in the blended fuels;

except for mixtures with methane whose LFLs change more with pressure when the fraction of hydrogen increases. Similarly, the UFLs of all mixtures increase when the fraction of hydrogen increases. For mixtures of hydrogen and the alkanes, the higher the fraction of hydrogen, the more the changes of the UFLs with pressure. In contrast, the UFL of mixture of hydrogen and ethylene change more with pressure when the fraction of hydrogen in the fuel composition decreases.

In summary, the flammable region of all mixtures widens when the fraction of hydrogen in the mixture increases. With respect to the influence of pressure, when the initial pressure decreases, the flammable region narrows, which is understandable since the UFL of the mixture decreases more significantly with decreasing pressure while the LFL does not vary much with pressure.

6.3.2. The application of Le Chatelier's rule and CAFT model

The application of Le Chatelier's rule and CAFT model was verified against the flammability limits of mixtures of hydrogen and the hydrocarbons. Table 27 summarizes the average relative differences between experimental and calculated flammability limits.

Table 23: Average relative differences between experimental and calculated flammability limits for Le Chatelier's rule and CAFT model at room temperature and initial pressures of 1.0 atm, 0.5 atm, and 0.1 atm

	Le Chatelier's rule		CAFT	
	Δ_{LFL} (%)*	Δ_{UFL} (%)	Δ_{LFL} (%)	Δ_{UFL} (%)
$H_2 + CH_4$	4.5	8.8	8.1	32.9
$H_2 + C_2H_6$	6.7	4.4	16.3	39.9
$H_2 + C_4H_{10}$	7.6	6.0	27.2	96.4
$H_2 + C_2H_4$	4.3	9.3	13.3	15.6

$$* \Delta = \frac{|(\text{Calculated} - \text{Experimental})|}{\text{Experimental}} \times 100\%$$

Overall, Le Chatelier's rule could predict the flammability limits (LFLs, UFLs) of mixtures of hydrogen and the hydrocarbons very well at room temperature and initial pressure from 1.0 atm to 0.1 atm: the average relative deviation is within 8.0% for the LFLs and within 10.0% for the UFLs. For mixtures of hydrogen and ethylene, Le Chatelier's rule gives higher deviation for the UFLs, especially when the fraction of hydrogen is higher than 50%. In general, the level of prediction by Le Chatelier's rule increases when the initial pressure decreases.

For the LFLs, Le Chatelier's rule provides a more conservative prediction of the LFLs (calculated LFLs are smaller than experimental LFLs), except for mixtures of hydrogen and methane whose calculated LFLs are slightly higher. For the UFLs, Le Chatelier's rule provides a less conservative prediction of UFLs (calculated UFLs are smaller than experimental UFLs), except for mixtures of hydrogen and ethylene whose calculated UFLs are slightly higher than.

Compared to Le Chatlier's rule, the CAFT model gives a much less accurate prediction of the flammability limits, especially of the UFLs where signification

deviations from experimental values are observed. For all mixtures, CAFT model provide much wider flammability regions (lower LFLs and higher UFLs). The reason for the large deviations and the wider flammability regions is that CAFT model does not take into account the heat loss by the product dissociation which absorbs energy of combustion and the interaction between the fuels which reduces the effective heat of combustion. Therefore, it is recommended that Le Chatelier's rule is used instead of CAFT model for the prediction of the flammability limits of the fuel mixtures.

7. CONCLUSIONS AND RECOMMENDATIONS

7.1. Conclusions

The flammability limits (UFLs and LFLs) of : i) pure hydrogen, and light hydrocarbons (methane, ethane, *n*-butane, and ethylene), and ii) binary mixtures of hydrogen and the hydrocarbons were experimentally determined at room temperature and initial pressure ranging from 1.0 atm to 0.1 atm. The influence of pressure on the flammability limits was investigated. It was found that:

- The flammability limits of hydrogen behave differently under the impact of pressure compared to those of the hydrocarbons. The flammability region of hydrogen widens (LFL decreases, UFL increases) when the initial pressure decreases from 1.0 atm to 0.3 atm, then the region narrows with the further decrease of pressure. Whereas the flammability regions of the hydrocarbons narrows (LFL increases, UFL decreases) when the initial pressure decreases. From a safety point of view, more precaution is recommended when handling hydrogen at low pressure conditions since its flammable region widens when the pressure decreases below 1.0 atm. In contrast, considering the flammable region, it is recommended to handle the hydrocarbons as a pressure as low as possible.
- The LFLs of hydrogen and the hydrocarbons don't change much with pressure compared to the UFLs. In other words, pressure has a much greater impact on the UFLs than on the LFLs for hydrogen and the hydrocarbons.

- For binary mixtures of hydrogen and the hydrocarbons, the flammability regions narrow when the initial pressure decreases from 1.0 atm to 0.1 atm. Pressure has much greater impact on the UFLs than the LFLs of the mixtures. And the higher the fraction of hydrogen in the blended fuel mixture, the more impact of the pressure on the UFL of the mixture; except for mixtures of hydrogen and ethylene where the opposite is observed.
- The flammable regions of all mixtures widen when the fraction of hydrogen in the fuel mixtures increases. Thus, the risk of fire/explosion increases when there is more hydrogen in the fuel mixture.

The constant volume adiabatic flame temperatures (AFTs) of hydrogen and hydrocarbons at the flammability limit concentrations and initial pressures ranging from 1.0 atm to 0.1 atm were calculated using the EQUILIBRIUM program in CHEMKIN package. The following conclusions were made:

- For hydrogen, at all initial pressures studied, the AFT at UFL is roughly 2 times the AFL at LFL. This suggests that the thermal impact of a flame at UFL is higher than that at LFL; thus, on the safety point of view, the consequence of a hydrogen flame at UFL is more severe than that at LFL. However, the risk of hydrogen flame, whether at lean or rich concentration, should be carefully analyzed holistically based on many other factors, such as the operating condition, proximity to other fuels.

- For hydrogen and the hydrocarbons, pressure has higher impact on the AFT at UFL than on the AFT at LFL.
- A linear relationship was derived between the AFT and the corresponding flammability limit for hydrogen and hydrocarbons, in which the AFTs at LFL are proportional to the LFLs whereas the AFTs at UFL are direct opposite to the UFLs.
- A thermodynamic method which does not consider the reaction equilibrium calculation, called Calculated Adiabatic Flame Temperature (CAFT), was also used to calculated the AFTs. Compared to the AFTs calculated using the CHEMKIN package, this method could provide very good estimates of the AFTs of hydrogen at all initial pressures studied. The same is not true for the AFTs of the hydrocarbons where there are large differences between the AFTs calculated by two methods. The differences are larger for the AFTs at UFLs than for the AFTs at LFLs. At all initial pressure, CAFT method provides higher AFTs. This is because CAFT method does not take into account the complex chemistry of the combustion reaction including the product dissociation and the formation of complex product mixtures (NOx, radicals, soot…) which consume energy.

The application of Le Chatelier's rule to the flammability limits of mixtures of hydrogen and hydrocarbons at room temperature and initial pressures of 1.0 atm, 0.5 atm, and 0.1 atm were verified. The application of CAFT model to predict the

flammability limits was also performed and compared with Le Chatelier's rule. It was found that:

- Le Chatelier's rule could predict the flammability limits (LFLs, UFLs) of mixtures of hydrogen and the hydrocarbons quite well: the average relative deviation is within 8.0% for the LFLs and within 10.0% for the UFLs. In general, the accuracy of prediction by Le Chatelier's rule increases when the initial pressure decreases.
- Compared to Le Chatlier's rule, the CAFT model gives a much less accurate prediction of the flammability limits, especially of the UFLs where signification deviations from experimental values are observed. For all mixtures, CAFT model provide much wider flammability regions (lower LFLs and higher UFLs).

7.2. Recommendations

The following future research topics are recommended in order to take advantage of the results of this research and further extend it.

- Pressure is found to have a much greater impact on the UFLs than on the LFLs of hydrogen and the hydrocarbons. This may be explained by a research into the reaction mechanism of hydrogen and the hydrocarbons at limiting concentrations (flammability limits) under the influence of pressure. For the case of ethylene, it was found by Carriere et al.[25] that for fuel-rich mixtures of ethylene (close to the UFL) the reaction mechanism is very sensitive to the variation of pressure. Specifically, the dominant ethylene consumption pathway and the route to the final oxidation products of the combustion of ethylene change greatly with

pressure. When the pressure increases, the destruction of ethylene changes from abstraction reaction forming C_2H_3 to addition reaction forming C_2H_5; consequently, the pathway to the formation of final products via oxygenated species appears and becoming more important.[25] Some reactions on this pathway are pressure dependent in a way that an increase in pressure further enhance the rates of these reactions[25] which promotes the flame propagation and results in a large increase of the UFL as observed in this study. Therefore, it is recommended that a similar research to that by Carriere et al.[25] is carried out in the future to be able to explain the greater influence of pressure on the UFLs of hydrogen and hydrocarbons.

- This research determined and analyzed the flammability limits of hydrogen and its mixtures with light hydrocarbons at atmospheric and sub-atmospheric pressures. The next step is to study the effect of inert gases on these flammability limits at sub-atmospheric pressures. The inert gases can be nitrogen, carbon dioxide, and water which are commonly used in the industry. A research on the interting effects, together with the results from this research, would provide valuable information and guidance on the prevention and mitigation of fire/explosion pertaining to hydrogen and its mixtures with light hydrocarbons.
- This study with mixtures of hydrogen and the hydrocarbons with mole fraction of hydrogen equal or less than 0.75 show that the flammable regions narrow when the pressure decreases from 1.0 atm to 0.1 atm. This behavior is similar to that of the hydrocarbons under the influence of pressure. It is expected that when the

fraction of hydrogen increases to a certain value, the flammable region will widen when the pressure decreases, similar to that observed for pure hydrogen. Therefore, it is recommended that this minimum fraction of hydrogen with various mixtures of hydrocarbons be determined in the future study.

- This research introduces a modified Le Chatelier's rule which incorporates the interaction between the fuel components. There are many ways this modified rule could be explored further in the future. For example, the modified rule could be verified with other fuel mixtures at different operating conditions. The coefficients of perturbation could be examined under the influence of pressure and/or temperature.
- A study on the behavior of the flammability limits of mixtures of hydrogen with hydrocarbons under the impact of temperature is recommended. This research is necessary since data/study on the influence of temperature on the flammability limits of mixtures of hydrogen and hydrocarbons is limited in the literature, and non-ambient temperature operating conditions are common in industry.

REFERENCES

(1) ASTM Standard Test Method for Concentration Limits of Flammability of Chemicals (Vapors and Gases). **2009,** *10.1520/E0681-09*.

(2) Coward, H. F.; Jones, G. W. Limits of flammability of gases and vapors. *Bureau of Mines Bulletin*, 1952; Vol. 503.

(3) Zabetakis, M. G. Flammability Characteristics of Combustible Gases and Vapors. *Bureau of Mines, Pittsburgh*, 1965; Vol. Bulletin 627.

(4) Schr¨oder, V.; Molnarne, M. Flammability of gas mixtures Part 1: Fire potential. *Journal of Hazardous Materials* **2005,** *121* (1-3), 37-44.

(5) Crowl, D. A.; Louvar, J. F. *Chemical Process Safety: Fundamentals with Applications, Second Edition*. Prentice Hall: 2001.

(6) NFPA 30: Flammables and Combustible Liquids Code. 1996.

(7) CCPS, A. *Guidelines for chemical process quantitative risk analysis*. New York: American Institute of Chemical Engineers: 2000.

(8) Wong, W. K. Measurement of flammability in a closed cylindrical vessel with thermal criterion. PhD Dissertation, 2006.

(9) Federal Institute for Materials Research and Testing (BAM). Determination of explosion limits, explosion pressure and rate of explosion pressure rise of gases and vapors at elevated initial pressure and temperature conditions. 2004.

(10) Britton, L. G. Two Hundred Years of Flammable Limits. *Process Safety Progress* **2002,** *21* (1), 1-11.

(11) EN 1839:2003. Determination of explosion limits of gases and vapours. BSI: 2003.

(12) BS EN 13673-1:2003. Determination of the maximum explosion pressure and the maximum rate of pressure rise of gases and vapours. Determination of the maximum explosion pressure. BSI: 2003.

(13) Mashuga, C. V.; Crowl, D. A. Application of the flammability diagram for evaluation of fire and explosion hazards of flammable vapors. *Process Safety Progress* **1998,** *17* (3), 176-183.

(14) DIN 51649-1. Bestimmung der Explosionsgrenzen von Gasen und Gasgemischen in Luft. 1986.

(15) ASTM E 918-83. Standard practice for determining limits of flammability of chemicals at elevated temperature and pressure. 1999.

(16) ASTM E 2079-01. Standard test methods for limiting oxygen (oxidant) concentration in gases and vapors. 2001.

(17) Heinonen, E. W.; Tapscott, R. E.; Crawford, F. R. *Methods Development for Measuring and Classifying Flammability/Combustibility of Refrigerants*; NMERI, The University of New Mexico, Albuquerque: 1994.

(18) ISO 10156. Gases and gas mixtures—Determination of fire potential and oxidizing ability for the selection of cylinder valve outlets. 1996.

(19) Shebeko, Y. N.; Tsarichenko, S. G.; Korolchenko, Y. A.; Trunev, A. V.; Navzenya, Y. V.; Papkov, S. N.; Zaitzev, A. A. Burning velocities and flammability limits of gaseous mixtures at elevated temperatures and pressures. *Combustion and Flame* **1995,** *102* (4), 427-437.

(20) Hustad, E. J. Experimental studies of lower flammability limits of gases and mixtures of gases at elevated temperatures. C*ombustion and Flame* **1988,** *71* (3), 283-294.

(21) Vanderstraeten, B.; Tuerlinckxa, D.; Berghmansa, J.; Vliegenb, S.; Van't Oostb, E.; Smitb, B. Experimental study of the pressure and temperature dependence on the upper flammability limit of methane/airmixtures. *Journal of Hazardous Materials* **1997,** *56* (3), 237-246.

(22) Goethalsa, M.; Vanderstraetena, B.; Berghmansa, J.; De Smedta, G.; Vliegenb, S.; Van't Oostb, E. Experimental study of the flammability limits of toluene–airmixtures at elevated pressure and temperature. *Journal of Hazardous Materials* **1999,** *70* (3), 93-104.

(23) Berl, E.; Werner, G. The limit of combustibility of flammable gas and vapor air mixtures at high pressure. *Ztschr. Angew. Chem.* **1927,** *40*, 245-250.

(24) Shebeko, Y. N.; Tsarichenko, S. G.; Korolchenko, A. Y.; Trunev, A. V.; Vavzenya, V. Y.; Papkov, S. N.; Zaizev, A. A. Burning velocities and flammability limits of gaseous mixtures at elevated temperatures and pressures. *Combustion and Flame* **1995,** *102* (4), 427-437.

(25) Carriere, T.; Westmoreland, P. R.; Kazakov, A.; Stein, Y. S.; Dryer, F. L. Modeling ethylene combustion from low to high pressure. *Proceedings of the Combustion Institute* **2002,** *29* (1), 1257–1266.

(26) Hoimstedt, G. S. The Upper Limit of Flammability of Hydrogen in Air, Oxygen and Oxygen-Inert Mixtures at Elevated Pressures. *Combustion and Flame* **1971,** *17*, 295-301.

(27) Pekalski, A.A.; Zevenbergen, J.F; Pasman, H.J.; Lemkowitz, S.M.; Dahoe, A.E; Scarlett, B. The relation of cool flames and auto-ignition phenomena to process safety at elevated pressure and temperature. *Journal of Hazardous Materials* **2002,** *93*, 93-105.

(28) Laffitte, P.; Delbourgo, R. Ignition by condenser sparks. Regions of flammability of ethane, propane, n-butane and n-pentane. *Fourth Symposium (International) on Combustion* **1953,** *Williams and Wilkins* 114.

(29) Piazza, J. T. D. Limits of flammability of pure hydrocarbon-air mixtures at reduced pressures and room temperature. *N.A.C.A. Research Memorandum* **1951,** *E51C28*.

(30) Winter, C. J. Hydrogen energy, Abundant, efficient, clean: A debate over the energy-system-of-change. *International Journal of Hydrogen Energy* **2009,** *34* (14), S1-S52.

(31) Ogden, J. M. Hydrogen: The Fuel of the Future? *Phys. Today* **2002,** *55* (4), 69.

(32) Dunn-Rankin, D. *Lean Combustion: Technology and Control*. Academic Press: 2008.

(33) Census Bureau; U.S. Department of Commerce. Current Industrial Reports: Industrial Gases, 2004. http://www.census.gov/industry/1/mq325c045.pdf.

(34) ARIA. Accidentology involving hydrogen. http://www.aria.developpement-durable.gouv.fr/ressources/etude_h2_gb.pdf.

(35) Glassman, I. *Combustion*. New York: Academic Press: 1996.

(36) Suzuki, T. *Fire and Materials: Volume 18*. 1994.

(37) Bartknecht, W. *Explosions-Schutz: Grundlagen und Anwendung*. New York: Springer: 1993.

(38) Kuchta, J. M. Investigation of fire and explosion accidents in the chemical, mining and fuel-related industries. *Bureau of Mines Bulletin*, 1985; Vol. 680.

(39) Daniel A. Crowl; Jo, Y.-D. The hazards and risks of hydrogen. *Journal of Loss Prevention in the Process Industries* **2007,** *20* (2), 158-164.

(40) Sherifa, S. A.; Barbirb, F.; Veziroglu, T. N. Wind energy and the hydrogen economy—review of the technology. *Solar energy* **2005,** *78* (5), 647-660.

(41) Fotis Rigas; Paul Amyotte. *Hydrogen Safety: Chapter 2: Historical Survey of Hydrogen Accidents*. CRC Press 2012.

(42) Bjerketvedt, D.; Mjaavatten, A. A. Hydrogen-Air Explosion in a Process Plant: A Case History. *1st International Conference on Hydrogen Safety* **2005**.

(43) The Sasakawa Peace Foundation.*The Fukushima Nuclear Accident and Crisis Management: Lessons for Japan-U.S. Alliance Cooperation*; 2012.

(44) http://navier.engr.colostate.edu/tools/equil.html.

(45) Enloe, J. D.; Thomson, J. D. Flammability limits of hydrogen-oxygen-nitrogen mixtures at low pressures. *Combustion and Flame* **1966,** *10*, 393-394.

(46) Kaldis, S. P.; Kapantaidakis, G. C.; Sakellaropoulos, G. P. Simulation of multicomponent gas separation in a hollow fiber membrane by orthogonal collocation — hydrogen recovery from refinery gases. *Journal of Membrane Science* **2000,** *173*, 61-71.

(47) Yufei Dong; Christina M. Vagelopoulos; Geoffrey R. Spedding; Fokion N. Egolfopoulos. Measurement of laminar flame speeds through digital particle image velocimetry: Mixtures of methane and ethane with hydrogen, oxygen, nitrogen, and helium. *Proceedings of the Combustion Institute* **2002,** *29* (2), 1419-1426.

(48) Tang, C.; Huang, Z.; Jin, C.; He, J.; Wang, J.; Wang, X.; Miao, H. Laminar burning velocities and combustion characteristics of propane–hydrogen–air premixed flames. *International Journal of Hydrogen Energy* **2008,** *33* (18), 4906-4914.

(49) Huang, Y.; Sung, C. J.; Eng, J. A. Laminar flame speeds of primary reference fuels and reformer gas mixtures. *Combustion and Flame* **2004,** *139* (3), 239-251.

(50) Kaskan, W. E. The dependence of flame temperature on mass burning velocity. *Symposium (International) on Combustion* **1957,** *6* (1), 134-143.

(51) Kuo, K. K. *Principles of Combustion 2nd Edition*. John Wiley & Sons, Inc. : 2005.

(52) Sivashinsky, G. I. Instabilities, pattern formation, and turbulence in flames. *Ann. Rev. Fluid Mech.* **1983,** *15* (1), 79-99.

(53) Melhem, G. A. A detailed method for estimating mixture flammability limits using chemical equilibrium. *Process Safety Progress* **2004,** *16* (4), 203-218.

(54) Vidal, M.; Wong, W.; Rogers, W. J.; Mannan, M. S. Evaluation of lower flammability limits of fuel–air–diluent mixtures using calculated adiabatic flame temperatures. *Journal of Hazardous Materials* **2006,** *130* (1-2), 21-27.

(55) Razus, D.; Molnarne, M.; Fu, O. Limiting oxygen concentration evaluation in flammable gaseous mixtures by means of calculated adiabatic flame temperatures. *Chemical Engineering and Processing: Process Intensification* **2004,** *43* (6), 775-784.

(56) Center for Chemical Process Safety. *Guidelines for Chemical Process Quantitative Risk Analysis (2nd Edition)*. Center for Chemical Process Safety/AIChE: 2000.

(57) Zhou, M.; Donald Gauthier, J. E. A new method for adiabatic flame temperature estimations of hydrocarbon fuels. *Fuel* **1999,** *78* (4), 471-478.

(58) Mashuga, C. V.; Crowl, D. A. Flammability zone prediction using calculated adiabatic flame temperatures. *Process Safety Progress* **1999,** *18* (3), 127-134.

(59) Gülder, Ö. L. Flame Temperature Estimation of Conventional and Future Jet Fuels. *J. Eng. Gas Turbines Power* **1986,** *108* (2), 376-380.

(60) Chang, S. L.; Rhee, K. T. Adiabatic flame temperature estimates of lean fuel/air mixtures *Combustion Science and Technology* **1983,** *35* (1-4), 203-206.

(61) EQS4WIN. http://www.mathtrek.com/.

(62) Kee, R. J.; Rupley, F. M.; Miller, J. A. *CHEMKIN-II: a Fortran chemical kinetics package for the analysis of gas phase chemical kinetics*; Sandia International Laboratories Report no. SAND89- 8009B: 1993.

(63) Kee, R. J.; Rupley, F. M.; Miller, J. A. *The CHEMKIN Thermodynamic Data Base*; SAND87-8215B; Sandia National Labs., Albuquerque, NM: 1992.

(64) Kee, R. J.; Dixon-Lewis, G.; Warnatz, J.; Coltrin, M. E.; Miller, J. A. *A FORTRAN Computer Code Package for the Evaluation of Gas-phase, Multicomponent Transport Properties*; SAND86-8246; Sandia National Labs., Albuquerque, NM: 1992.

(65) Smith, G. P.; Golden, D. M.; Frenklach, M.; Moriarty, N. W.; Eiteneer, B.; Goldenberg, M.; Bowman, C. T.; Hanson, R. K.; Song, S.; William C. Gardiner, J.; Lissianski, V. V.; Qin, Z. http://www.me.berkeley.edu/gri_mech/

(66) Combustion Chemistry Center. http://c3.nuigalway.ie/

(67) Liu, F.; Guo, H.; Smallwood, G. J.; Gülder, Ö. L. Numerical study of the super adiabatic flame temperature phenomenon in hydrocarbon premixed flames. *Proceedings of the Combustion Institute* **2002,** *29* (2), 1543-1550.

(68) Davis, S. G.; Quinarda, J.; Searby, G. Markstein numbers in counterflow, methane- and propane- air flames: a computational study. *Combustion and Flame* **2002,** *130* (1-2), 123-136.

(69) EN 1839. Determination of explosion limits of gases and vapours. 2003.

(70) Efunda Engineering Fundamentals. Wheatstone Bridges: Introduction. http://efunda.com/designstandards/sensors/methods/wheatstone_bridge.cfm.

(71) Mashuga, C. V. Determination of the combustion behavior for pure components and mixtures using a 20L sphere. Ph.D. Dissertation, Michigan, 1999.

(72) Wierzba, I.; Wang, Q. The flammability limits of H2-CO-CH4 mixtures in air at elevated temperatures. *International Journal of Hydrogen Energy* **2006,** *31* (4), 485-489.

(73) Bone, W. A.; Newitt, D. M.; Smith, C. M. Gaseous combustion at high pressures IX. The influence of pressure upon the explosion limits of inflammable gas-air, etc. mixtures. *Proceedings of the Royal Society* **1928,** *117*, 553-576.

(74) Terres, E.; Plenz, F. Influence of pressure on the burning of explosive gas mixtures. *Journal Gasbel.* **1914,** *57*, 990-995, 1001-1007, 1016-1019, and 1025-1027.

(75) Dougherty, E. P.; Rabitz, H. Computational Kinetics and Sensitivity Analysis of Hydrogen-Oxygen Combustion. *J. Chem. Phys* **1980,** *72* (12), 65-71.

(76) Law, C. K.; Egolfopoulos, F. N. Kinetic criterion of flammability limits: The C-H-O-Inert system. *Twenty-Third Symposium (International) on Combustion/The Combustion Institute* **1990**, 413-421.

(77) Sohn, C. H.; Chung, S. H. Effect of Pressure on the Extinction, Acoustic Pressure Response, and NO Formation in Diluted Hydrogen–Air Diffusion Flames. *Combustion and Flame* **2000,** *121* (1-2), 288-300.

(78) Le, H.; Nayak, S.; Mannan, M. S. Upper Flammability Limits of Hydrogen and Light Hydrocarbons In Air at Sub-atmospheric Pressures. *Industrial & Engineering Chemistry Research* **2012,** *51* (27), 9396-9402.

(79) Holmstedt, G. S. The upper limit of flammability of hydrogen in air, oxygen, and oxygen-inert mixtures at elevated pressures. *Combustion and Flame* **1971,** *17* (3), 295-301.

(80) Mason, W.; Wheeler, R. V. Effect of Temperature and of Pressure on the Limits of Inflammability of Mixtures of Methane in Air. *Jour. Chem. Soc.* **1918,** *113*, 45-57.

(81) Van den Schoor, F.; Verplaetsen, F. The upper explosion limit of lower alkanes and alkenes in air at elevated pressures and temperatures. *Journal of Hazardous Materials* **2006,** *128* (1), 1-9.

(82) Craven, A. D.; Foster, M. G. The limits of flammability of ethylene in oxygen, air and air –nitrogen mixtures at elevated temperatures and pressures. *Combust. Flame* **1966,** *10* (2), 95-100.

(83) Hashiguchi, Y.; Ogahara, T.; Iwasaka, M.; Ozawa, K. Effect of pressure on the detonation limit of ethylene. *Int. Chem. Eng.* **1966,** *6*, 737-743.

(84) Hertzberg, M.; Cashdollar, K. L.; Zlochower, I. A. Flammabilitylimitmeasurements for dusts and gases: Ignition energy requirements and pressure dependences. *Symposium (International) on Combustion* **1988,** *21* (1), 303-313.

(85) Kondo, S.; Takahashi, A.; Takizawa, K.; Tokuhashi, K. On the pressuredependence of flammabilitylimits of CH_2=$CFCF_3$, CH_2F_2 and methane. *Fire Safety Journal* **2011,** *46* (5), 289-293.

(86) Zabetakis, M. G.; Lambiris, S.; Scott, G. S. Flame temperature of limit mixture. In: seventh Symposium (international) on Combustion. *The Combustion Institute, Pittsburgh* **1959**, 484-487.

(87) Sukesh Roy; Waruna D Kulatilaka; Robert P Lucht; Nick G Glumac; Tailai Hu.Temperature profile measurements in the near-substrate region of low-pressure diamond-forming flames. *Combustion and Flame* **2002,** *130* (3), 261-276.

(88) Siegel, R.; Howell, J. R. *Thermal Radiation Heat Transfer, 3rd ed.* . New York: Hemisphere: 1991.

(89) Lewis, B.; Von Elbe, G. *Combustion, Flames and Explosions of Gases, 3rd ed*. Academic Press: 1987.

(90) Reynolds, W. C. *The Element Potential Method for Chemical Equilibrium Analysis: Implementation in the Interactive Program STANJAN*; Department of Mechanical Engineering, Stanford University: 1986.

(91) Chen, C. C. A Study on Estimating Flammability Limits in Oxygen. *Ind. Eng. Chem. Res.* **2011,** *50* (17), 10283–10291.

(92) Law, C. K.; Makino, A.; Lu, T. F. On the off-stoichiometric peaking of adiabatic flame temperature. *Combustion and Flame* **2006,** *145*, 808–819.

(93) Albert Greville White. Limits for the propagation of flame in inflammable gas–air mixtures. Part III. The effects of temperature on the limits. *J. Chem. Soc., Trans* **1925,** *127*, 672-684.

(94) Sandler, S. I. *Chemical, Biochemical, and Engineering Thermodynamics*. 4 ed.; John Wiley & Sons, Inc.: 2006.

(95) Kaldis, S. P.; Kapantaidakis, G. C.; Sakellaropoulos, G. P. Simulation of multi-component gas separation in a hollow fiber membrane by orthogonal collocation — hydrogen recovery from refinery gases. *Journal of Membrane Science* **2000,** *173*, 61-71.

(96) TerMaath, C. Y.; Skolnik, E. G.; Schefer, R. W.; Keller, J. O. Emissions reduction benefits from hydrogen addition to midsize gas turbine feedstocks. *Int J Hydrogen Energy* **2006,** *31* (9), 1147-1158.

(97) Guo, H.; Smallwood, G. J.; Liu, F.; Ju, Y.; Gülder, Ö. The effect of hydrogen addition on flammability limit and NOx emission in ultra-lean counterflow CH4/air premixed flames. *Proc Combust Inst* **2005,** *30* (1), 303-311.

(98) Hawkes, E. R.; Chen, J. H. Direct numerical simulation of hydrogen-enriched lean premixed methane–air flames. *Combust Flame* **2004,** *138* (3), 242-258.

(99) Bell, S. R.; Gupta, M. Extension of the lean operating limit for natural gas fueling of a spark ignited engine using hydrogen blending. *Combust Sci Technol* **1997,** *123* (1-6), 23-48.

(100) Van den Schoor, F.; Verplaetsen, F. The upper flammability limit of methane/hydrogen/air mixtures at elevated pressures and temperatures. *International Journal of HydrogenEenergy* **2007,** *32* (13), 2548-2552.

(101) Wierzba, I.; Ale, B. B. Rich flammability limits of fuel mixtures involving hydrogen at elevated temperatures. *International Journal of Hydrogen Energy* **2000,** *25* (1), 75-80.

(102) Wierzba, I.; Harris, K.; Karim, G. Effect of low temperature on the rich flammability limits in air of hydrogen and some fuel mixtures containing hydrogen. *International Journal of Hydrogen Energy* **1992,** *17* (2), 149-152.

(103) Van den Schoor, F.; Verplaetsen, F.; Berghmans, J. Calculation of the upper flammability limit of methane/hydrogen/air mixtures at elevated pressures and temperatures. *Journal of Hazardous Materials* **2008,** *153* (4), 1301-1307.

(104) Wierzba, I.; Karim, G. A.; Cheng, H. The Flammability of Rich Gaseous Fuel Mixtures Including Those Containing Propane in Air,. *Journal of Hazardous Materials* **1988,** *20*, 303-312.

(105) Wierzba, I.; Karim, G.A.; Cheng, H.; Hanna, M. The flammability of rich mixtures of hydrogen and ethylene in air. *Journal of Institute of Energy* **1987**, 3-7.

(106) Zhao, F.; Rogers, W. J.; Mannan, M. S. Experimental measurement and numerical analysis of binary hydrocarbon mixture flammability limits. *Process Safety and Environmental Protection* **2009,** *87* (2), 94-104.

(107) Kondo, S.; Takizawa, K.; Takahashi, A.; Tokuhashi, K.; Sekiya, A. A study on flammability limits of fuel mixtures. *Journal of Hazardous Materials* **2008,** *155* (3), 440-448.

(108) Crowl, D. A. *Understanding Explosions - A CCPS Concept Book*. Center for Chemical Process Safety (CCPS), AIChE, John Wiley & Sons: New York, 2003.

(109) Wierzba, I.; Karim, G. A.; Cheng, H.; Hanna, M. The flammability of rich mixtures of hydrogen and ethylene in air. *Journal of the Institute of Energy* **1988**, 4-9.